Report No. FAA-RD-72-149, I

JET ENGINE BURN-THROUGH INVESTIGATION
VOLUME I: SONIC ANALYSIS

Richard W. Schumacker

MARCH 1973

FINAL REPORT

Document is available to the public through the National Technical Information Service, Springfield, Virginia 22151

Prepared for

DEPARTMENT OF TRANSPORTATION
FEDERAL AVIATION ADMINISTRATION
Systems Research & Development Service
Washington D. C., 20591

TECHNICAL REPORT STANDARD TITLE PAGE

1. Report No.	2. Government Accession No.	3. Recipient's Catalog No.
FAA-RD-72-149, I		

4. Title and Subtitle	5. Report Date
Jet Engine Burn-Through Investigation - Vol. I Sonic Analysis	March 1973
	6. Performing Organization Code ASW-587

7. Author(s)	8. Performing Organization Report No.
R.W. Schumacker	FAA-NA-72-96

9. Performing Organization Name and Address	10. Work Unit No.
The Magnavox Company Government and Industrial Group Fort Wayne Division Fort Wayne, Indiana 46804	11. Contract or Grant No. DOT-FA72-575
	13. Type of Report and Period Covered Final Report June - September 1972
12. Sponsoring Agency Name and Address DEPARTMENT OF TRANSPORTATION FEDERAL AVIATION ADMINISTRATION Systems Research and Development Service Washington, D. C. 20590	14. Sponsoring Agency Code

15. Supplementary Notes

This study was made under a contract administrated by the National Aviation Facilities Experimental Center, Atlantic City, N.J.

16. Abstract

The work performed during this program was directed toward determining the acoustic characteristics of simulated burn-through failures. To determine the feasibility of detecting this failure acoustically two types of jet engines (J-47 and J-57) were modified to simulate burn-through failures. Magnetic tape recordings of the modified engines were made to determine the extent of the acoustic spectrum, the relationship of engine speed to failure related sound pressure levels and acoustic spectrum, the effect of sensor location to detect the failure acoustically and characteristic acoustic spectra at burn-through. The recorded data was analyzed by real time spectrum analysis and mean square techniques. Results indicated that the simulated burn-through failure acoustic spectra consists primarily of broadband random noise above 5 kHz. It was also determined that sensor location is an important factor in detecting burn-through failures. Based on the results it is concluded that acoustic detection of a burn-through failure is feasible. Recommendations for a monitor and detector based on the results of this program have been included. Volume II contains engine tests raw data and is available on loan from the DOT Library Services Division, TAD-494, 800 Independence Avenue, Washington, D.C. 20591

17. Key Words	18. Distribution Statement
Burner-Can Burn-Through Sonic Engine Analyzer Jet Engine Combusters Combustion Chamber Failure	Availability is unlimited. Document may be released to the National Technical Information Service, Springfield, Virginia 22151, for sale to the public.

19. Security Classif. (of this report)	20. Security Classif. (of this page)	21. No. of Pages	22. Price
Unclassified	Unclassified	80	$3.00PC .95MF

Form DOT F 1700.7 (8-69)

PREFACE

This report was prepared by the Government and Industrial Group, Fort Wayne Division, The Magnavox Company, Fort Wayne, Indiana, for the National Aviation Facilities Experimental Center (NAFEC), Atlantic City, New Jersey. The work was administered under the direction of Richard Hill, Project Engineer, Propulsion and Fire Protection Branch, Aircraft Safety Division, NAFEC. Appreciation is expressed to Mr. Hill and his staff for their valuable assistance while executing the tests at the NAFEC facility.

TABLE OF CONTENTS

LIST OF ILLUSTRATIONS

LIST OF ILLUSTRATIONS (CONT)

LIST OF ILLUSTRATIONS (CONT)

1.0 INTRODUCTION

1.1 Purpose

The purpose of this program is to record and analyze acoustical energy produced by jet engines which have been modified to produce burn-through failures. Conclusions based on the frequency spectral content and the power spectral density of the data analysis will be used to determine the feasibility of detecting burn-through failures by acoustic means and recommendations made for achieving this means.

1.2 Background

Burn-through failures in jet engines appear to be random in nature and cannot be isolated to any particular aircraft or engine. Information on this failure mode is sketchy, but both airlines and engine manufacturers alike acknowledge the existence of the problem. Jet engine burn-through failures generally occur in close proximity (forward or aft) to the fuel nozzles. Failure modes include cracked burner cans, worn burner can locator lugs and pins, fuel manifold failures, and fuel line failures. The result is a high-temperature, high-velocity (supersonic) flame that burns through the engine housing and cowling. The acoustic energy created by the burn-through suggests a possible method of detecting an engine failure.

The National Aviation Facilities Experimental Center (NAFEC), Aircraft Safety Division, at Atlantic City, New Jersey has taken an active role in investigating the nature of burn-through failures. Initial investigations were made using a J-47 engine mounted on a test stand with remote engine control from a nearby blockhouse. Burner cans were modified to establish standard test conditions for testing materials for possible use as a fire barrier for protection against burn-through failures.* Subsequent work accomplished includes analyzing the complex properties of the burn-through flame.**

A second and third jet engine have been added to the facility by utilizing a surplus Air Force B-57 aircraft. The B-57 is equipped with J-57 engines which have a higher pressure ratio than the J-47 engine and more closely approximates aircraft currently in commercial and military inventory. The aircraft was modified such that each engine could be

---

*Rust, Thomas Jr., Investigation of Jet Engine Combustion Chamber Burn-Through Fire, National Aviation Facilities Experimental Center, Atlantic City, New Jersey, Report No. FAA-RD-70-68, March 1971.

**Pergament, H.S. & Mikatarian, R.R., Evaluation of Test Data on Jet Engine Combustion Burn-Through Flames, AeroChem Research Laboratories, Inc., Princeton, New Jersey, Report No. FAA-RD-71-100, March 1972.

remotely operated from the blockhouse. Engine burner cans were modified to create conditions which simulate burn-throughs. The facility is shown in Figure 1-1.

Acoustic recordings have been made of simulated burn-through failures using limited range (100 Hz to 10 kHz) instrumentation equipment. The recordings were analyzed for spectral content and power density. The results indicated that acoustic techniques might very well develop into a feasible method of detecting burn-through failures. This program is a direct result of that effort and utilizes more sophisticated instrumentation recording equipment.

1.3 Program Objectives

The objective of this program is to accurately determine the acoustic characteristics of burn-through failure. In particular, it is desired to ascertain the following:

(1) The extent of the acoustic spectrum

(2) Characteristic line spectra at burn-through

(3) Sound pressure level relationship to orifice size and engine speed

(4) Acoustic spectrum relationship to orifice size and engine speed

(5) Effect of sensor locations on acoustic spectrum and sound pressure levels

(6) Effect of extraneous sound sources.

A J-47 engine and two J-57 engines, located at the NAFEC facility in Atlantic City, New Jersey, were instrumented in a manner deemed most likely to satisfy these objectives. The J-47 engine was open and the two J-57 engines were cowled. Five microphones, placed on or about the engine under test, were used to record each event. One of the five was an extended range instrumentation microphone. The recordings were analyzed by two different methods; real time spectrum analysis and broadband energy level detection. The results of the real time spectrum analysis are permanent records made on electrosensitive paper called spectrograms or grams (time record of intensity versus frequency). The broadband energy analysis were recorded on a dual channel chart recorder (time record of average power level in a broad frequency band) and may be called energy grams. In addition, spectrum photographs (amplitude versus frequency) were made from an oscilloscope display of each event as well as before and after burn-through.

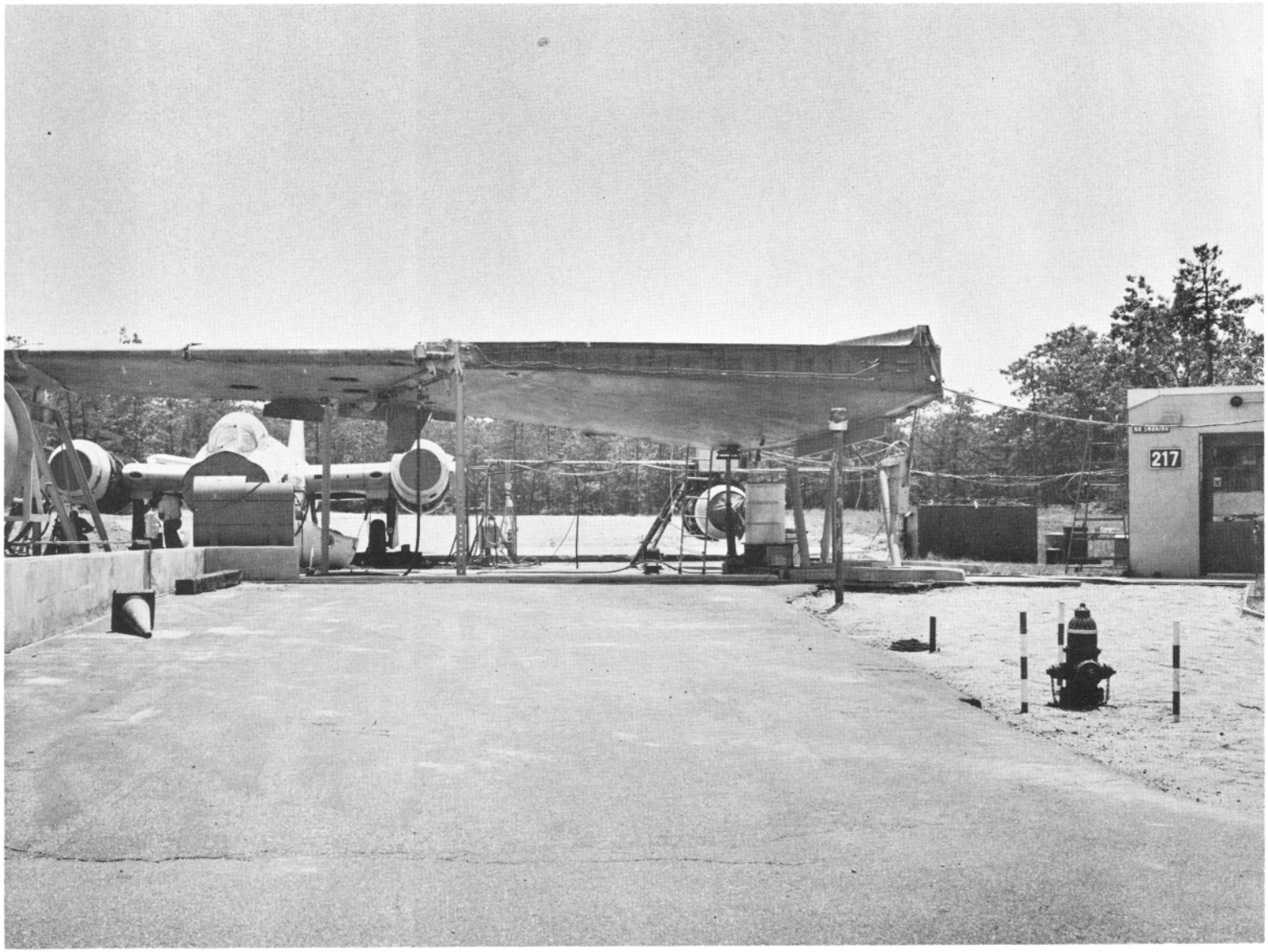

Figure 1-1. NAFEC Jet Engine Test Facility

2.0 ENGINE TESTS AND RECORDING INSTRUMENTATION

2.1 General

Two primary types of tests were run on each type engine. They were constant aperture tests and burn-through tests. In the constant aperture tests the engine was run at three different diffuser case pressure levels with 0.75, 1.0, and 1.5 inch orifices representative of engine burn-through failures. For purposes of comparison, a closed orifice test was run representing normal engine operation. The three diffuser case pressures for the J-47 engine were:

(1) 46 in. Hg gage 70% RPM

(2) 70 in. Hg gage 80% RPM

(3) 97 in. Hg gage 90% RPM

The three diffuser case pressures for the J-57 engines were:

(1) 150 in. Hg gage 82% RPM

(2) 240 in. Hg gage 90% RPM

(3) 270 in. Hg gage Maximum power.

Diffuser case pressures and approximate equivalent RPM will be used synonymously throughout this report. The fixed and closed orifice tests served to produce a steady state sound pressure level and acoustic spectrum.

In the burn-through tests, the same orifice size (1.5 inch) was always used, but the modified burner can hole was capped. The J-47 engine was capped with a 0.1-inch thick lead plate to facilitate rapid burn-through. The J-57 engine modified burner can was capped with 0.062-inch thick aluminum and the cowling was covered with 0.050-inch thick aluminum. Burn-through was created on both engine types by running the engine to speed and turning on the fuel to the modified burner can. The hot flame and gasses burned through the cap creating the dynamic characteristics of a burn-through. In the J-57 engine, the flame burned through the cap and the cowling.

A third test, which created a burn-through similar to those experienced by operational aircraft, was run with a 0.040-inch hole drilled in the primary and secondary fuel lines between the No. 7 and No. 8 fuel nozzle clusters. The fuel in the No. 8 nozzle cluster and the release of fuel in the altered fuel lines was controlled by shut-off valves installed in the lines. The engine was run to speed and the valves opened to release the fuel and cause burn-through. This simulated a burn-through caused by a cracked fuel line or fuel manifold.

A series of tests were also run to determine the interference effect of extraneous engine noise on the engine under test. This was accomplished by installing microphones on the center test engine (J-57 engine; see Figure 1-1). The J-47 engine to the left and then the J-57 engine to the right were run to speed while the center test engine was quiet. These tests established an interference standard. In addition, a burn-through test was run on the center test engine while the J-47 engine was running at maximum RPM.

In every test, five microphones were employed for data collection. One broadband instrumentation microphone and four general-purpose microphones were used. The former was a Bruel and Kjaer (B & K) Model 4138 with specifications as outlined in Appendix E. The general purpose microphones were Shure Model 515SB low impedance types also specified in Appendix E.

In general, the B & K microphone was placed close to the modified burner can orifice in order to detect any characteristic high frequency discrete or broadband random noise energy that might emanate from that source. The Shure microphone, in addition to detecting characteristic discrete frequencies and broadband noise, were used to determine the effects of distance from the orifice by comparing the relative sound pressure levels, and were strategically located about the engine. At least one, however, was always in close proximity to the modified burner can orifice.

During the course of each constant orifice event (here defined as one engine run from start to shut down), the microphone output voltages were measured and recorded at each engine speed. Attempts were also made to measure the output level during each burn-through event (before and after burn-through), but were not always successful due to rapid burn-through. The readings thus taken were indicative of the sound pressure level at the specific microphone locations.

Processing of the taped data by real time spectrum analysis and broadband energy detection produced results that provide answers to the questions set forth earlier. That is, the frequency spectrum is clearly evident from the spectrum analysis spectrograms. Relative power levels are easily determined from the mean square analysis recordings and the microphone output readings allow correlation of the relative measurements with actual sound pressure levels at the microphones.

2.2 Recording Instrumentation

Figure 2-1 is a block diagram of the electrical equipment used to monitor, record, and play back engine data during the recording phase of the program. The Shure type 515SB microphones were connected by 125 feet of shielded pair cable to a buffer amplifier with a differential input. The cable capacitance of approximately 18 pF per feet (2200 pF total) shunting the microphone coil (150 ohm resistive) produced a negligible low-pass filtering effect with a corner frequency of 500 kHz.

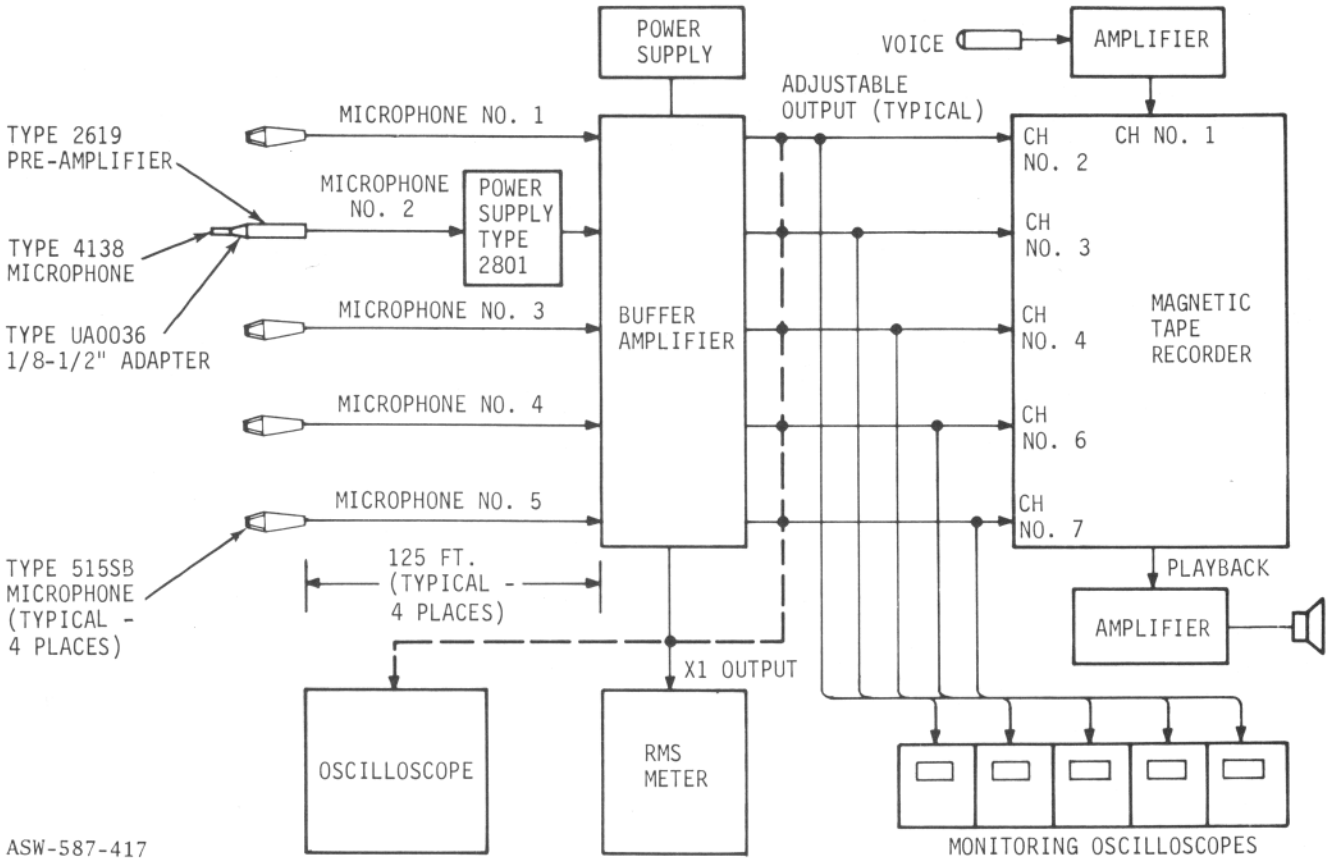

Figure 2-1. Recording, Monitoring, and Playback Equipment Block Diagram

The connections for the B & K microphone are shown in Figure 2-1. The type 4138 cartridge and the type 2619 preamplifier (a FET follower amplifier) form a single unit connected to the type 2801 power supply (for the preamplifier) by 95 feet of cable. In addition to the signal lines, the cable also carries the preamplifier power line, the cartridge bias voltage, and a ground.

The type 2801 power supply also contains a buffer amplifier with a 50 ohm output impedance. This amplifier and its output transformer introduce a loss of 16 dB to the incoming signal. The loss is recovered, however, in the buffer amplifier (Figure 2-2) following the type 2801 power supply. All other connections and equipment are the same as was used for the other microphones.

The B & K microphone was connected to recorder channel 3 for all events up to and including a fire on the starboard J-57 engine. The microphone connecting cable was destroyed by the fire and the microphone was damaged. (See Figures 2-3 and 2-4.) Following the fire, the B & K microphone was replaced by a Shure 515SB microphone since a replacement could not be obtained in sufficient time to meet the schedule.

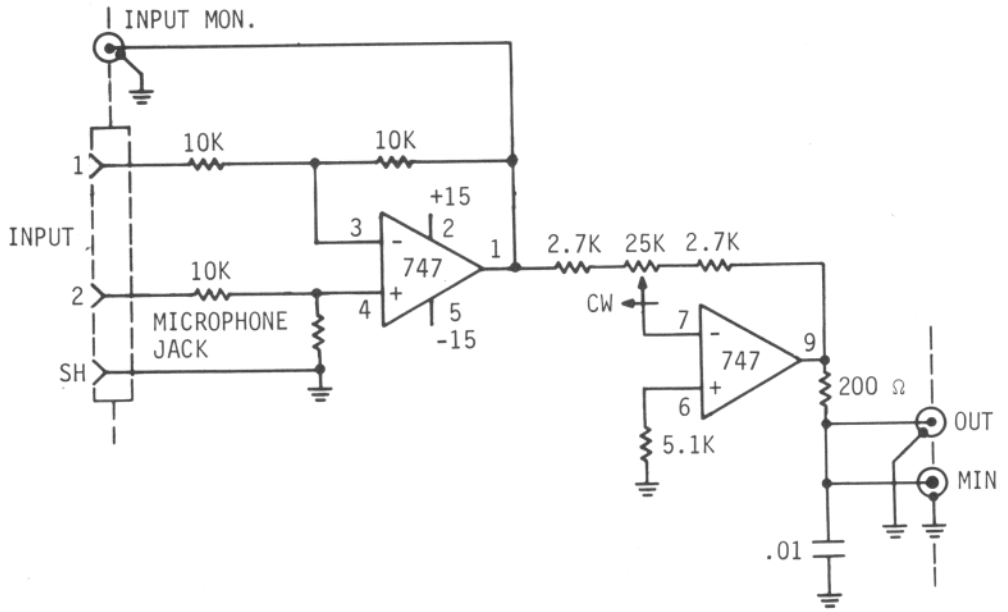

Figure 2-2. Buffer Amplifier

Recorder channels 2, 4, 6, and 7 were connected to Shure 515SB microphone for all tests. However, channel 2 and 6 microphones were also damaged during the fire and were replaced for subsequent tests.

2.3 Microphone Locations

2.3.1 J-47 Engine

The microphones were installed on the J-47 test stand support structure as shown in Figure 2-5. Distances from the modified burner can orifice are as noted on the diagram. Figure 2-6 is a photograph of the installation showing the arrangement more clearly.

2.3.2 J-57 Port Engine

The microphones were installed on the engine housing as shown in Figure 2-7 with distances from the modified burner can orifice as indicated. The installation is also pictured in Figures 2-8, 2-9, and 2-10.

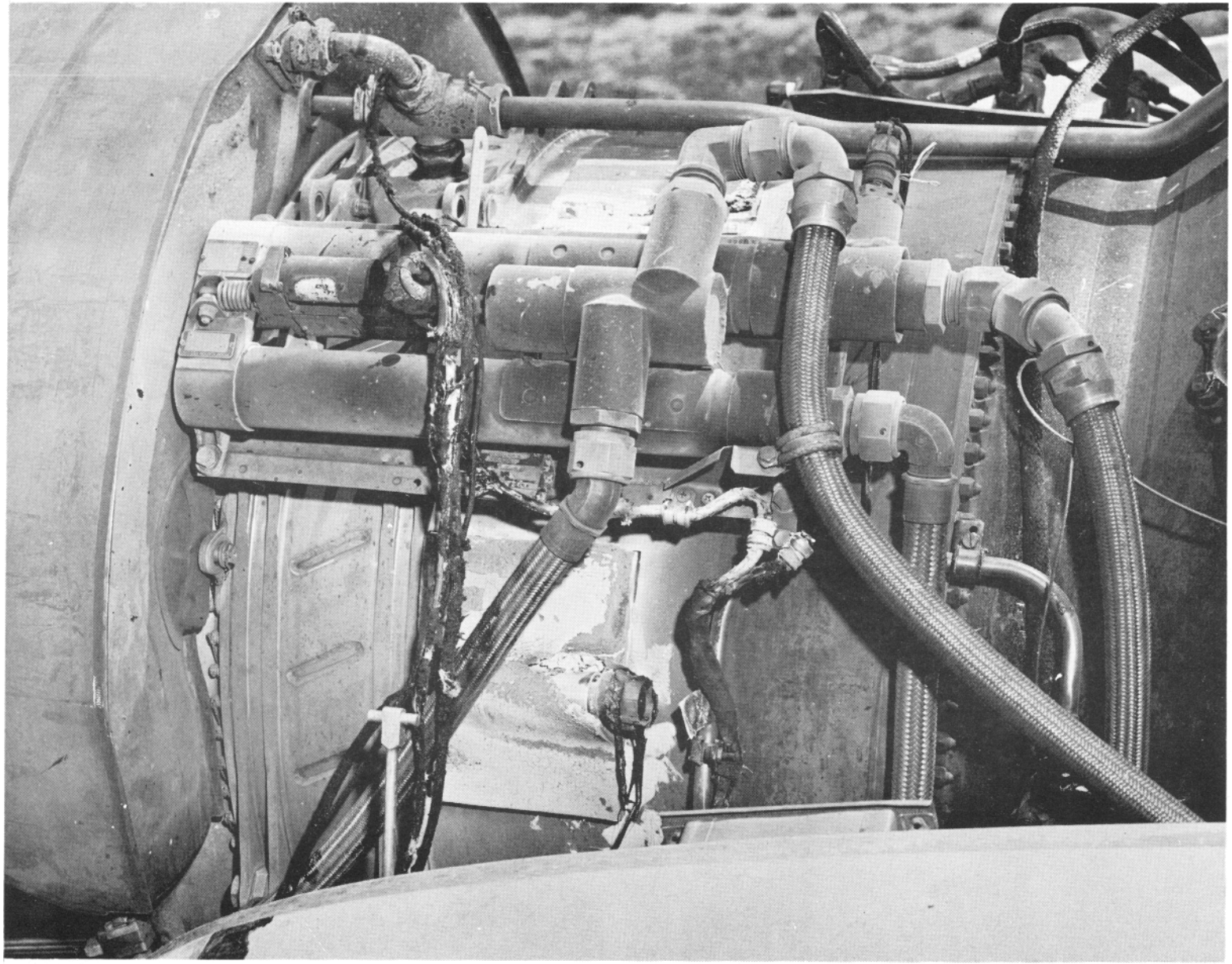

Figure 2-3. Microphone No. 2 (Upper Center) and Microphone No.4 (Bottom Center) After Flash Fire

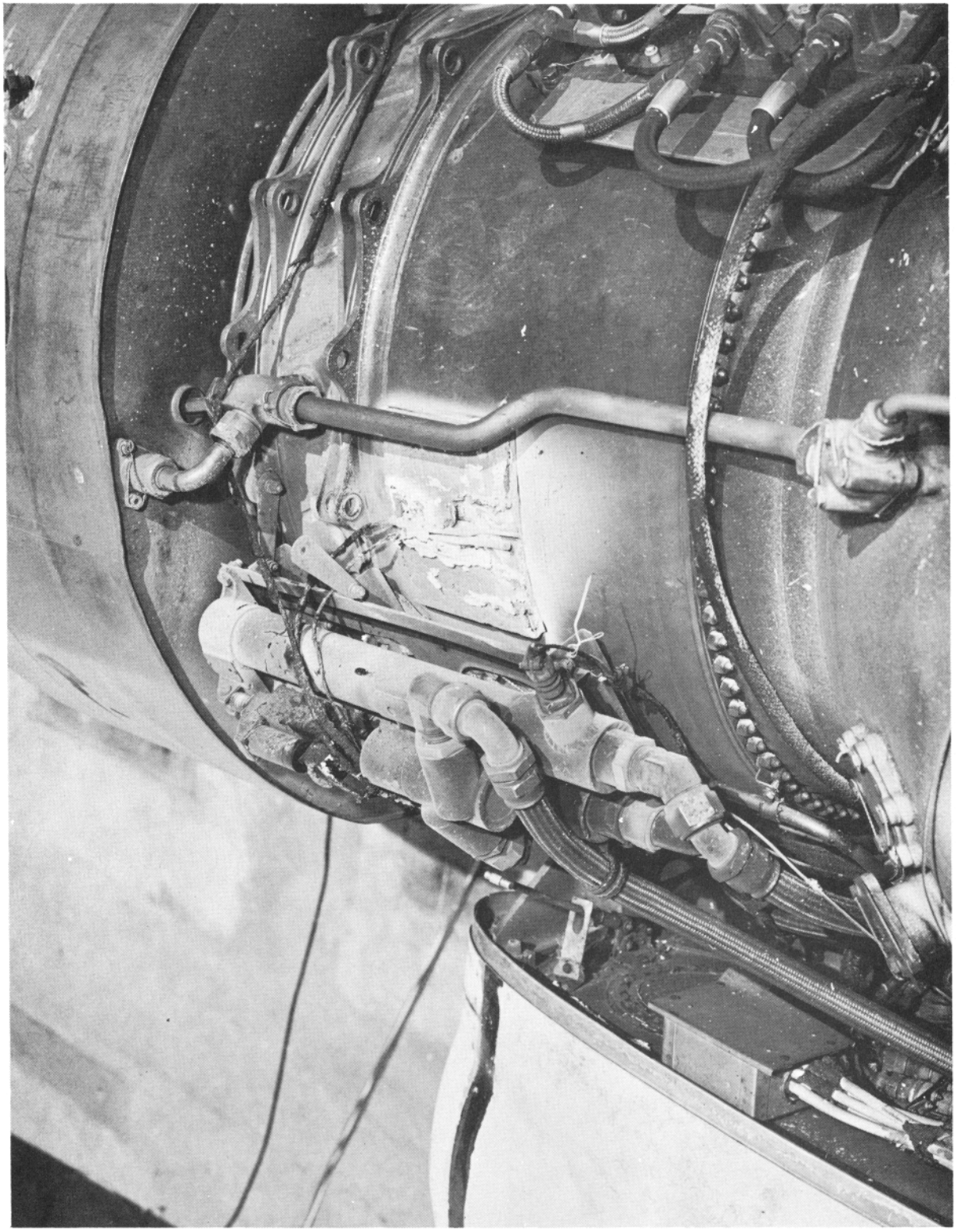

Figure 2-4. Microphone No. 2 and a NAFEC Instrumentation Microphone After Flash Fire

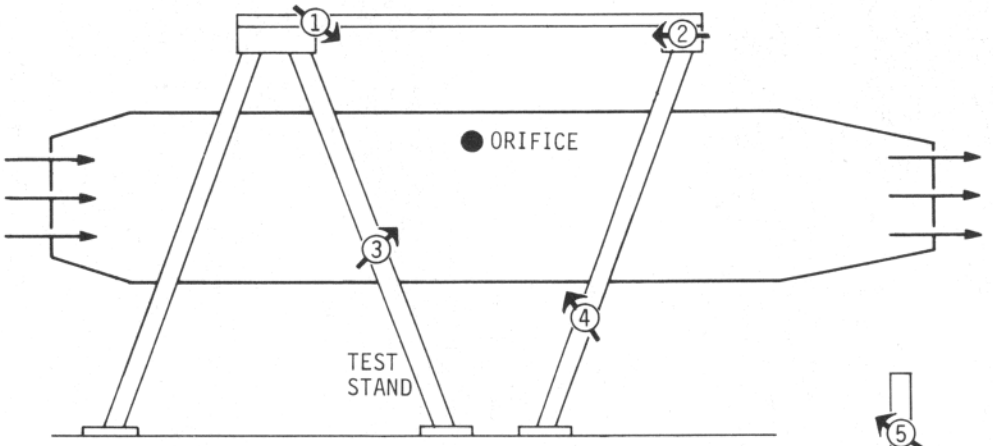

MICROPHONE DISTANCES FROM
ORIFICE IN MODIFIED BURNER CAN

MICROPHONE NO. 1 - 30¼"
MICROPHONE NO. 2* - 28"
MICROPHONE NO. 3 - 22½"
MICROPHONE NO. 4 - 50"
MICROPHONE NO. 5 - 12' 9"

} SHORTEST PATH

*B & K TYPE 4138, THE BALANCE ARE SHURE 515SB

ASW-587-421

Figure 2-5. Diagram of Microphone Locations on the J-47 Test Stand

2.3.3 J-57 Starboard Engine

Two installations were used on the J-57 starboard engine. Figure 2-11 shows location of the microphones for reel 2, event 6 only, with distances from the modified burner can orifice. The second installation and the distances from the burn-through area are shown in Figure 2-12. This installation was used for reel 3, event 6 only.

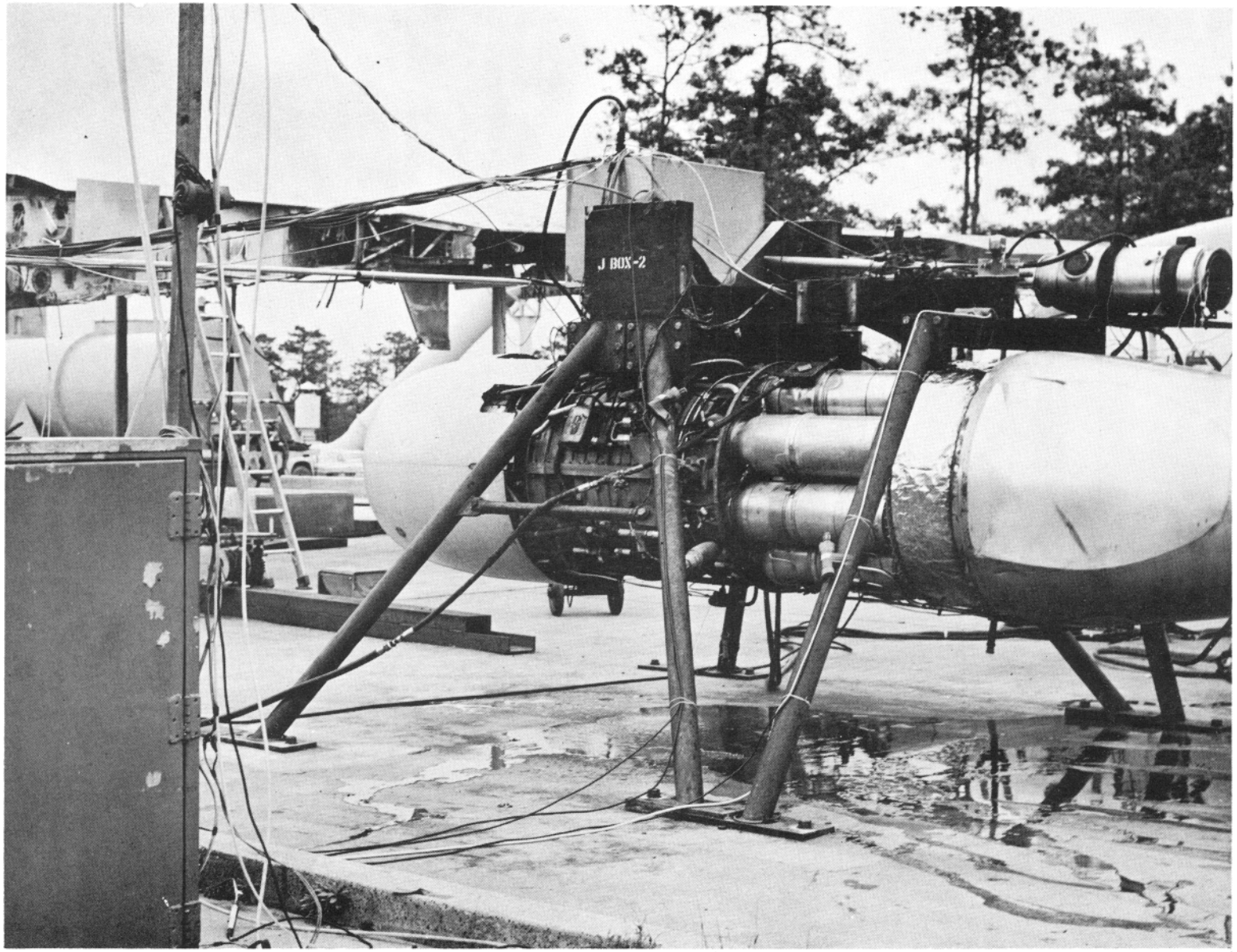

Figure 2-6. Microphones Installed on the J-47 Test Stand and on a Nearby Post

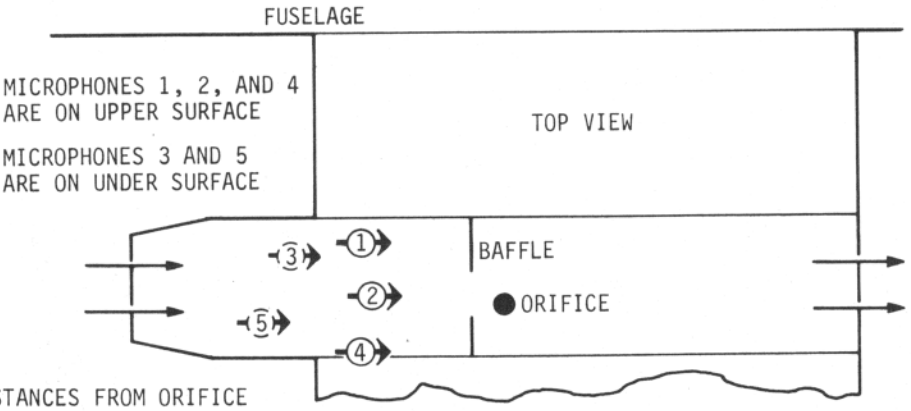

MICROPHONE DISTANCES FROM ORIFICE
IN MODIFIED BURNER CAN

MICROPHONE NO. 1 - 43"
MICROPHONE NO. 2* - 29"
MICROPHONE NO. 3 - 85"
MICROPHONE NO. 4 - 34"
MICROPHONE NO. 5 - 79"

} SHORTEST PATH

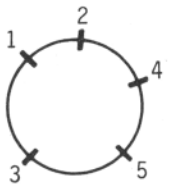

FRONT VIEW

*B & K TYPE 4138, THE BALANCE ARE SHURE 515SB.

NOTE 1: MICROPHONES NO. 1, 2, AND 4 REPLACED AS NOTED IN THE TEXT AFTER ENGINE FIRE.

NOTE 2: DISTANCE FROM ORIFICE TO J47 EXHAUST PORT - 19'
DISTANCE BETWEEN J57 ENGINES - 31'

ASW-587-423

Figure 2-7. Diagram of Microphone Locations on the J-57 Port Engine Housing

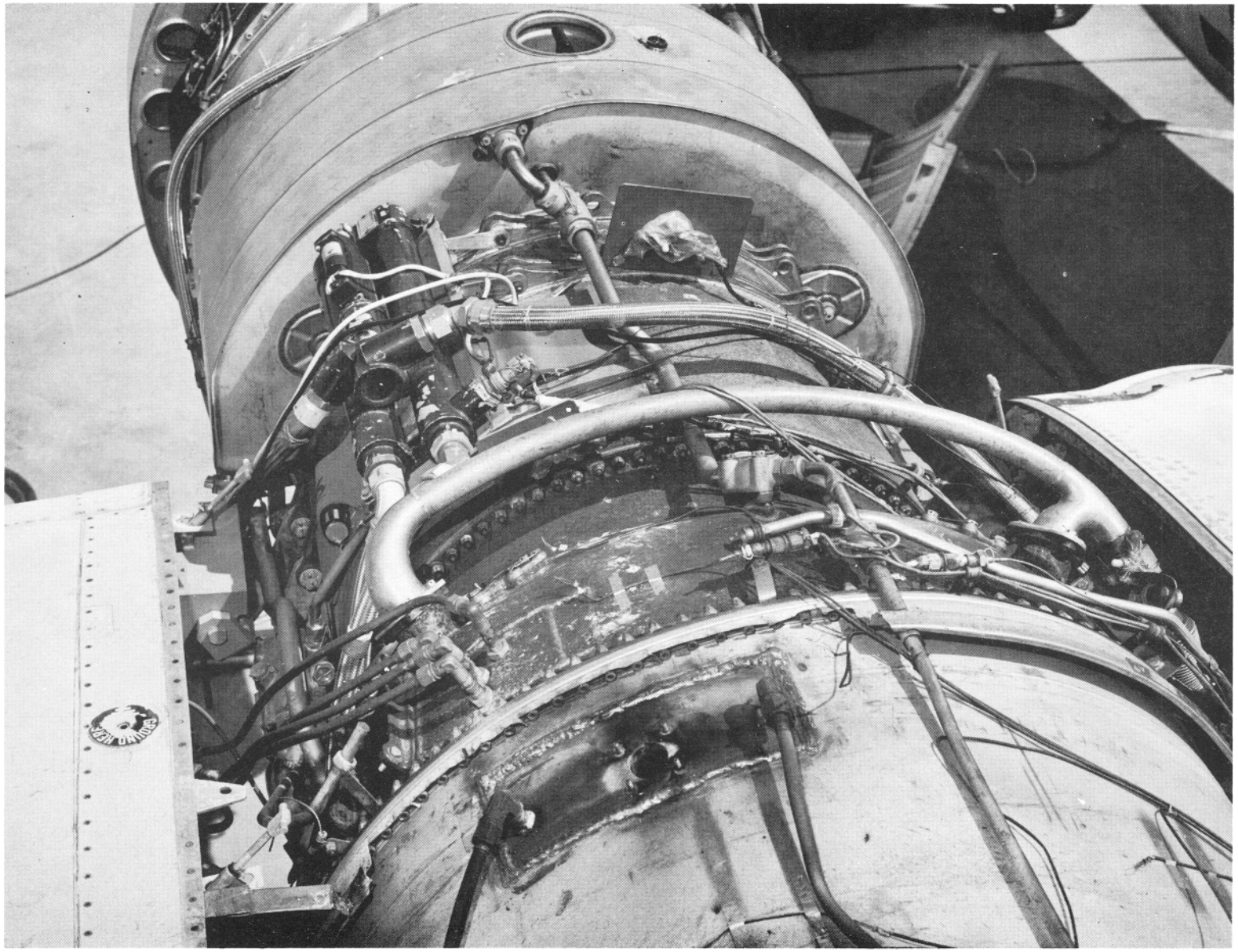

Figure 2-8. Microphone 1, 2, and 4 Mounted on the Housing of the J-57 Port Engine

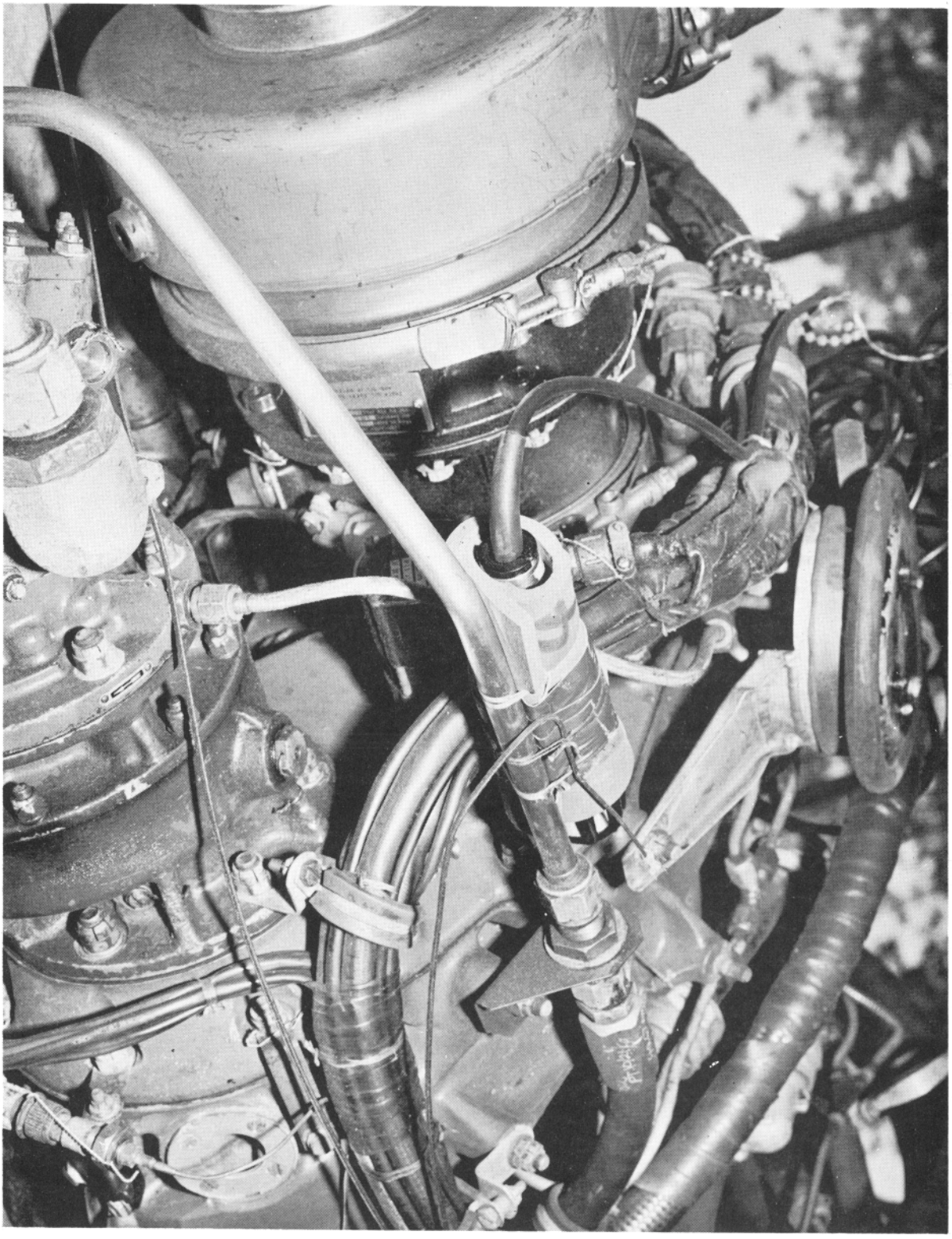

Figure 2-9. Microphone No. 3 Mounted on the J-57 Port Engine

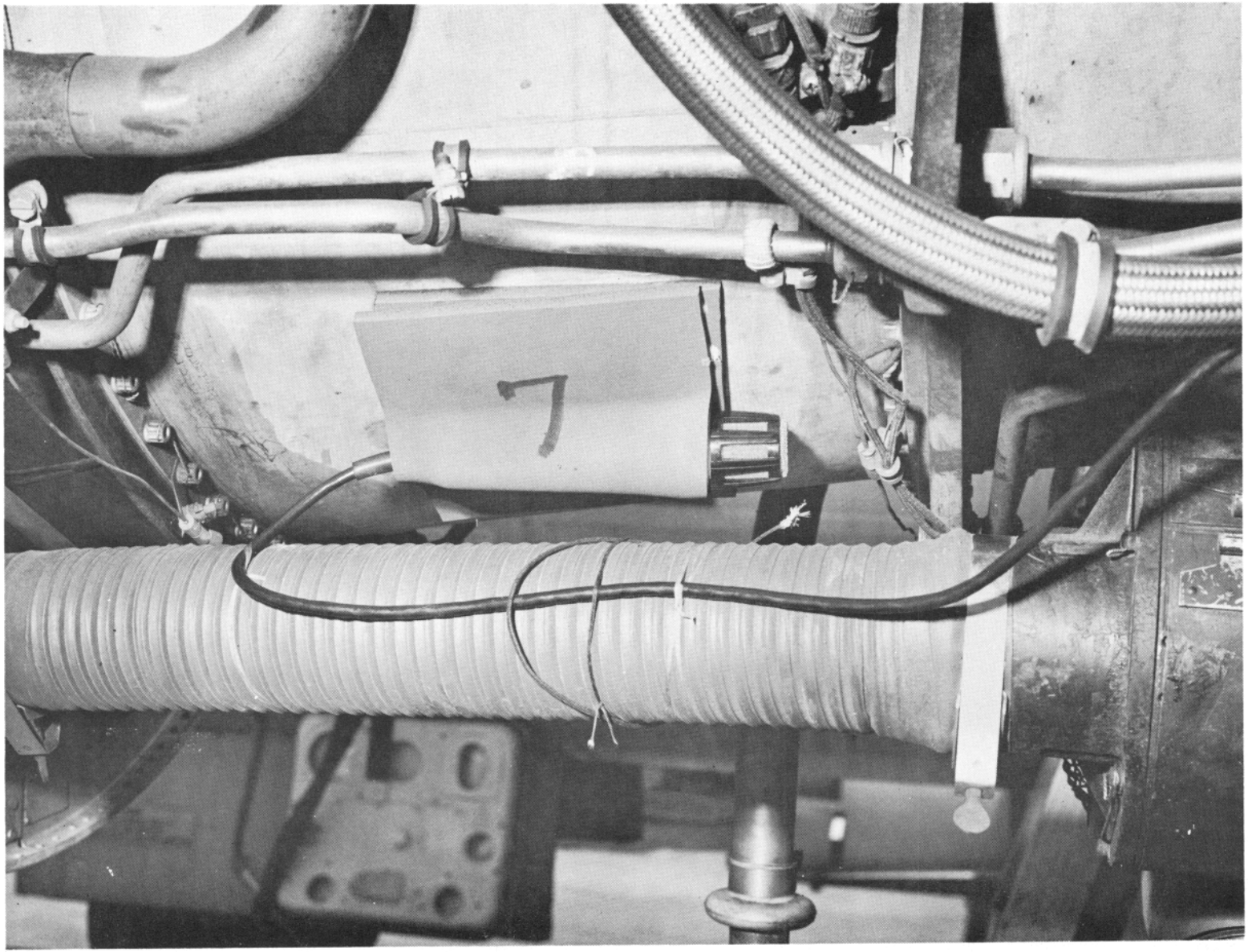

Figure 2-10. Microphone No. 5 Mounted on the J-57 Port Engine

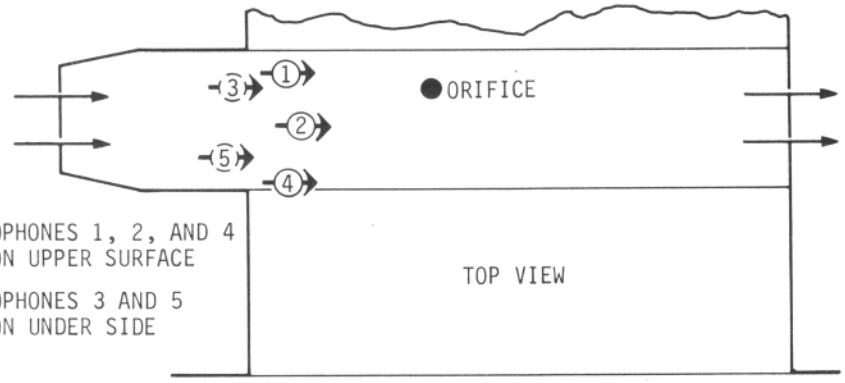

MICROPHONE DISTANCES FROM ORIFICE IN MODIFIED BURNER CAN.

MICROPHONE NO. 1	32½"	SHORTEST PATH
MICROPHONE NO. 2*	29"	
MICROPHONE NO. 3	51"	
MICROPHONE NO. 4	42"	
MICROPHONE NO. 5	79"	

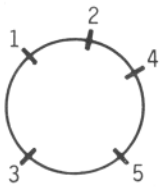

*B & K TYPE 4138, THE BALANCE ARE SHURE 515SB

ASW-587-427

Figure 2-11. Diagram of the Location of Microphones on the J-57 Starboard Engine Housing

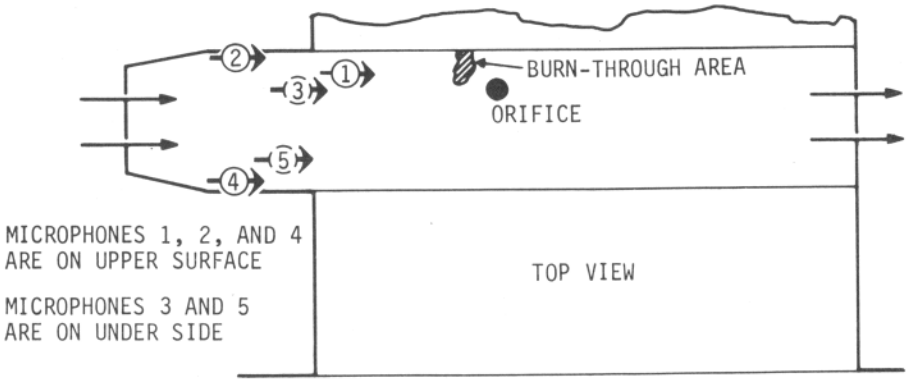

MICROPHONE DISTANCES FROM ORIFICE
IN MODIFIED BURNER CAN

MICROPHONE NO. 1 - 33"
MICROPHONE NO. 2 - 66"
MICROPHONE NO. 3 - 85"
MICROPHONE NO. 4 - 76"
MICROPHONE NO. 5 - 79"

} SHORTEST PATH

ALL ARE SHURE 515SB

ASW-587-428

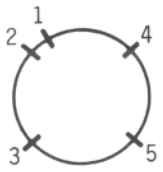

FRONT VIEW

Figure 2-12. Diagram of the Location of Microphones on the J-57 Starboard Engine Housing for Fuel Line Failure Test

3.0 DATA REDUCTION METHODS AND INSTRUMENTATION

Two methods of data reduction were used for analysis of the recorded signals: real time spectrum analysis and broadband energy detection.

3.1 Real Time Spectrum Analysis

With this processing mode, a plot of intensity (amplitude) versus frequency versus time is generated to show the spectral content of the signal as a function of time. Figure 3-1 is a diagram of the data processing instrumentation.

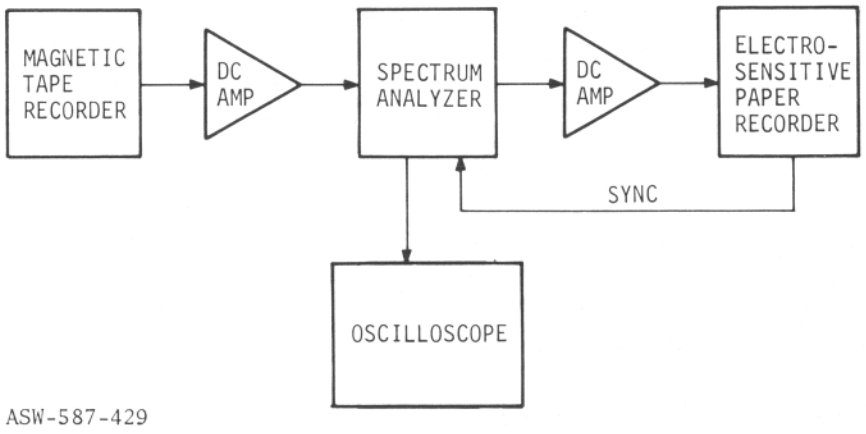

Figure 3-1. Real Time Spectrum Analysis and Recording Instrumentation Block Diagram

The tape recorder is operated in the reproduce mode. One channel at a time is analyzed by the real time spectrum analyzer and the intensity output of the analyzer modulates the recording pen write voltage as the pen sweeps across the recorder paper.

The analyzer operates on a frequency band extending from dc to 10 kHz. It analyzes this band in 20-Hz increments by rapidly scanning a stored replica (8-bit quantized) of 50 ms of the input signal. Using digital frequency multiplication techniques, the analyzer determines the amplitude of each 20-Hz segment in 0.1 ms and thus searches the whole 10-kHz band in 5 ms. With this method, no portion of the input signal is ignored while another segment is being analyzed since the analyzer completely reduces each 50 ms input segment in 50 ms.

The paper recorder triggers the analyzer spectrum search each time one of three pens starts to sweep across the chart paper. Thus, as the analyzer puts out an intensity voltage as a function of frequency, the recorder writes the amplitude as a dark spot on the paper. Signal frequency

thus corresponds to pen position. The chart paper is continuously advancing at a rate of 0.0465 inch per second and each successive pen sweep is written next to the previous one.

In addition to the electrosensitive paper recording or spectrogram generated in this manner, each 50 ms sweep of the analyzer is displayed on an oscilloscope. Photographs made from this display give an XY plot of amplitude versus frequency.

In order to cover the full 40-kHz spectrum recorded on channel 3 with the instrumentation microphone, the tape recorder played back the data at ¼ of the record speed or 3 3/4 ips. In effect then, the frequency spectrum of the recorded signal was divided by four and the analyzer processed a 0- to 40-kHz real signal band although it was operated at its maximum bandwidth of 10 kHz. The analysis resolution was also multiplied by four so that the resolution is 80 Hz. Channels 2, 4, 6, and 7 were analyzed at ½ speed for an effective band coverage of 20 kHz with a resolution of 40 Hz.

The 125 spectrograms generated in this manner provide sufficient data to analyze the acoustic spectra of steady state tests and burn-through failures. In particular, the spectrograms give a good indication of the bandwidth and nature of the acoustic spectrum most likely to produce reliable burn-through indication signals.

3.2 Broadband Energy Detection

This processing technique produces a paper recording of the mean square value of the signal level in a broad frequency band. Two such bands were analyzed for each recorded signal using the instrumentation shown in Figure 3-2.

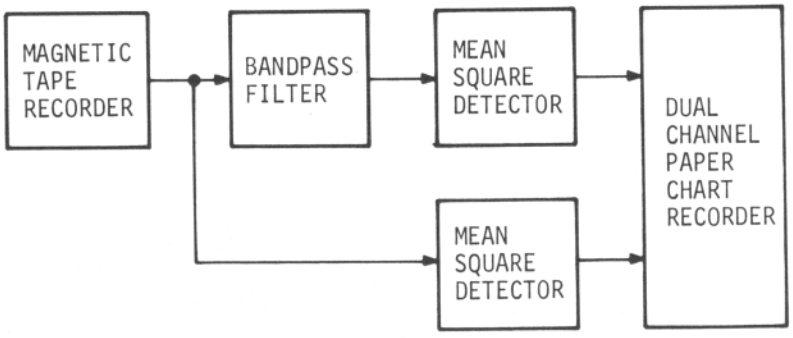

Figure 3-2. Mean Square Detection and Recording Instrumentation Block Diagram

The signal was analyzed in its unfiltered form (limited in frequency only by the microphone response) and also analyzed after bandpass filtering from 5 to 20 kHz. The two analyzer outputs were then recorded on a dual channel paper chart recorder for direct comparison. The plots represent the relative average power level at the microphone. All charts were recorded at a speed of 1 mm/sec and sensitivity scale at 2 V/cm.

Comparison of the average power plots with corresponding spectrograms reveals the spectral power density distribution more clearly. In several instances, as discussed in a later section, it was noted that engine machinery produced signals having sound pressure levels as high as those caused by burn-through failures. Cross correlating filtered and unfiltered data shows that methods of discriminating against interferring signals are available.

Finally, correlation of the average power grams with sound pressure level data derived from microphone output voltage readings provides a means of relating the grams for different microphone positions. It also gives insight into the relation of sensor location in reference to the orifice.

4.0 DATA REDUCTION RESULTS AND ANALYSIS

All pertinent processed data in the form of spectrograms, spectrum photographs, energy grams, and sound pressure level tables appear in Appendix A through D. In many cases, only a representative section of a gram was used because of space limitation. The J-57 port engine tests were instrumented with either a combination of the broadband instrumentation microphone and the general-purpose microphones or with just the general-purpose microphone.

As noted earlier in the text, a fire destroyed the instrumentation microphone before tests were completed making it necessary to substitute a general purpose microphone for the instrumentation microphone. As a result, there is mixed data in the fixed orifice test for the J-57 port engine. Instrumentation microphone data was used whenever possible to take advantage of the broadband characteristics of this sensor.

Analysis of the reduced data showing significant trends and supporting conclusions responsive to the original objectives of the program is given in the following paragraphs. The broadband instrumentation microphone data was used except as noted.

4.1 Acoustic Spectrum

Figure 4-1 is a composite of spectrum analysis grams made from the J-47 engine tests at 90% RPM. The figure shows the spectrum with the orifice closed, with a 0.75-inch orifice, and a 1.5-inch orifice. The closed orifice is representative of an engine operating normally and the open orifices are representative of a failure mode. These grams are typical of the acoustic spectrum of the J-47 engine for closed and open orifice conditions. Only spectrum intensity changes are evident when the engine speed is changed.

Discrete frequencies are visible on the closed orifice gram up to 27 kHz. It should be noted that discrete frequency lines are visible up to 35 kHz on some grams shown in Appendix A and B. Strong discrete frequency lines are present at 8 and 10 kHz. The discrete frequency lines are due to engine machinery such as pumps, bearings, etc. With the orifice open, these discrete frequencies are masked out by complex nonperiodic signals or random noise which is present in varying degrees across the entire processing bandwidth (0 to 40 kHz).

Figure 4-2 shows photographs of the same series of tests with a single 50 ms segment (amplitude as frequency) of the processed data frozen on the oscilloscope representative of a single line on the grams. The discrete frequency lines are always present but the noise signals, being of a random nature, change for every processing sweep. The photographs are therefore only relative indications of the processed spectrum as a whole. In order to segregate discrete frequencly lines, it is necessary to use the grams.

Figure 4-3 is a composite of spectrum analysis grams made from the J-57 port engine at maximum RPM. The figure shows the spectrum with the orifice closed, with a 0.75-inch orifice, and with a 1.5-inch orifice.

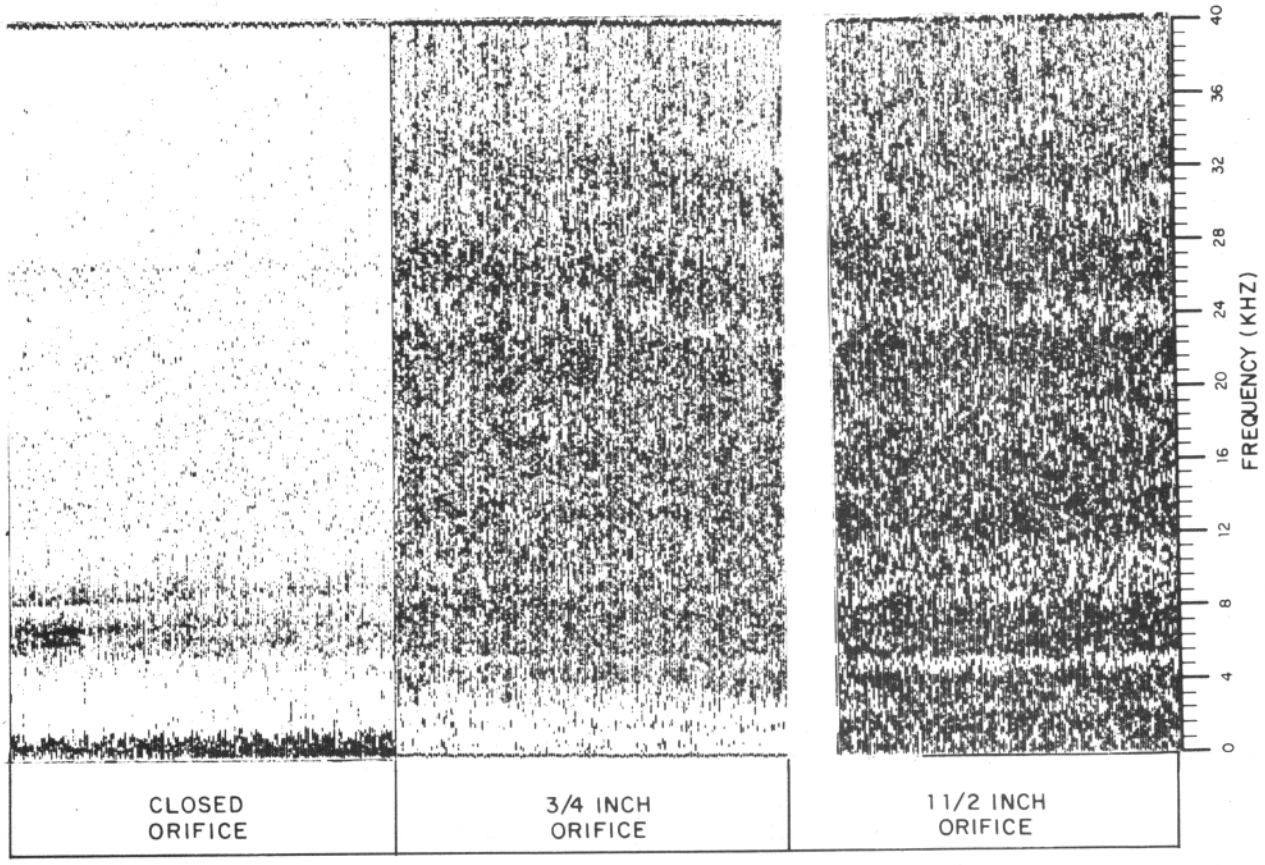

ASW-587-431

Figure 4-1. J-47 Engine Acoustic Spectra at 90% RPM

These grams are typical of the J-57 engine for open and closed orifice conditions. Only spectrum intensity changes are evident as a function of speed.

Discrete frequency lines in the closed orifice grams are less evident than on the J-47 engine. This is partially due to the J-57 engines being cowled and the J-47 engines being open. The lines that do appear are at 10 kHz and lower. At this engine speed and microphone location, the J-57 engine is quieter than the J-47 engine. The open orifice grams again contain random noise in varying degrees across the entire processing bandwidth, but are less intense than on those grams produced from J-47 engine data.

4.2 Characteristics of Burn-Through Failures

In order to determine the feasibility of detecting burn-through failures, it is necessary to understand the characteristics of burn-through, i.e., the spectral content, discrete frequencies, sound pressure levels, and any other factors which may be related to burn-through failure.

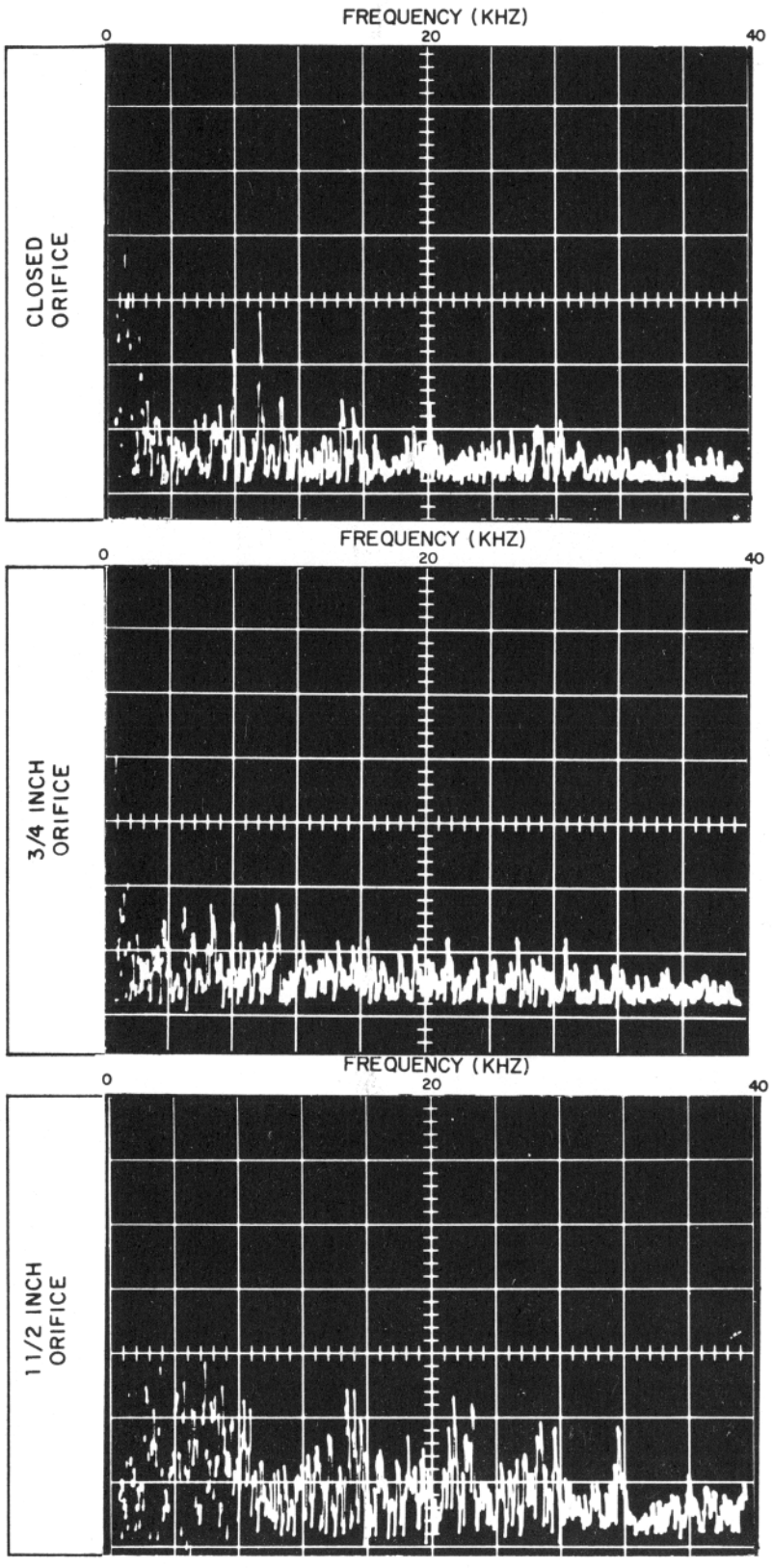

ASW-587-432

Figure 4-2. J-47 Engine Acoustic Spectra at 90% RPM

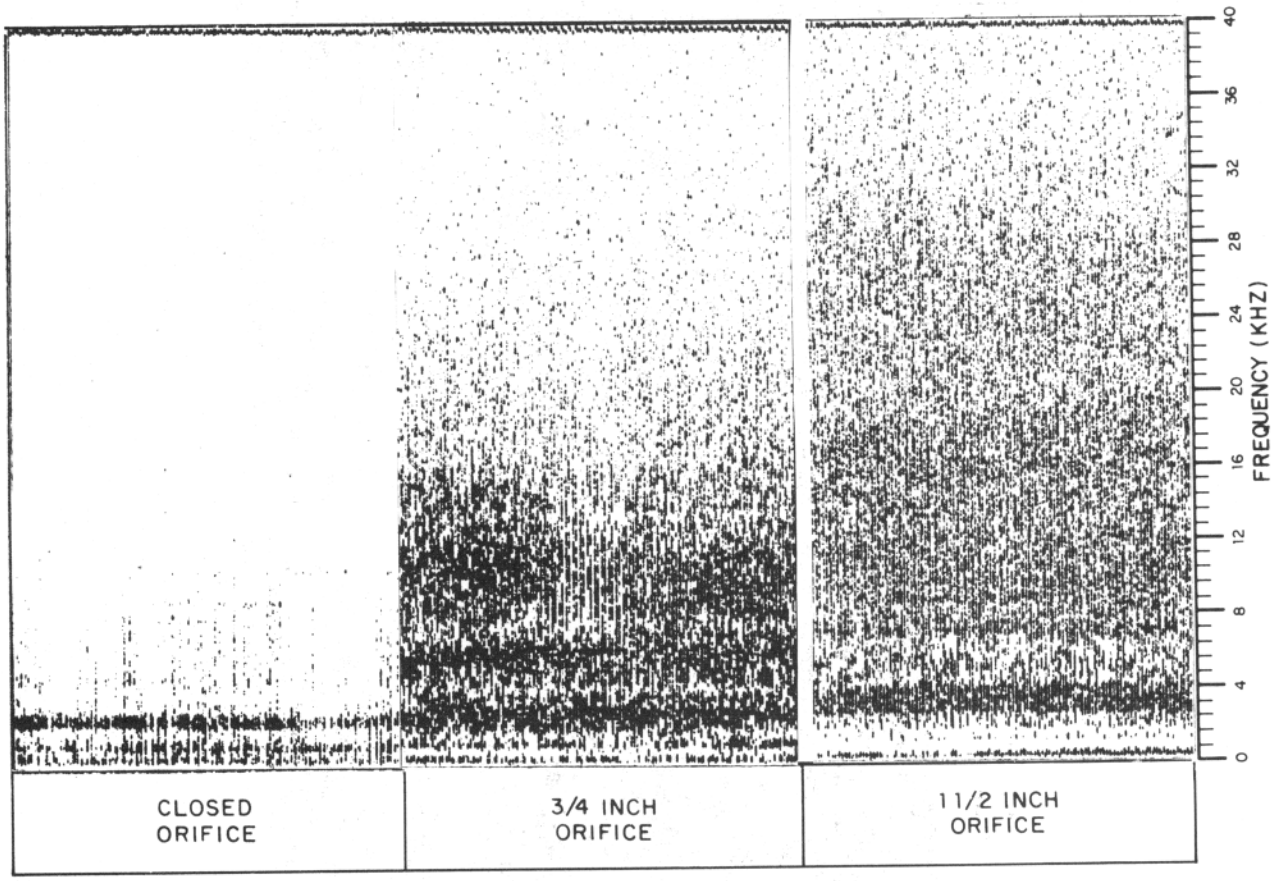

ASW-587-433

Figure 4-3. J-57 Port Engine Acoustic Spectra at Maximum RPM

Two types of tests were incorporated into the program to determine burn-through characteristics. One type is a series of steady state tests, discussed in detail later in the text, and the other type was simulated burn-through failures. The latter was achieved by modifying a burner can such that the flame was diverted toward the burner can wall. An orifice was built into the can to allow the diverted flame to spew through simulating a burn-through failure. The orifice was set inside a water jacket to prevent the flame from destroying it. By capping the orifice with a plate bolted to the can and controlling the fuel to the can, and hence the intensity of the flame, a burn-through was simulated. The engine was run to speed and the fuel and flame turned on causing the metal cap to burn away. Tests were performed on both the J-47 and J-57 engines in this manner.

The J-47 engine has a low pressure ratio. This factor, combined with the burner can modification, required that a cap made of material with a low melting point be used. A lead plate 0.1-inch thick satisified these conditions. Two simulated burn-through tests were run on this engine. Figure 4-4 and 4-5 show the spectrum and the mean square analysis chart of the same two microphones for each of the simulated burn-throughs. Inspection of the spectrum reduced from data recorded from

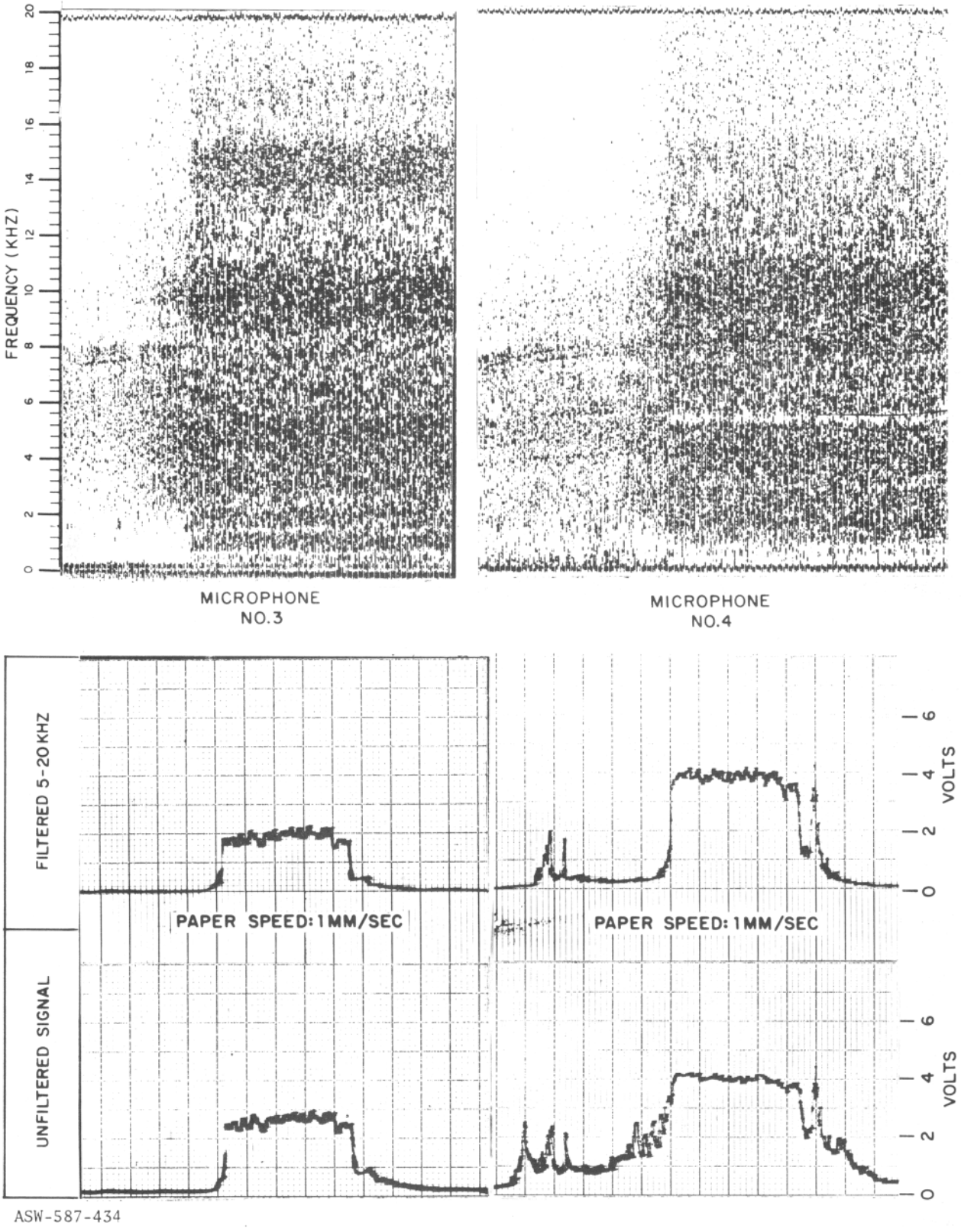

Figure 4-4. Burn-Through Failure No. 1 on the J-47 Engine (Sheet 1 of 2)

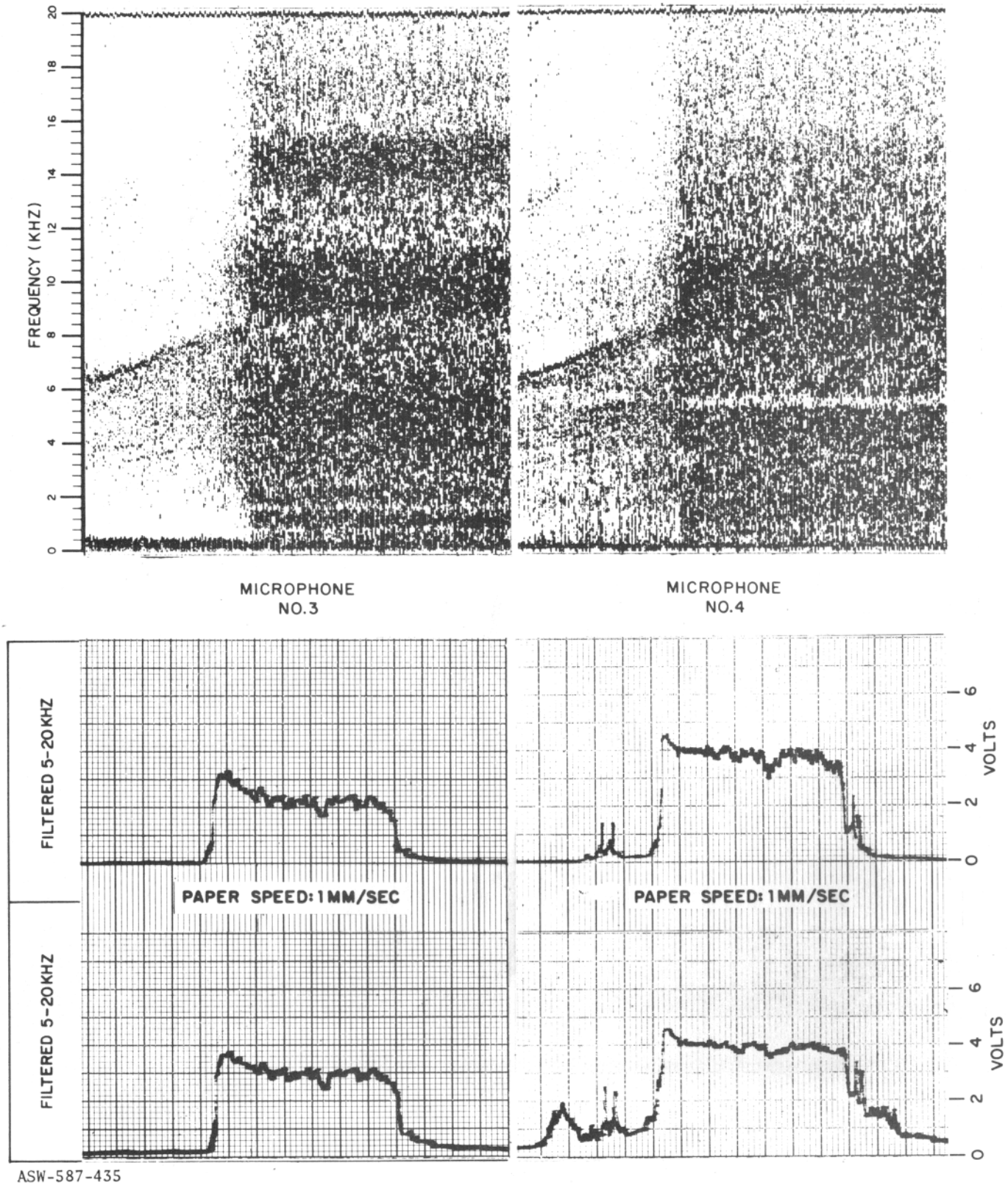

Figure 4-5. Burn-Through Failure No. 2 on the J-47 Engine

microphone No. 3 on Figure 4-4 indicates that as the engine gained speed, random noise as well as discrete frequency lines produced by the engine and auxilliary machinery (fuel pumps, oil pumps, etc.) were present. Random noise increased just prior to burn-through and at burn-through increased almost instantaneously to the full processed bandwidth of 0 to 20 kHz. The discrete frequency lines created by the engine were masked out by the intense random noise. The microphone sensed what appears to be two broad energy bands centered at 10 and 14.5 kHz each approximately 2 kHz wide.

Inspection of the No. 4 microphone gram indicates a slight difference in burn-through detection. More engine lines are present and random noise is more intense, covering a greater bandwidth prior to burn-through. At burn-through, the random noise appears less intense at higher frequencies and a discrete frequency line appears at 4.5 kHz. Figure 4-5 is similar to Figure 4-4. Each of the five microphones used in the test sensed the spectrum in a different manner. (Refer to Appendix A, Burn-Through No. 1 and Burn-Through No. 2 to review the grams for all five microphones.) There are no apparent discrete frequency lines associated with or characteristic to a simulated burn-through.

The recorded data (Figure 4-4) was simultaneously processed raw and filtered (5 to 20 kHz) using a mean square analysis technique. This technique sums the total spectrum resulting in a pair of traces showing relative energy levels at any given time. The unfiltered lower trace, processed from microphone No. 3, shows about 0.2 volt of amplitude prior to burn-through. At burn-through, the amplitude increases to approximately 2.25 volts in about two seconds. The upper trace shows that all of the spectral content prior to burn-through is below 5 kHz and after burn-through is primarily above 5 kHz. This is true for all simulated burn-throughs analyzed for this program with exceptions which will be noted in the text of this report.

Microphone No. 4 mean square traces have a greater amplitude than microphone No. 3 (4 volts as opposed to 2 volts for the filtered trace). Microphone locations, sensitivity, and distance from the orifice are all factors which affect the amplification or attenuation of sound. Microphone No. 4 also sensed frequencies above 5 kHz prior to burn-through as evidenced by the upper trace which shows about 0.2 volt steady state and two 2-volt spikes. These spikes or erratic frequency changes are usually due to momentary resonances created by engine machinery as the engine is run up to speed. As noted, they are not sensed by all microphones. The traces in Figures 4-4 and 4-5 are typical of burn-throughs for this engine.

Burn-through tests were run on the J-57 port engine in a manner similar to those on the J-47 engine. The J-57 engine, however, has a greater pressure ratio and a more intense flame which burned through higher temperature materials. A cap of 0.052-inch aluminum plate was used to cover the modified burner can orifice for this test. In addition, the J-57 engine

was cowled. A cutout was made on the cowling above the orifice and clinch-nuts mounted around its periphery to secure an additional 0.050-inch replaceable plate. A simulated burn-through on the engine burned through both the orifice plate and the cowling patch. Figure 4-6 is a photograph of the orifice and cowling rupture which occurred at 90% RPM simulating a burn-through.

Three tests were run to simulate burn-through failure on the J-57 port engine at 82%, 90%, and maximum RPM. Figure 4-7 and 4-8 shows the spectrum and the mean square analysis charts for all three runs as sensed by broadband instrumentation microphone No. 2. The grams are not unlike those produced by the J-47 engine, i.e., discrete engine frequency lines with light random noise followed by a heavy band of random noise at burn-through. The processing bandwidth for these grams is 0 to 40 kHz. The J-57 engine characteristics are noticeably different than those for the J-47 engine. Burn-through at each of the three engine speeds shows a multitude of discrete frequency lines at or below 12 kHz. These lines are most pronounced at 82% RPM and least pronounced at 90% RPM.

NOTE: The discrete frequency lines to the left of the 82% and maximum RPM tests are engine startup lines (idle). The burn-through on the three grams also varies. At 82% RPM the burn-through appears as a sharp change in random noise whereas the random noise change is more gradual at 90% RPM, but changes again appear to be sharper at maximum RPM.

Relating to the mean square analysis filtered traces, the time for burn-through at 82% RPM occurrs in a period of six seconds. The burn-through period at 90% RPM is four seconds and at maximum RPM, 2 seconds.

The mean square analysis traces for the 82% RPM test in Figure 4-7 vividly show the effect of filtering low frequency spectrum to aid in detecting burn-through failure. Prior to burn-through, the unfiltered trace has an amplitude equal to or greater than after burn-through. The high-pass 5 kHz filter removed the low frequency spectrum allowing only the high frequency spectrum to pass. Burn-through spectra has consistently been observed to consist primarily of frequencies above 5 kHz. Figure 4-9 shows the effect of filtering in greater detail for the 90% and maximum speed runs.

In addition to the burn-through tests discussed in the preceding paragraphs, the J-57 starboard engine was modified by drilling a hole 0.040-inch in diameter in the primary and secondary fuel lines between the No. 7 and No. 8 nozzle clusters. This modification resulted in a burn-through that very closely simulated a cracked fuel line or manifold failure. Figures 4-10 through 4-14 show the spectrum and mean square analysis traces for all five microphones. The burn-through detectability on the grams varies from gram to gram. Microphone No. 1, closest to the engine housing and cowling ruptures, detected the failure quite clearly. While it was apparent that the other microphone detected the failure in varying degrees, detection was dependent upon microphone location. (Refer to paragraph 2-3.)

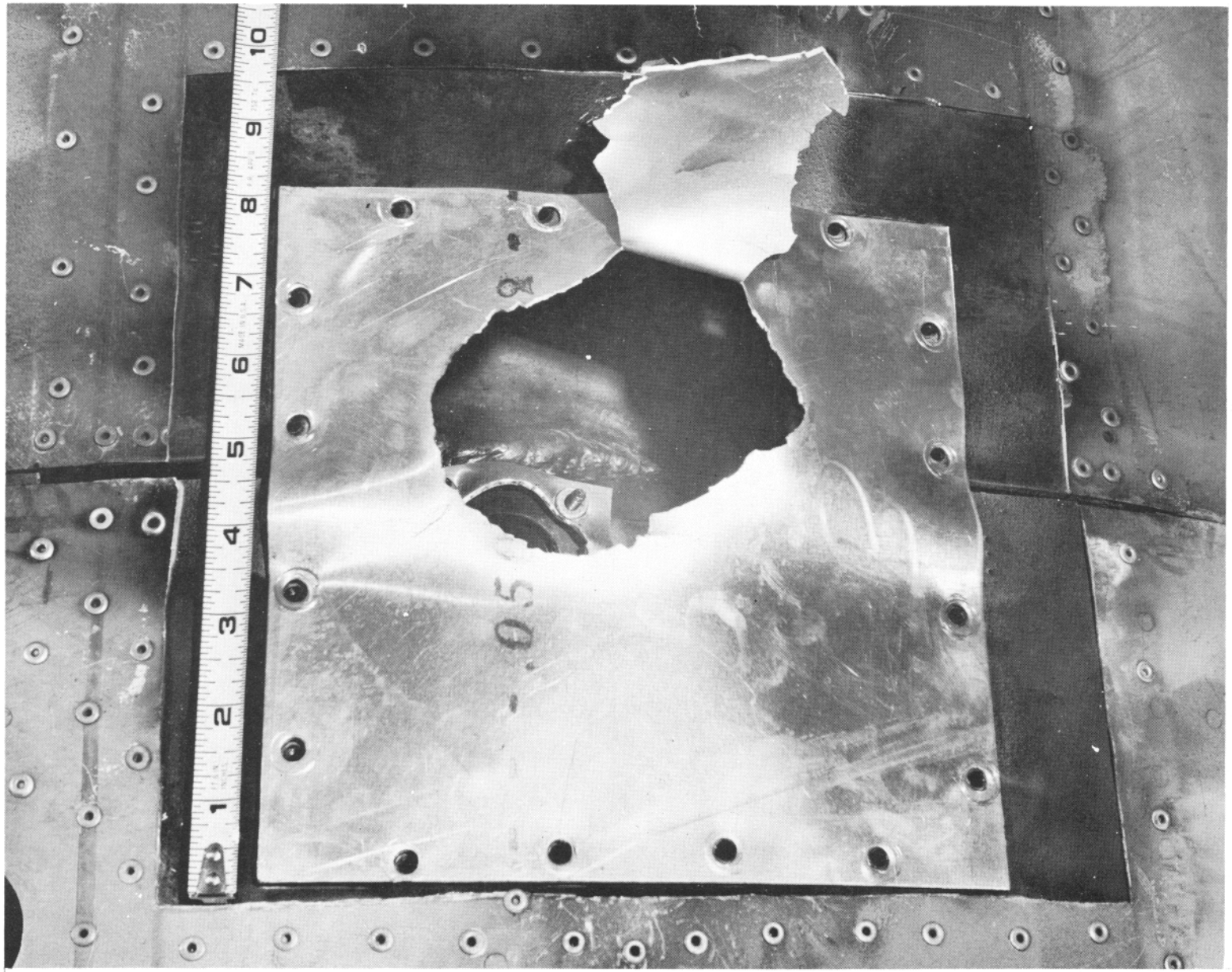

Figure 4-6. Ruptured Orifice Plate and Cowling Cover Due to Burn-Through Failure on the J-57 Port Engine

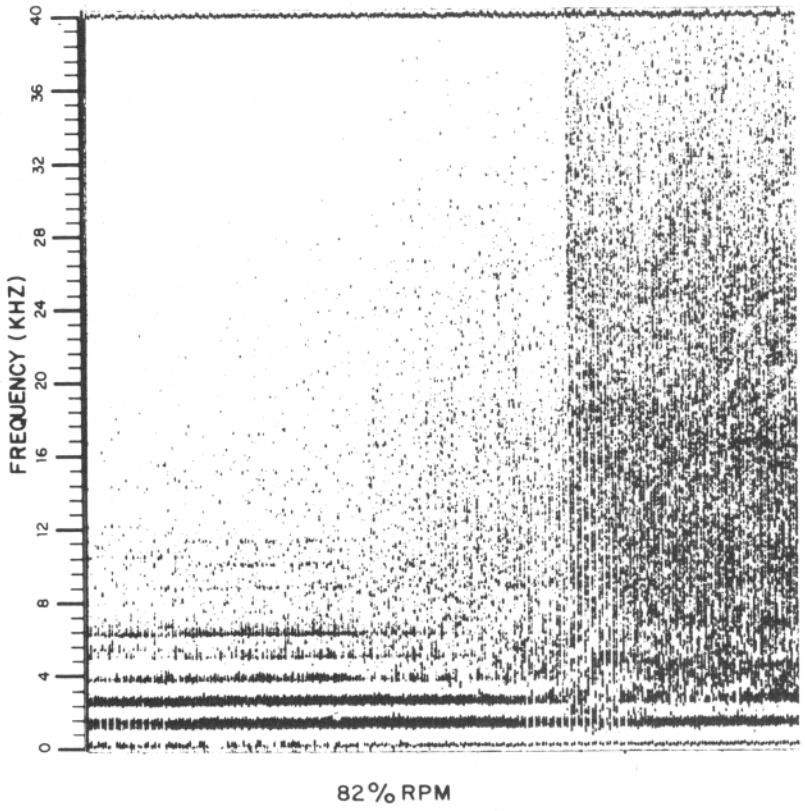

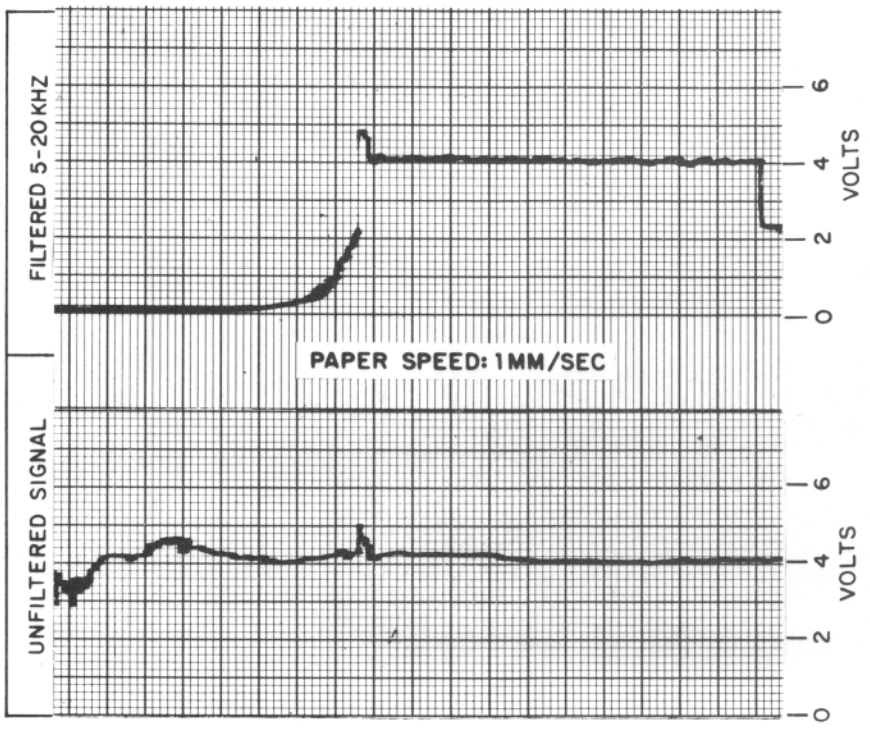

Figure 4-7. Burn-Through Failure on J-57 Port Engine at 82% RPM and 90% RPM (Sheet 1 of 2)

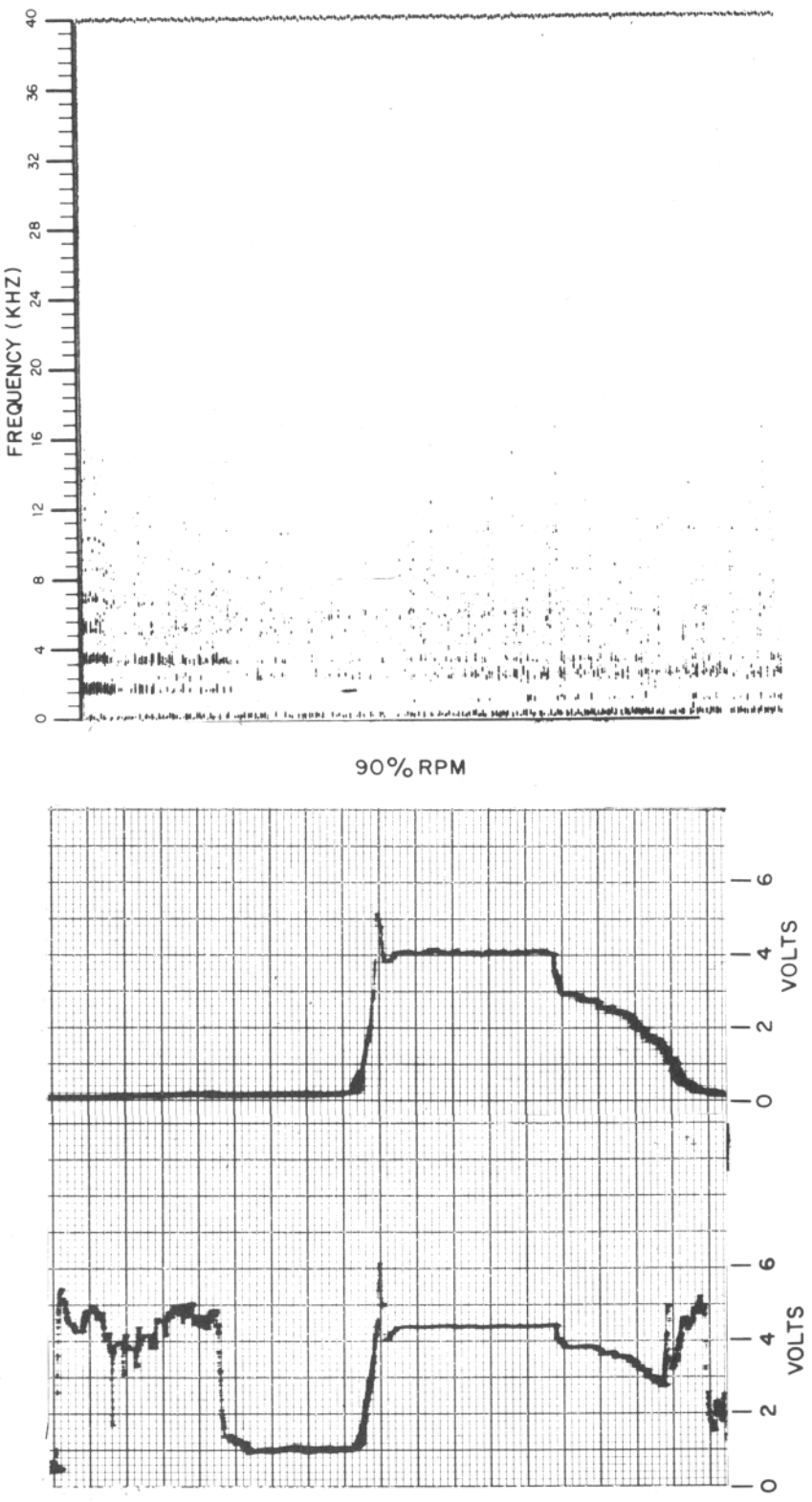

Figure 4-7. Burn-Through Failure on J-57 Port Engine at 82% RPM and 90% RPM (Sheet 2 of 2)

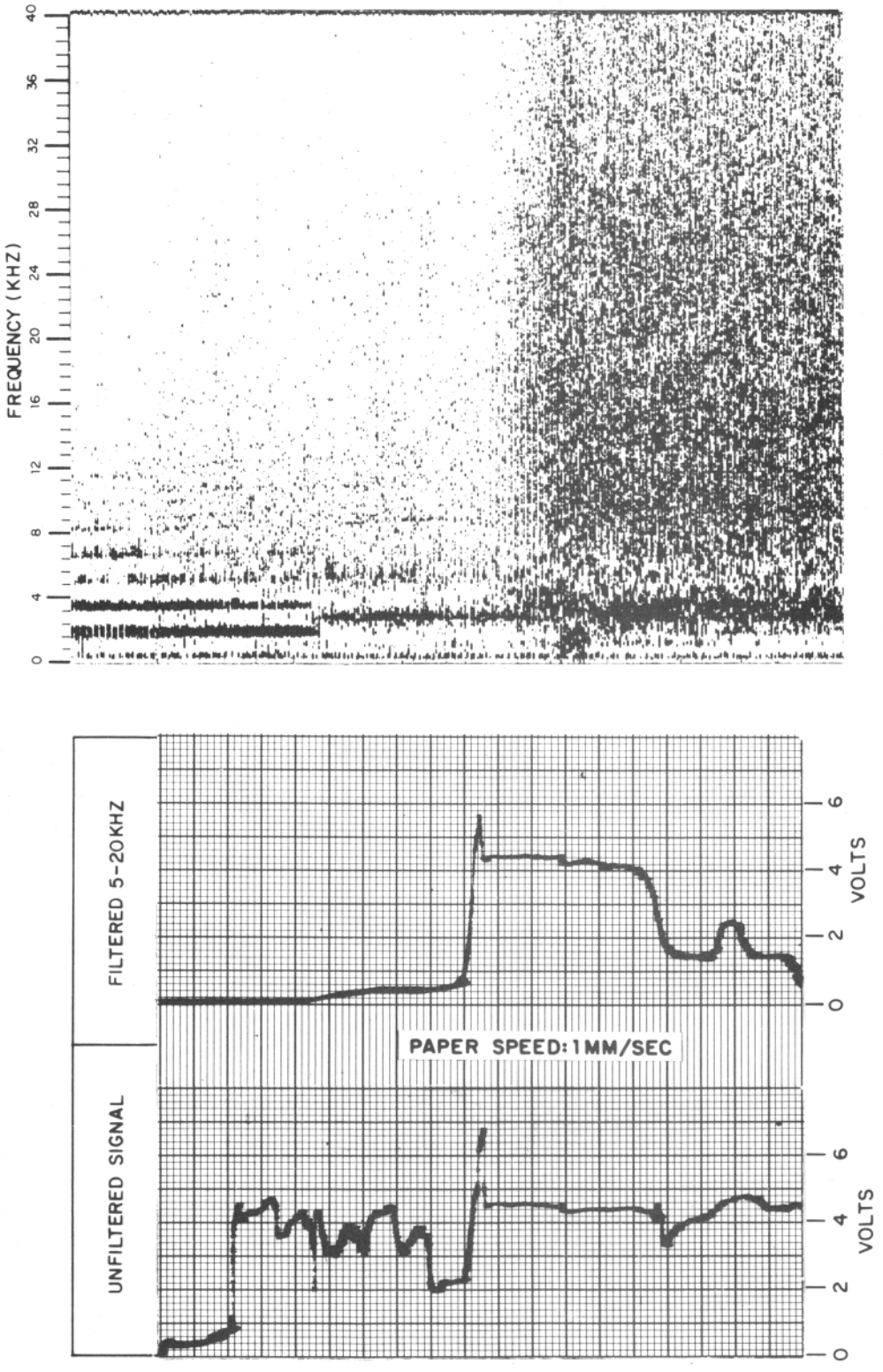

Figure 4-8. Burn-Through Failure on J-57 Port Engine at Maximum RPM

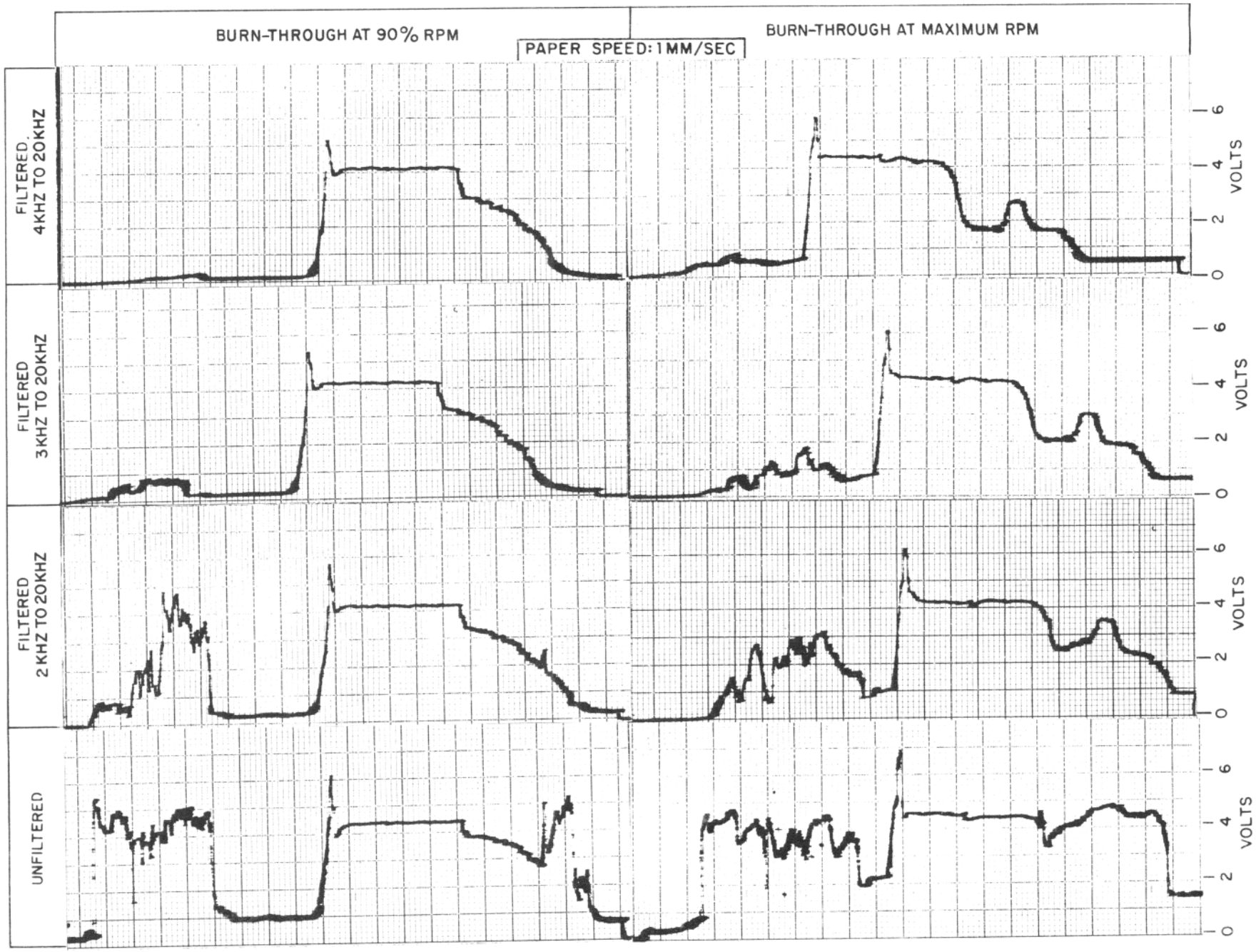

Figure 4-9. The Effect of Filtering Burn-Through Failure Signals at 90% RPM and Maximum RPM on the J-57 Port Engine

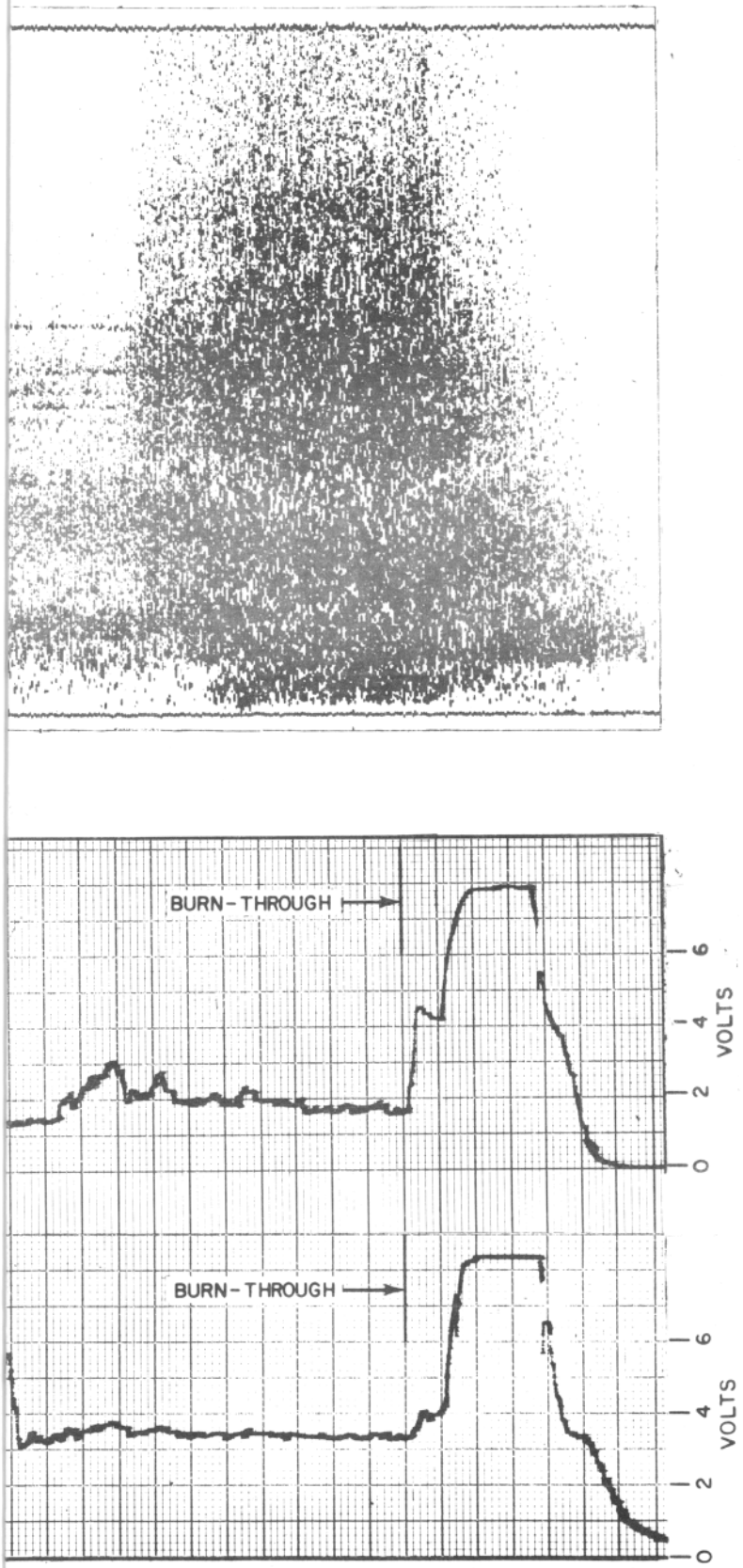

Figure 4-10. Fuel Line Burn-Through Failure as Sensed by Microphone No. 1

4-13/4-14 (Blank)

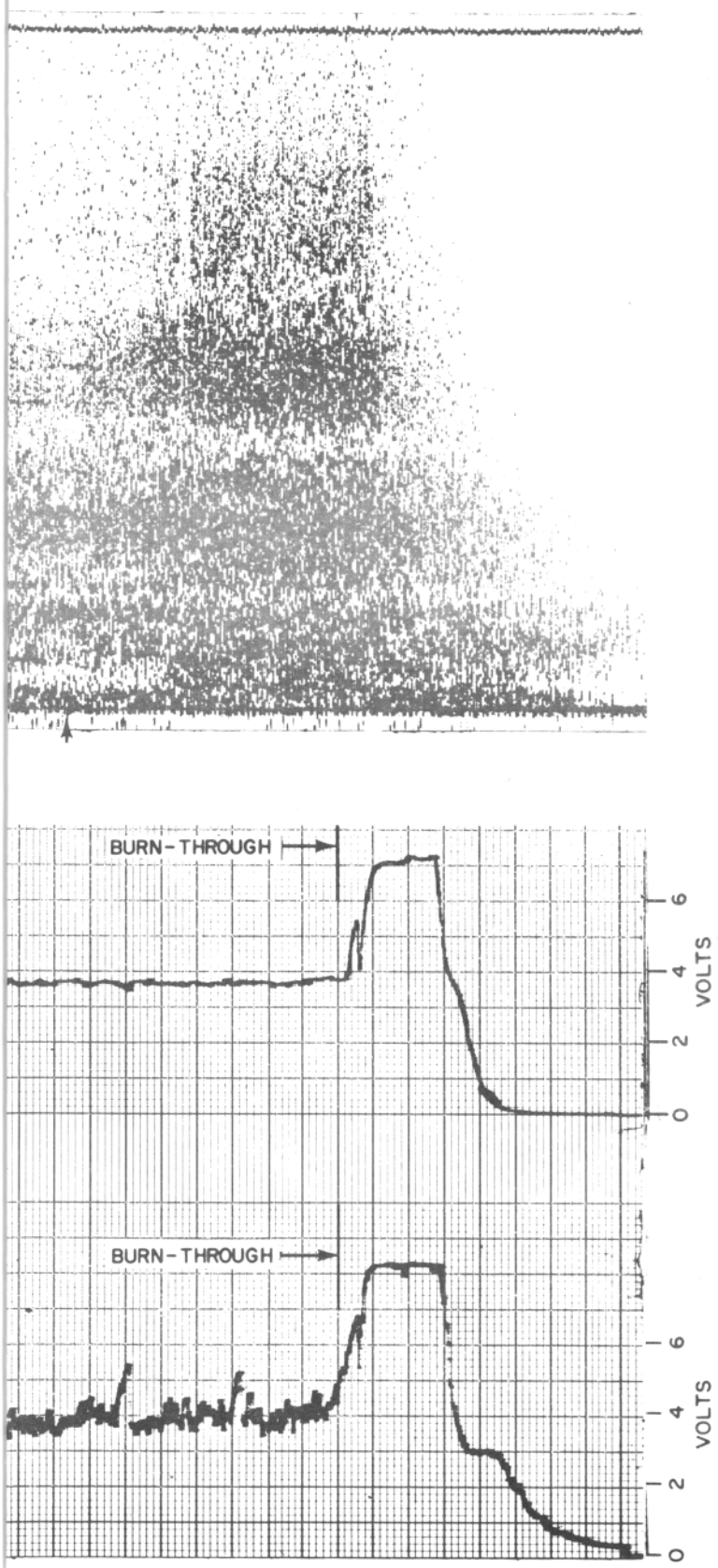

Figure 4-11. Fuel Line Burn-Through Failure as Sensed by Microphone No. 2

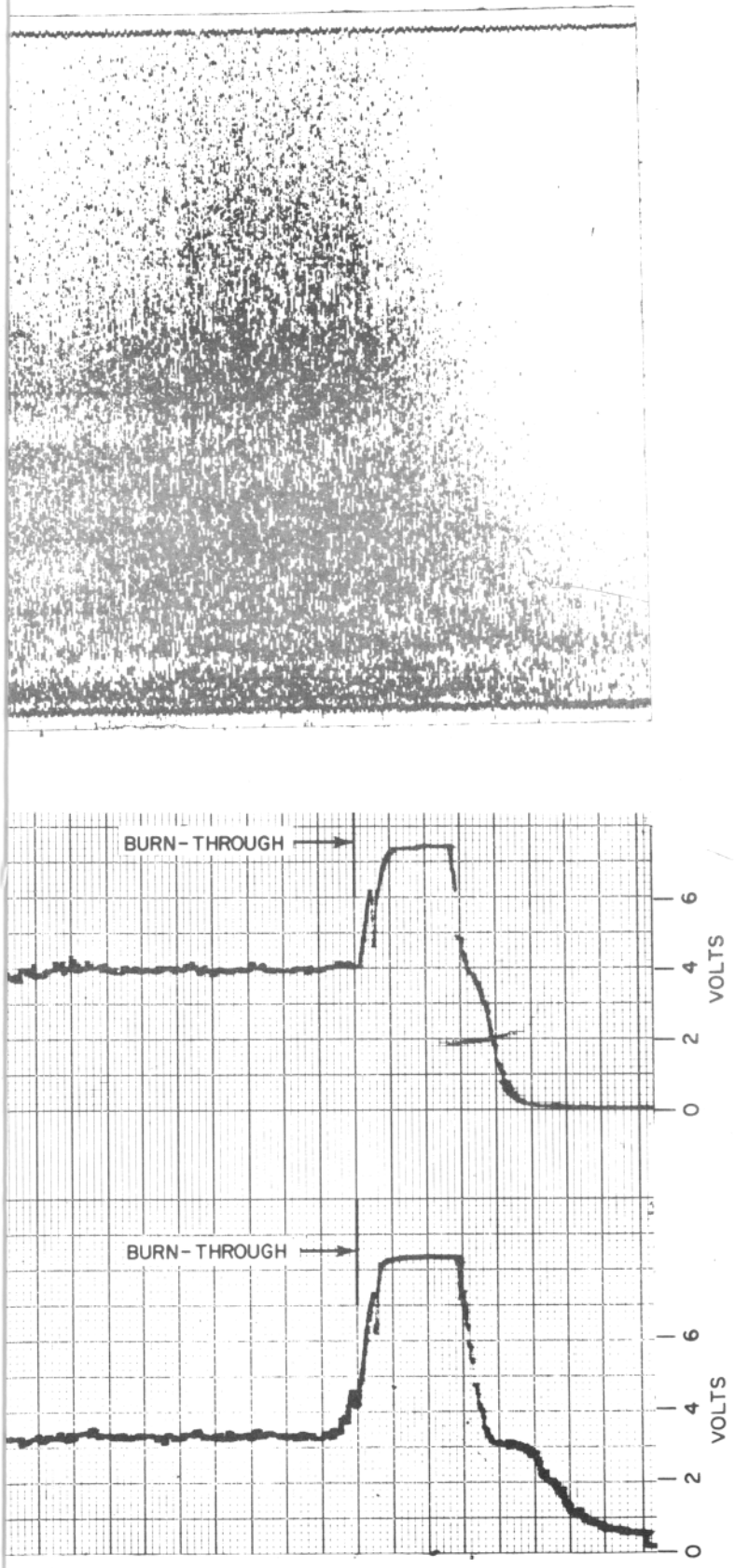

Figure 4-12. Fuel Line Burn-Through Failure as Sensed by Microphone No. 3

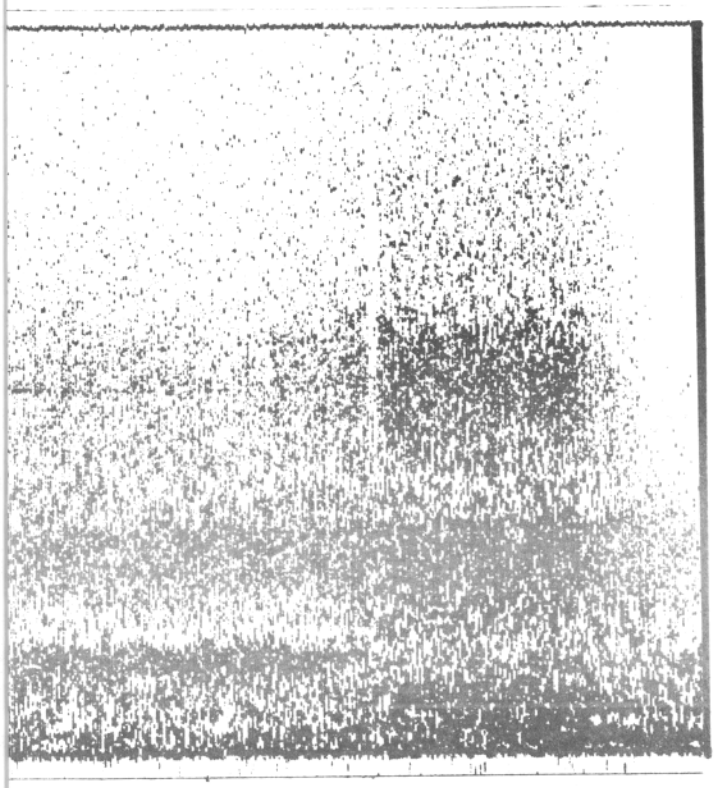

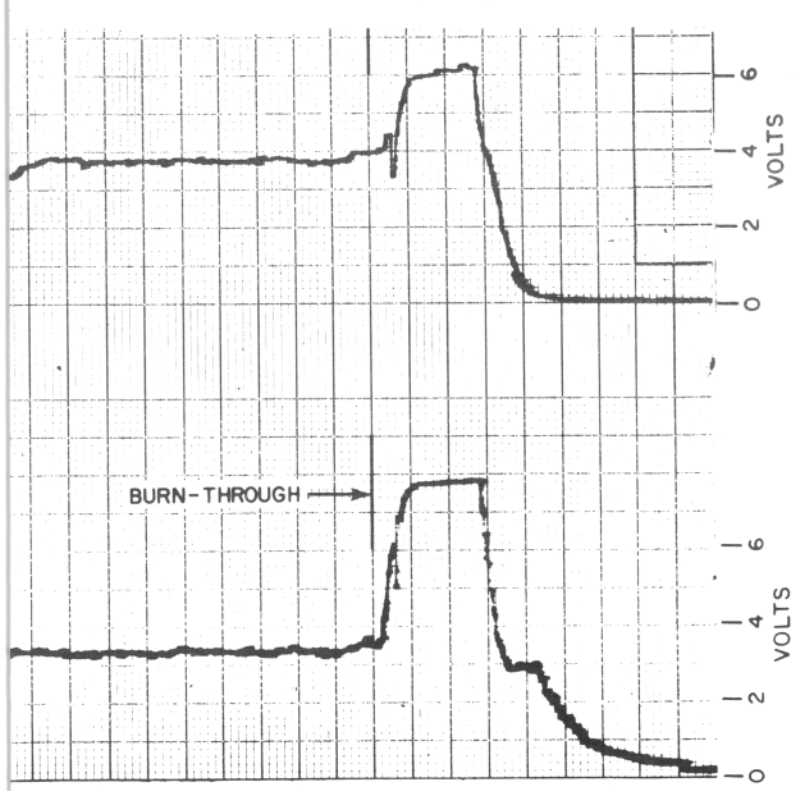

Figure 4-13. Fuel Line Burn-Through Failure as Sensed by Microphone No. 4

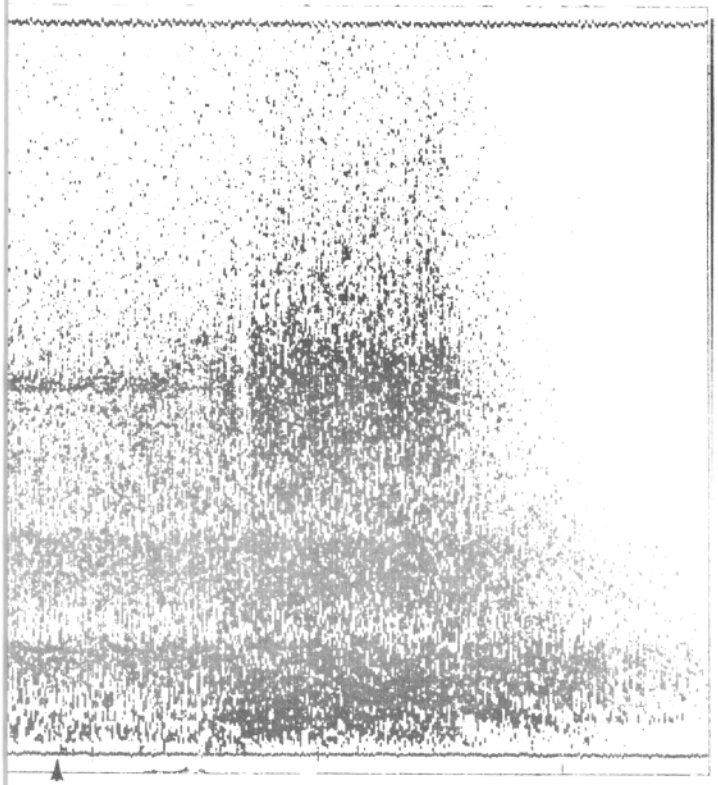

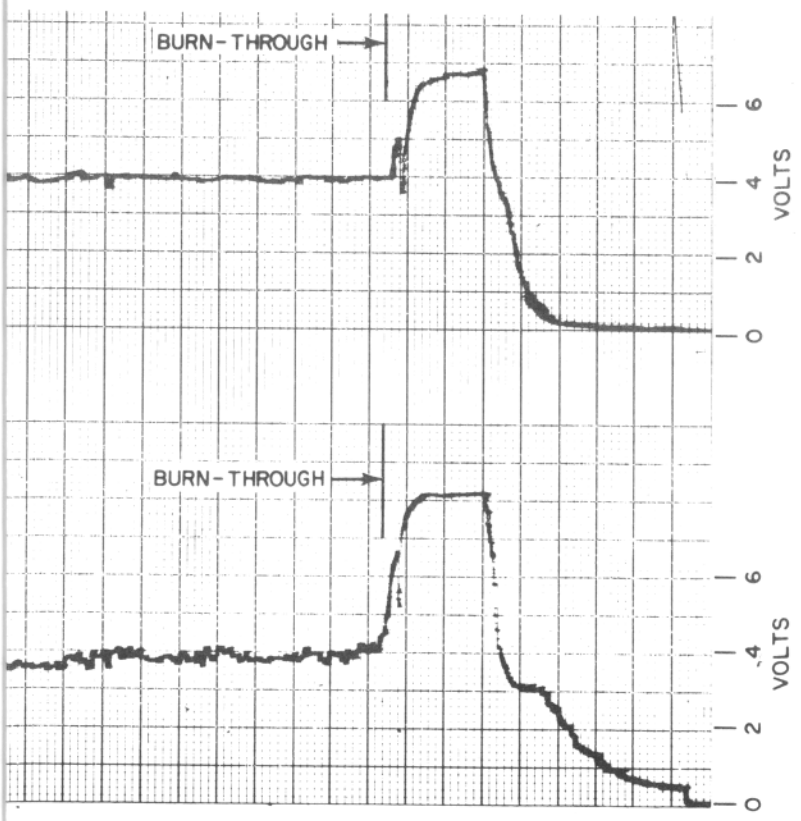

Figure 4-14. Fuel Line Burn-Through Failure as Sensed by Microphone No. 5

Those microphones farthest away detected the secondary rupture through the cowling much better than they did the engine housing rupture. All grams again showed the pre-burn-through and burn-through spectrum which has been observed to be characteristic of the failure mode.

The mean square analysis traces are a more reliable indicator of burn-through failure as can be observed by refering to the traces on Figures 4-10 through 4-14. In every case, the burn-through is plainly visible. In the upper trace, the highpass filter tends to dampen the extraneous low frequency spectra. The remaining spectra tends to be more stable, aiding in detection of burn-through failures.

The burn-through duration as detected by the microphones is listed below. Further examination of the microphone locations and the traces indicates that proximity to the rupture point is related to the failure duration sensed by the microphone. Although microphone 4 is the third farthest from the failure point, it is located well forward on the opposite side of the engine. Cowling and miscellaneous engine machinery have attenuated the sound transmission. Microphone 2 appears to have sensed the engine housing and cowling burn-through. There was a four-second lag between the two ruptures. Figures 4-15 and 4-16 are photographs which show the engine housing rupture and the cowling rupture, respectively.

Microphone	Time (Seconds)
1	8
2	4
3	4
4	3
5	4

4.3 Sound Pressure Level Relationship to Orifice Size and Engine Speed

Tests for both the J-47 and J-57 engines were run with varying engine speeds and orifice openings in the modified burner can. The purpose of these tests was to determine the relationship between engine speed and orifice size and between orifice size, engine speed, and burn-through failure.

Data from microphones 1, 3, and 4, installed on the J-47 engine, was used to produce Figures 4-17 through 4-19. By plotting microphone output versus orifice size and microphone output versus engine speed on the same graph, the relationship of sound pressure level to orifice size and engine speed became apparent. In all cases, an increase in orifice size increased the sound pressure level to a degree that varied with microphone location. The abscissa was expanded for microphones 3 and 4 to supplement location attenuation and emphasize the trends. Microphone No. 1 was located above and pointed toward the orifice while microphones 3 and 4 were mounted below the orifice. It is apparent that as engine speed is increased, the sound pressure level for a given orifice size increases.

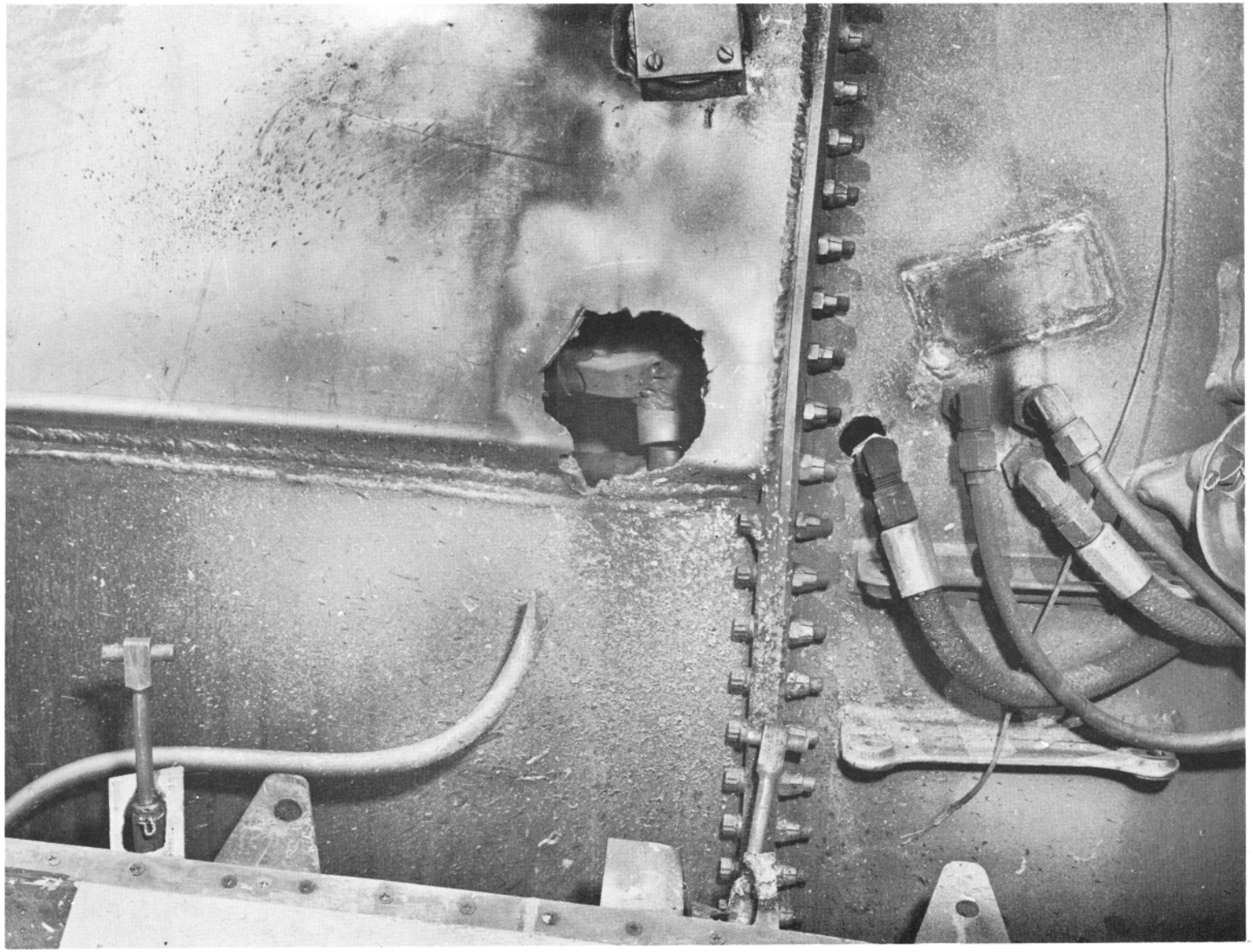

Figure 4-15. Engine Housing Rupture Due to Fuel Line Failure on the J-57 Starboard Engine

Figure 4-16. Engine Cowling Rupture Due to Fuel Line Failure on the J-57 Starboard Engine

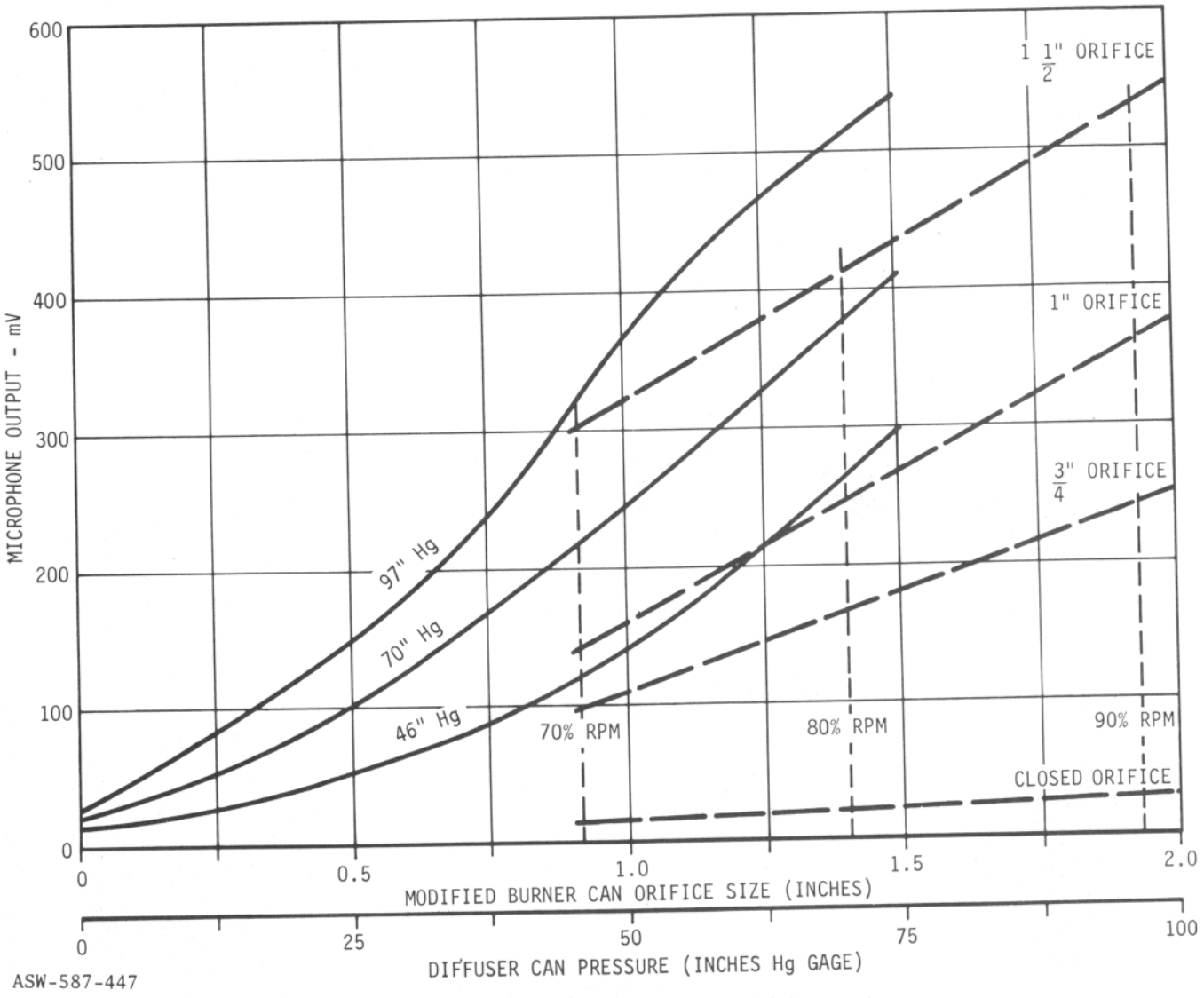

Figure 4-17. J-47 Engine Orifice Size, Engine Speed, and Sound Pressure Level Relationship for Microphone No. 1

A different situation exists on the J-57 engine. Data from microphones 1, 2, and 3, mounted on the J-57 port engine, was plotted in the same manner as above. (See Figures 4-20 through 4-22.) The previous relationship noting an increase in sound pressure level with an increase in orifice size is still evident but to a lesser degree. The prime difference is the unpredictable nature of the curve due to engine speed. In most cases, for a given orifice size, the 82% RPM sound pressure level is higher than the 90% RPM sound pressure level and in some cases is higher than the maximum engine speed sound pressure level. It has been determined that this factor is caused by characteristic discrete frequency lines produced by the J-57 engine. Mean square analysis of recorded data vividly shows that the effect

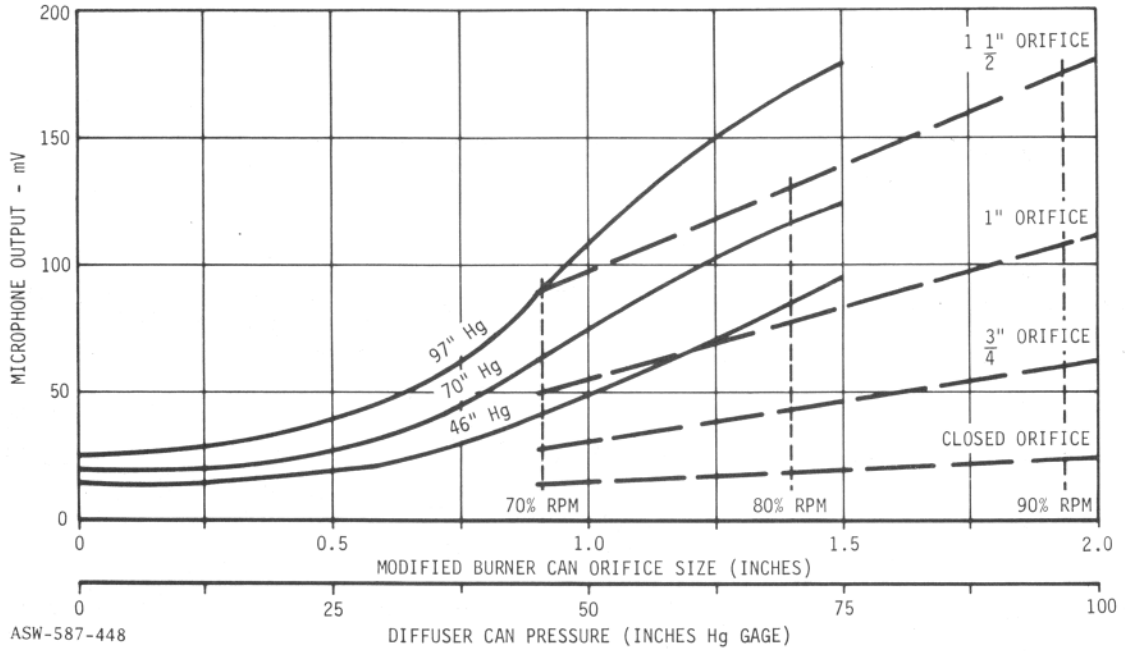

Figure 4-18. J-47 Engine Orifice Size, Engine Speed, and Sound Pressure Level Relationship for Microphone No. 3

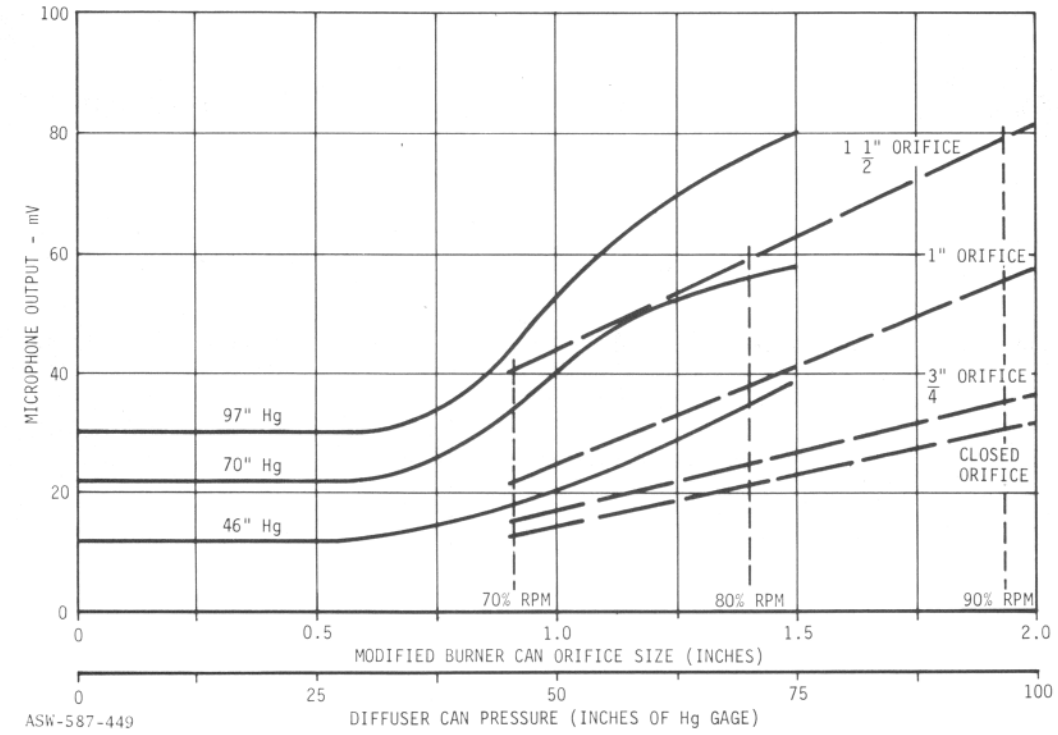

Figure 4-19. J-47 Engine Orifice Size, Engine Speed, and Sound Pressure Level Relationship for Microphone No. 4

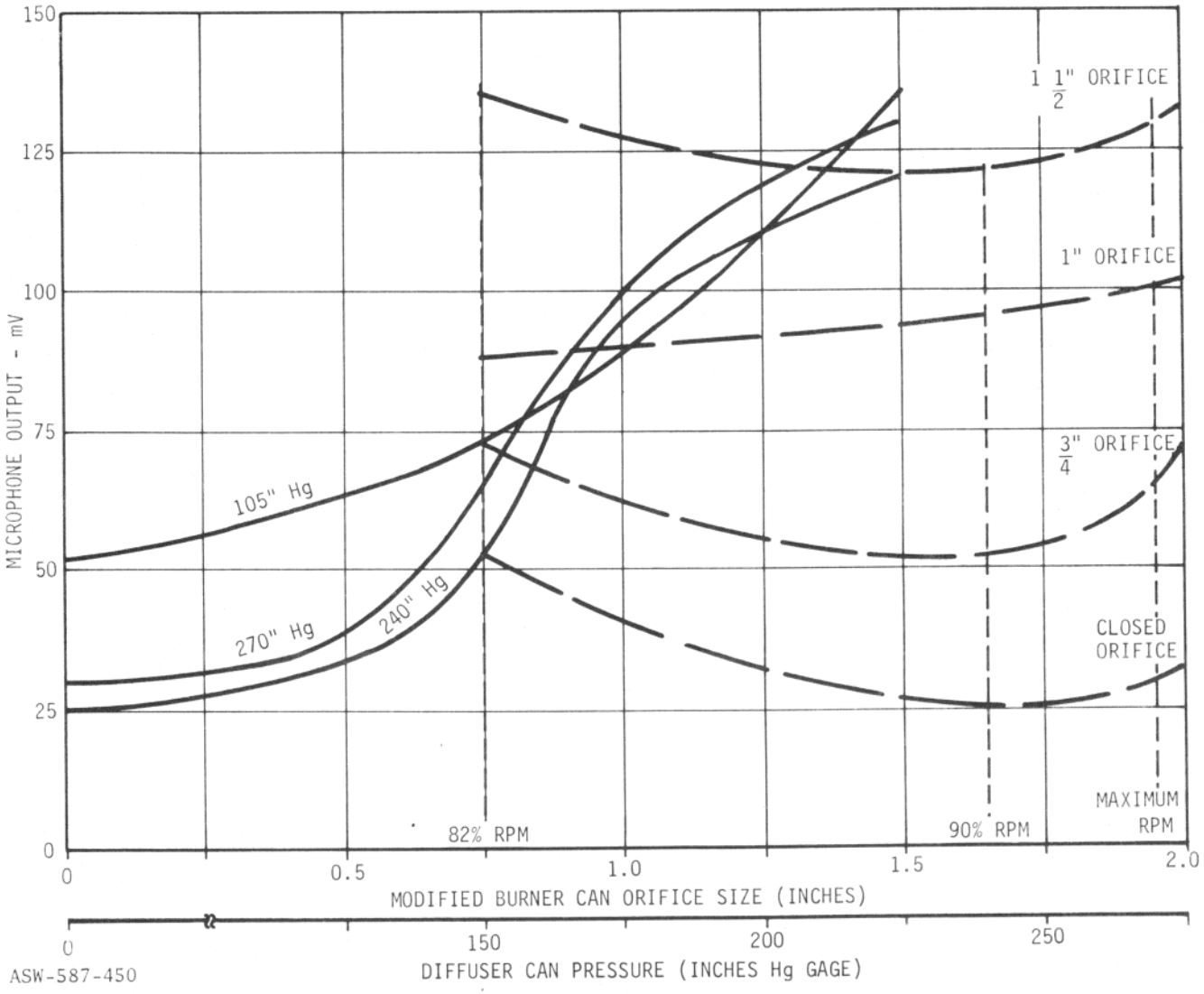

Figure 4-20. J-57 Engine Orifice Size, Engine Speed, and Sound Pressure Level Relationship for Microphone No. 1

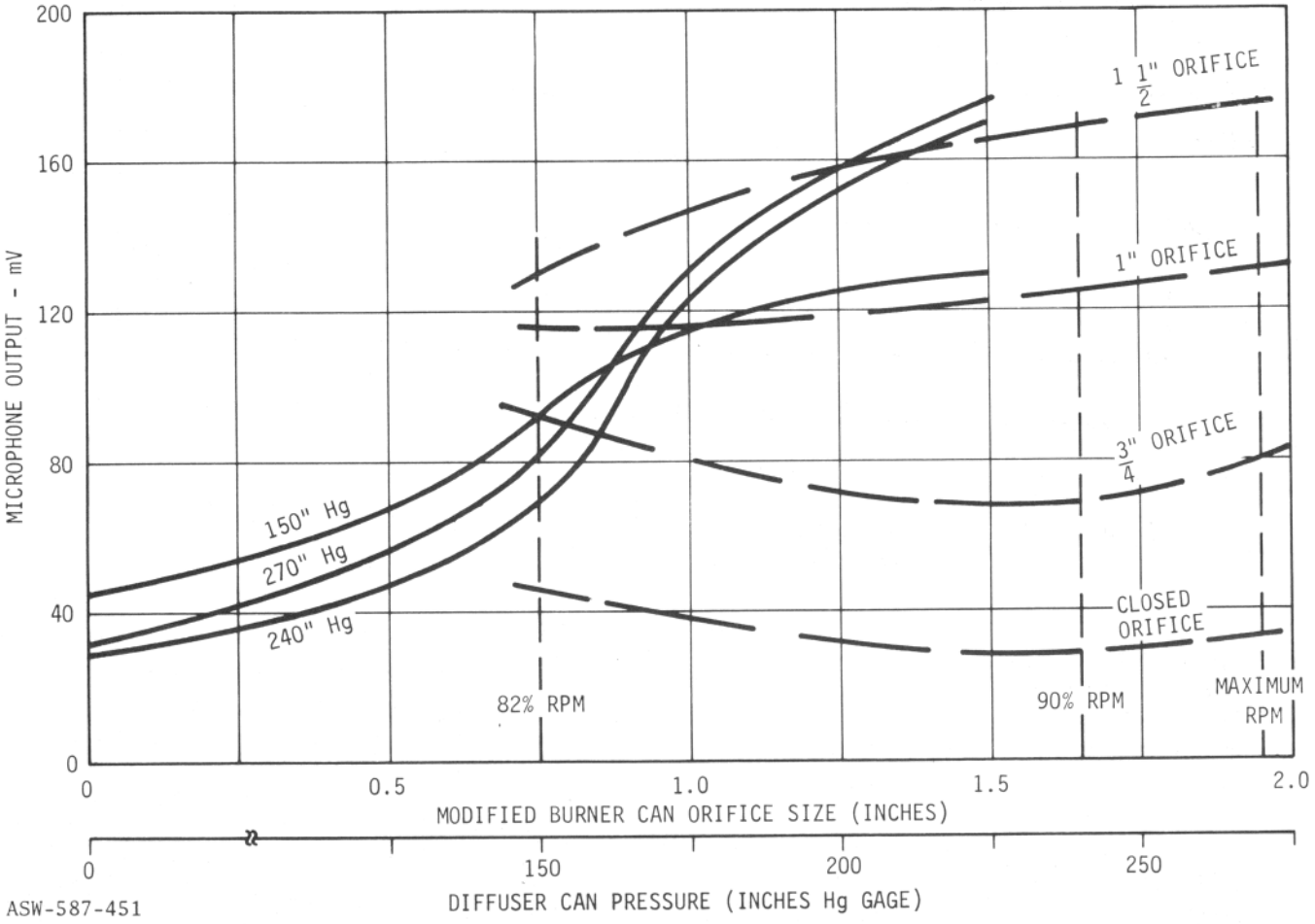

Figure 4-21. J-57 Engine Orifice Size, Engine Speed, and Sound Pressure Level Relationship for Microphone No. 2

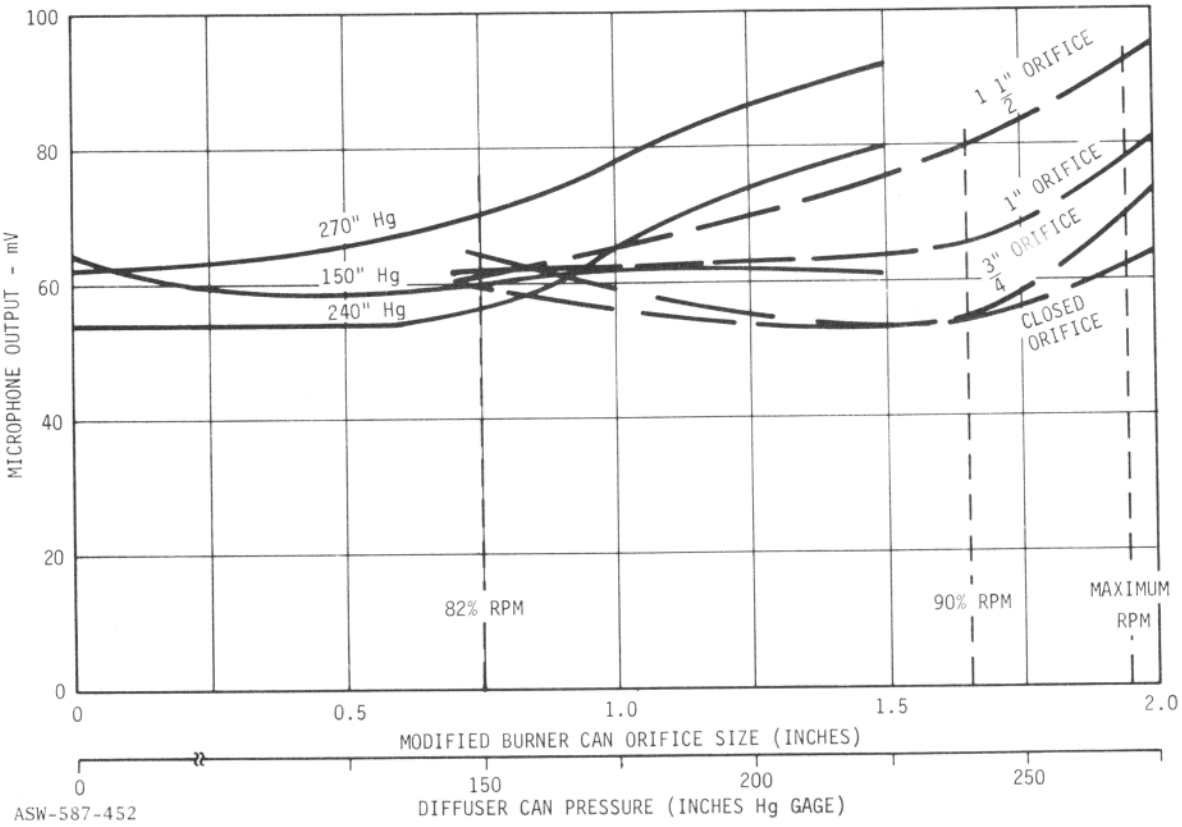

Figure 4-22. J-57 Engine Orifice Size, Engine Speed, and Sound Pressure Level Relationship for Microphone No. 3

is caused by characteristic discrete frequency lines produced by the J-57 engine. Mean square analysis of recorded data vividly shows the effect of filtering this low frequency energy and spectrograms show the frequency lines. (See Appendix B, engine speed and orifice variation analysis for the J-57 port engine.)

The J-57 engine was noticeably quieter than the J-47 engine and similar variations in sound pressure levels were noted due to microphone location. The J-57 engine was cowled causing restricted sound transmission. Microphone 3 was the farthest from the orifice and was least sensitive to orifice variation and engine speed.

Sound pressure level data taken during closed orifice and 1.5-inch open orifice tests was compared with before and after burn-through sound pressure levels. Figures 4-23 and 4-24 show microphone 1 and 3 sound pressure levels before and after burn-through superimposed on microphone output versus orifice size plots. After reviewing spectrograms of the burn-throughs and comparing frequencies at burn-through with 1.5-inch orifice steady state tests, it was verified that there is a direct correlation between engine speed, orifice size, and burn-through characterisitics. J-57 burn-through data was plotted in the same manner as discussed above. (See Figure 4-25.) Similar correlation is evident.

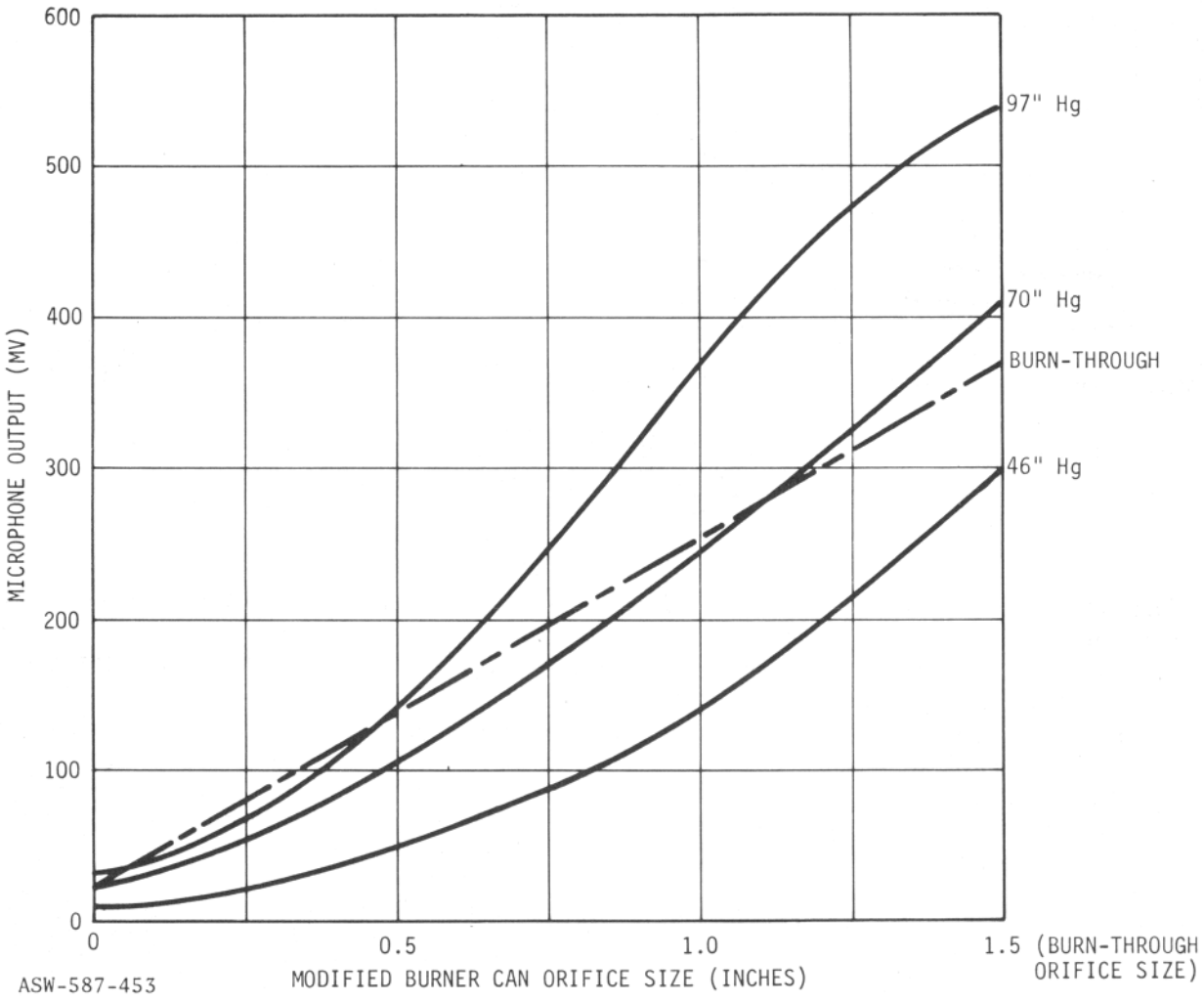

Figure 4-23. J-47 Engine Orifice Size, Engine Speed, and Sound Pressure Level Correlation to Burn-Through for Microphone No. 1

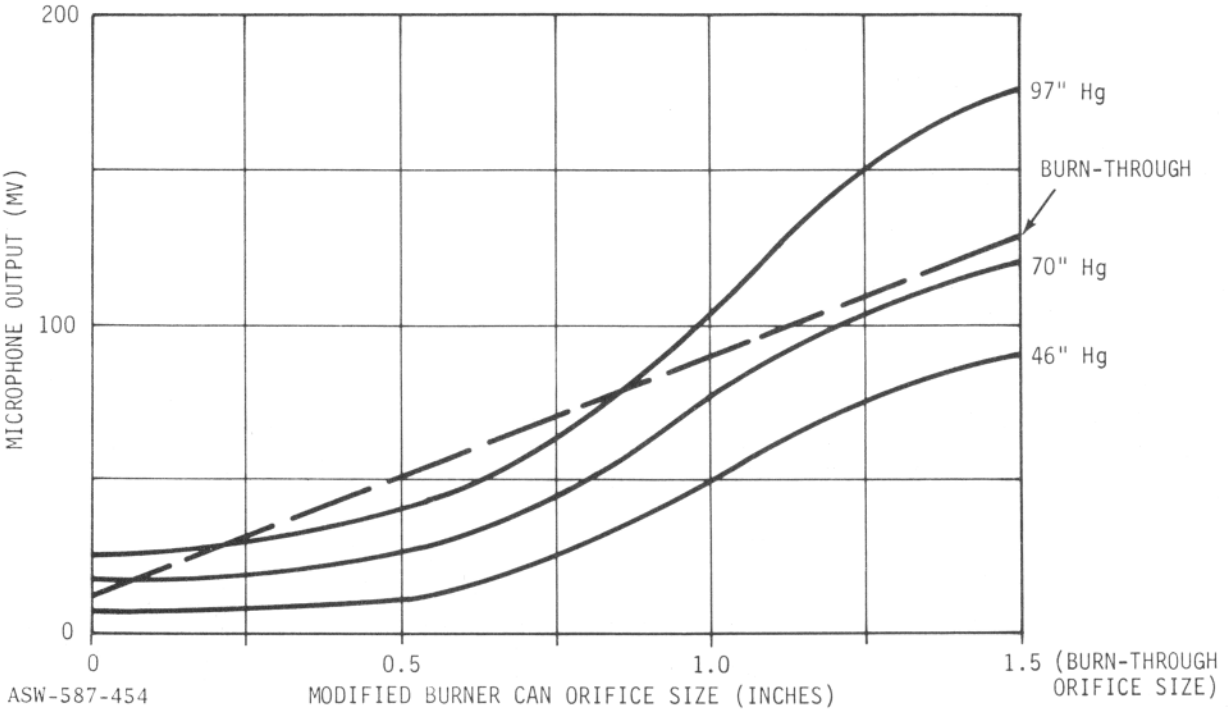

Figure 4-24. J-47 Engine Orifice Size, Engine Speed, and Sound Pressure Level Correlation to Burn-Through for Microphone No. 3

The pre-burn-through sound pressure levels are higher than the steady state closed orifice tests as was the case with the burn-through and 1.5 inch open orifice tests. The former is probably due to error in selecting the correct moment to read the meter and the latter may be due to increased sound pressure level after burn-through caused by the flame spewing through both the modified burner can orifice and the engine cowling. The sound pressure levels before and after burn-through for both the J-47 and J-57 engines definitely establish a correlation trend with steady state closed and 1.5 inch open orifice sound pressure levels.

4.4 Acoustic Spectrum Relationship to Orifice Size and Engine Speed

The same series of tests discussed in paragraph 4.3 were used again to determine the relationship between acoustic spectrum due to orifice size and engine speed.

Figures 4-26 and 4-27 compare engine speed to orifice size for the J-47 engine. Closed orifice and 0.75, 1.0, and 1.5 inch open orifice sizes were compared individually at 70%, 80%, and 90% RPM. All data was sensed by microphone No. 2 and the analysis bandwidth is 0 to 40 kHz. The closed orifice spectrum shows very little random noise and a number of discrete frequencies. The discrete lines below 10 kHz can be seen to

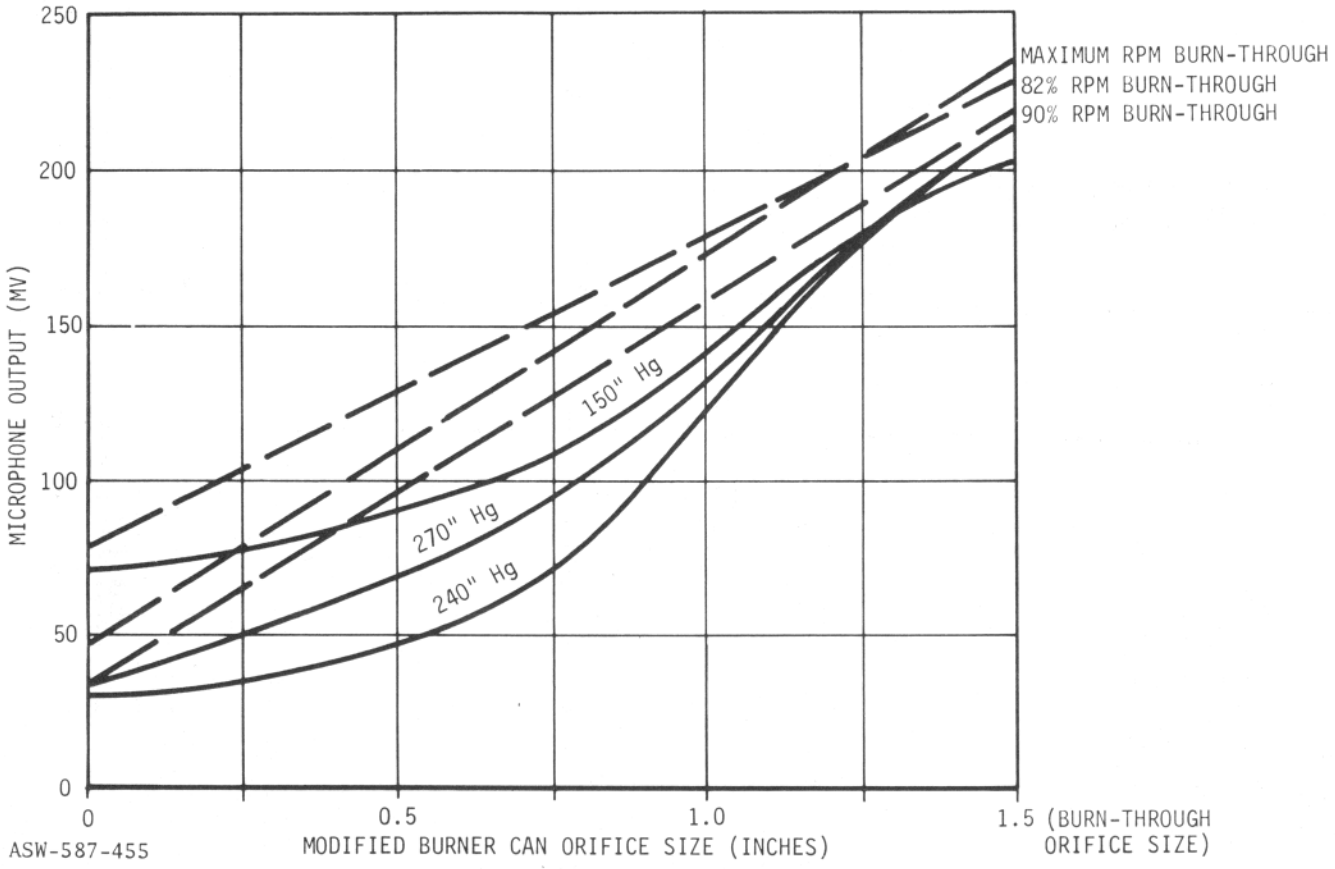

Figure 4-25. J-57 Engine Orifice Size, Engine Speed, and Sound Pressure Level Correlation to Burn-Through for Microphone No. 1

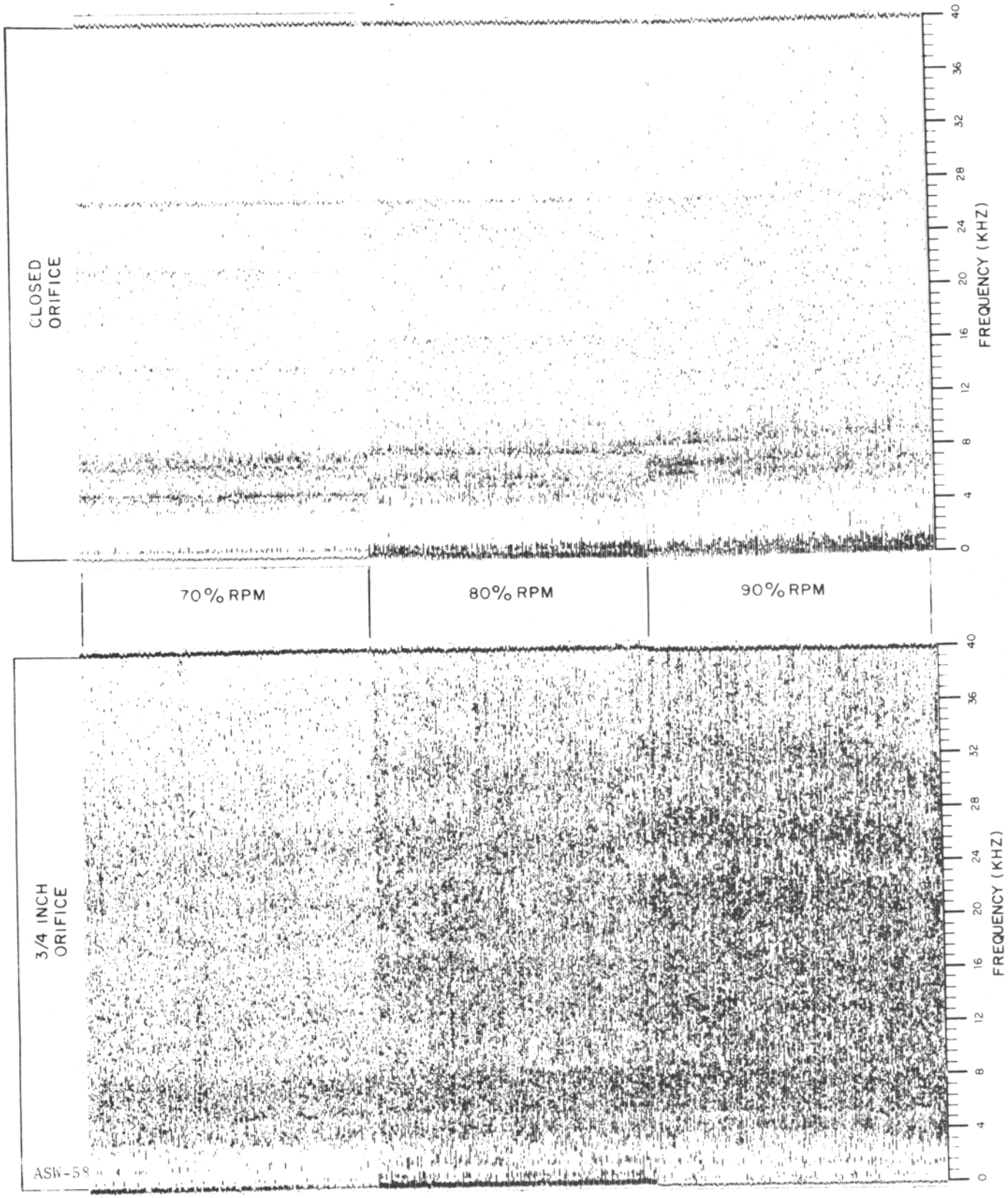

Figure 4-26. Spectral Comparison of 0.75 Inch Open and Closed Orifice at 70, 80, and 90% RPM of the J-47 Engine

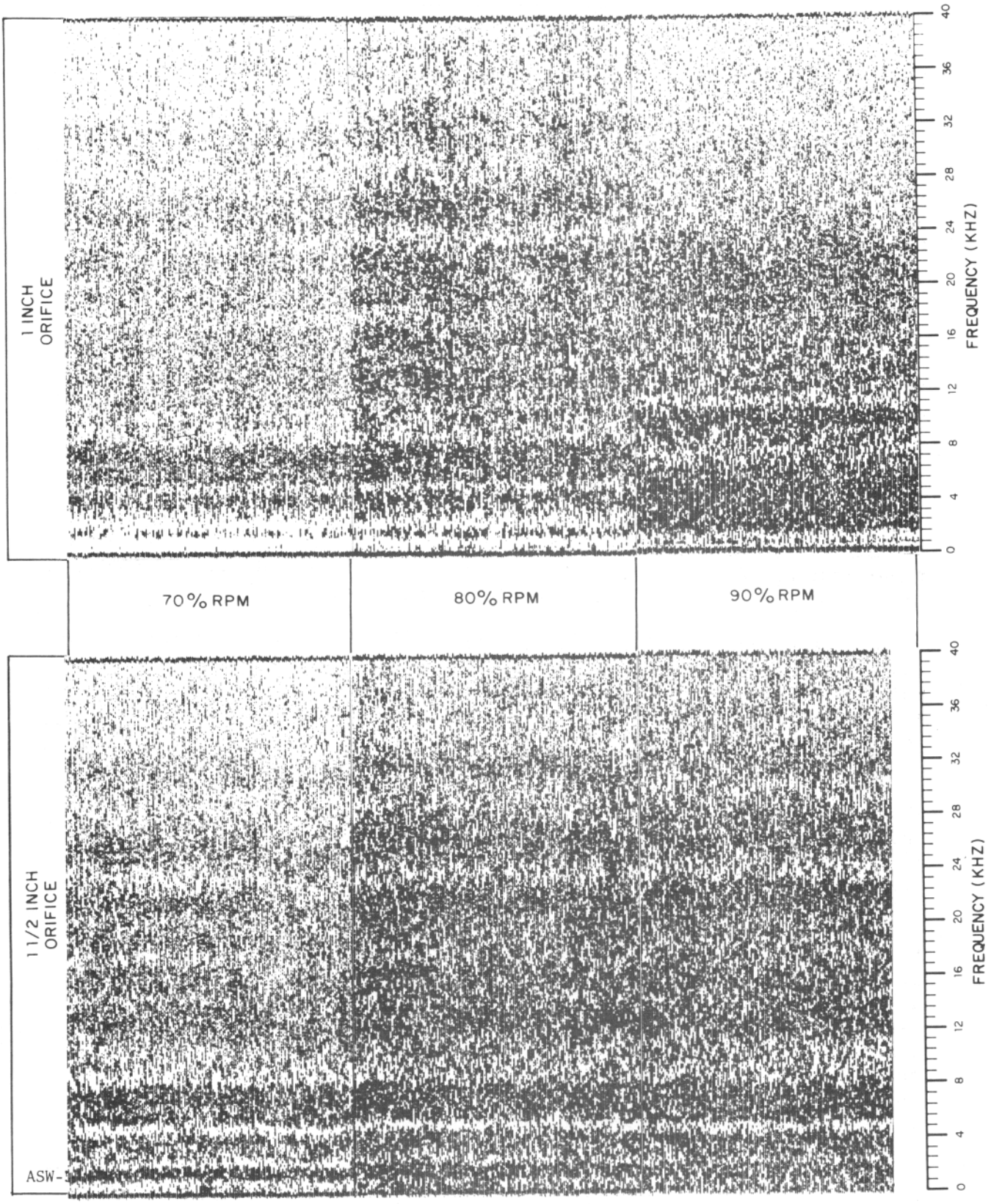

Figure 4-27. Spectral Comparison of 1.0 and 1.5 Inch Open Orifice at 70, 80, and 90% RPM of the J-47 Engine

increase directly with engine speed. The line at about 27 kHz, however, is relatively stable at both 70% and 80% RPM but becomes unstable at 90% RPM. There is also an increase in random noise density and frequency in relation to engine speed. The general pattern of the closed orifice spectrum as the engine speed increased also applies to the open orifice tests, except that the random noise increased to such an extent that discrete lines are not visible. Instead, the discrete line appear as bands of energy 4 or 5 kHz wide. (Note the lines between 6 and 10 kHz on the closed orifice grams as compared to those on the open orifice grams.)

Figures 4-28 through 4-30 reverse the above data. The grams have been rearranged such that RPM is held constant and orifice size increased. The banding effect noted above is further emphasized. The grams for the J-47 engine indicate that as engine speed is increased, random noise increases. It can also be observed that discrete engine frequencies increase in proportion to the engine RPM. Likewise, as the orifice increased in size, random noise increases. The spectrum behaves, as could be expected, in the same manner as the sound pressure level.

Figures 4-31 and 4-32 compare engine speed to orifice size for the J-57 port engine as was previously observed for the J-47 engine grams. Closed orifice and 0.75, 1.0, and 1.5 inch open orifice sizes were compared individually at 82%, 90%, and maximum RPM. All data was sensed by microphone No. 1 and the analysis bandwidth is 0 to 20 kHz.

The closed orifice grams for this engine are quite different from the J-47 engine. At 82% RPM, this engine resonates and produces a multitude of discrete frequency lines. Aurally, the tape playback sounds like a 2-kHz oscillator. At 90% and maximum RPM, the engine is relatively quiet. Open orifice spectrum is similar to that of the J-47 engine except that the change in random noise density is not as noticeable. The 1.0 inch orifice gram appears to be more dense than the 1.5 inch orifice gram. The recording levels were apparently not properly compensated when the data was processed. (The sound pressure levels, which are direct microphone readings, indicate that the density increased proportional to the orifice size.)

Figures 4-33 through 4-35 reverses the above data. The grams have been rearranged such that engine speed is held constant and orifice size increased. The grams for the J-57 engine indicate that as engine speed increases, random noise increases, but to a lesser degree than for the J-47 engine. The low speed resonances, which appear as discrete frequency lines primarily below 10 kHz on the grams, are a characteristic of the engine. The grams also show that at a given engine speed, an increase in aperture size increases random noise. The spectral behavior of the J-57 engine responds in a similar manner to orifice size and speed changes as sound pressure level.

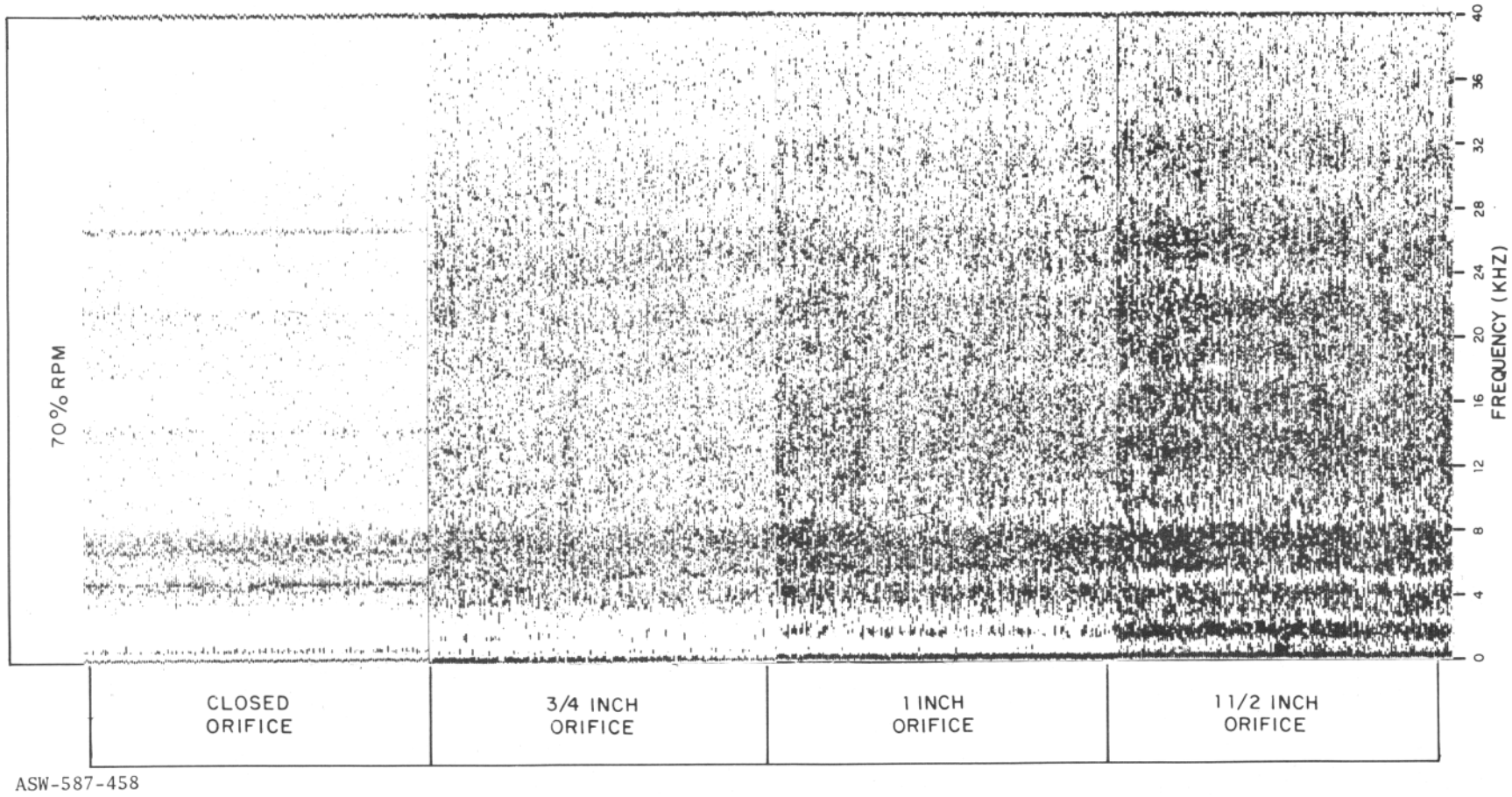

Figure 4-28. Spectral Comparison of Open and Closed Orifice at 70% RPM of the J-47 Engine

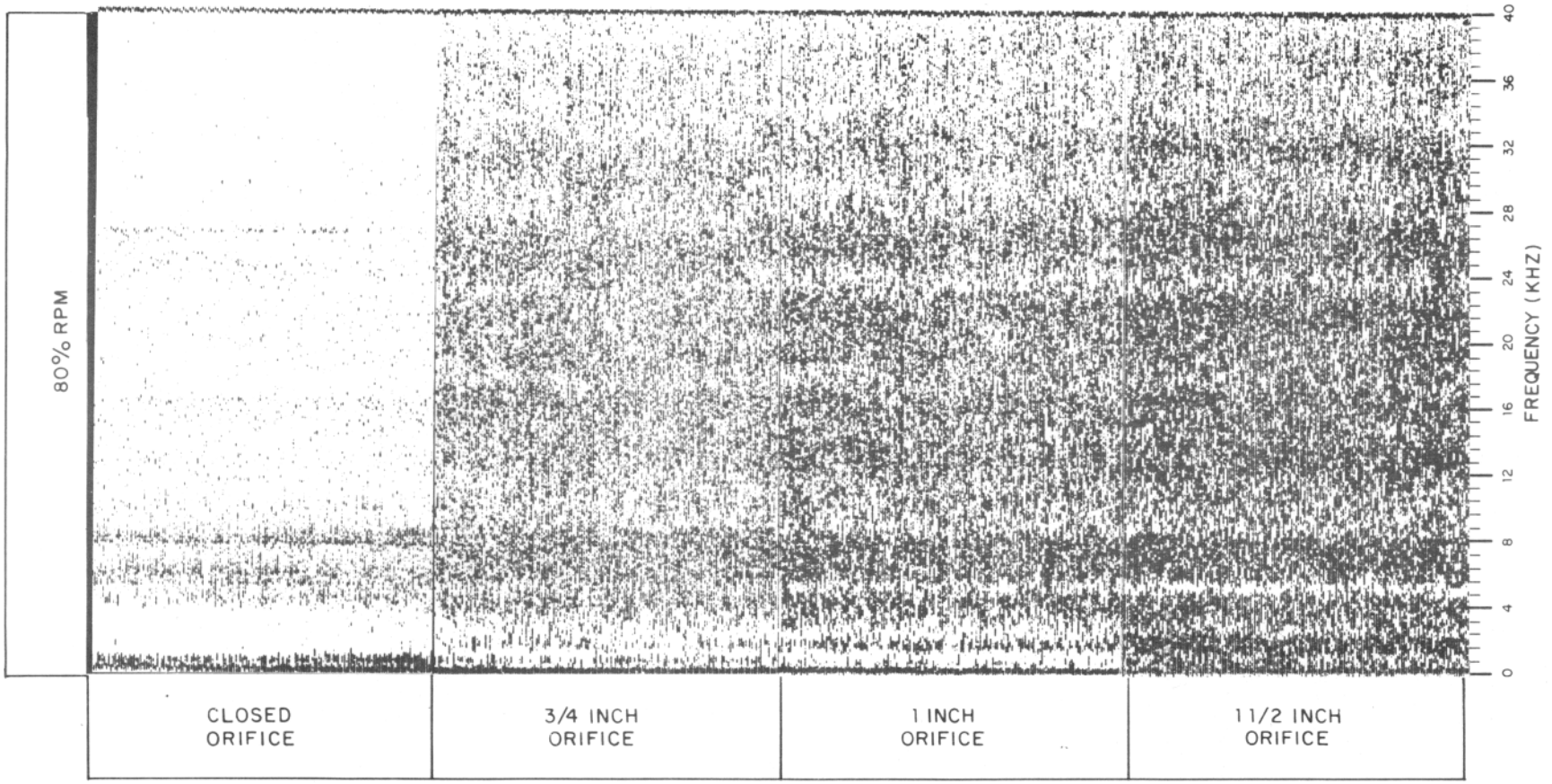

ASW-587-459

Figure 4-29. Spectral Comparison of Open and Closed Orifice at 80% RPM of the J-47 Engine

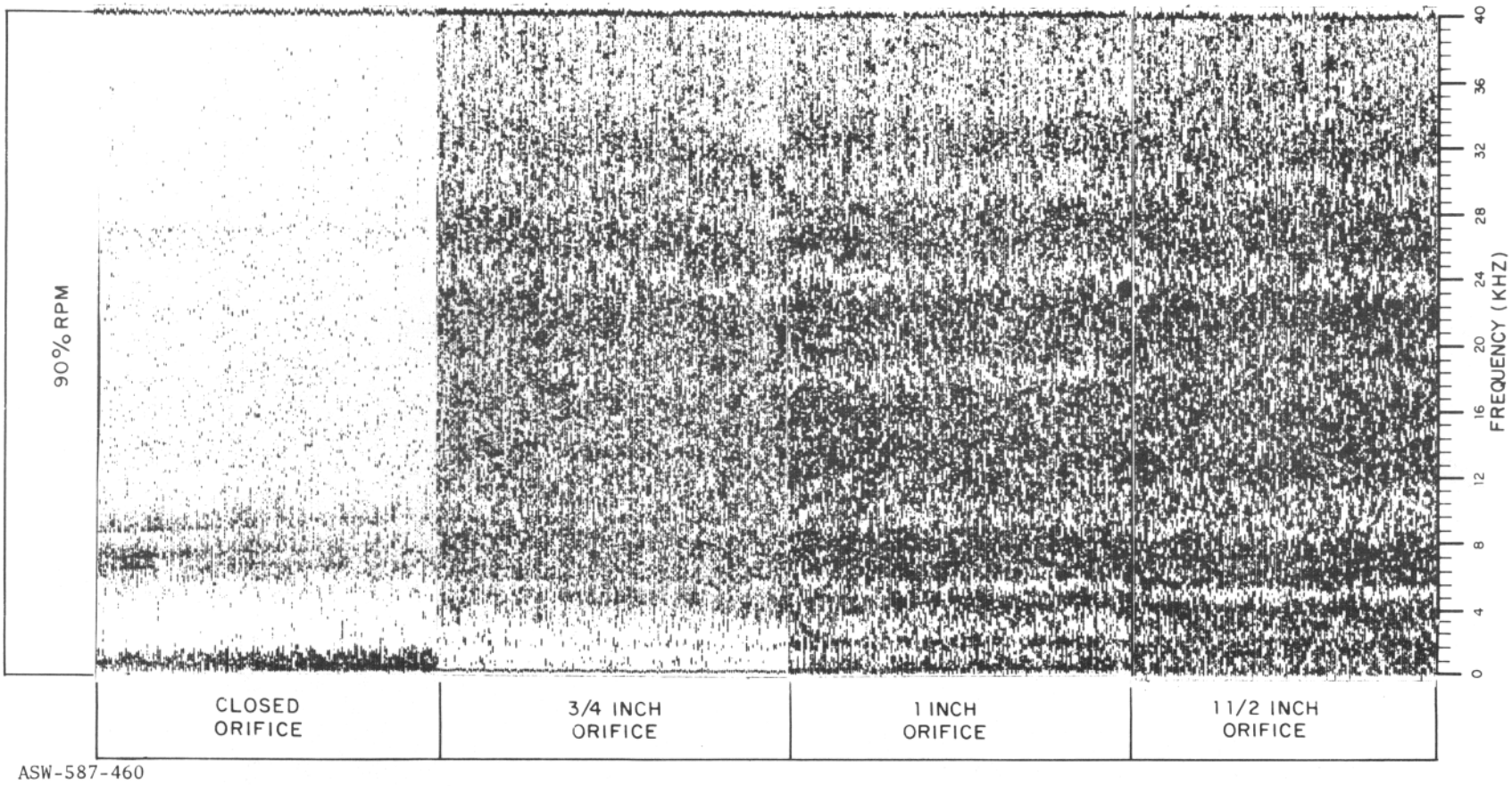

Figure 4-30. Spectral Comparison of Open and Closed Orifice at 90% RPM of the J-47 Engine

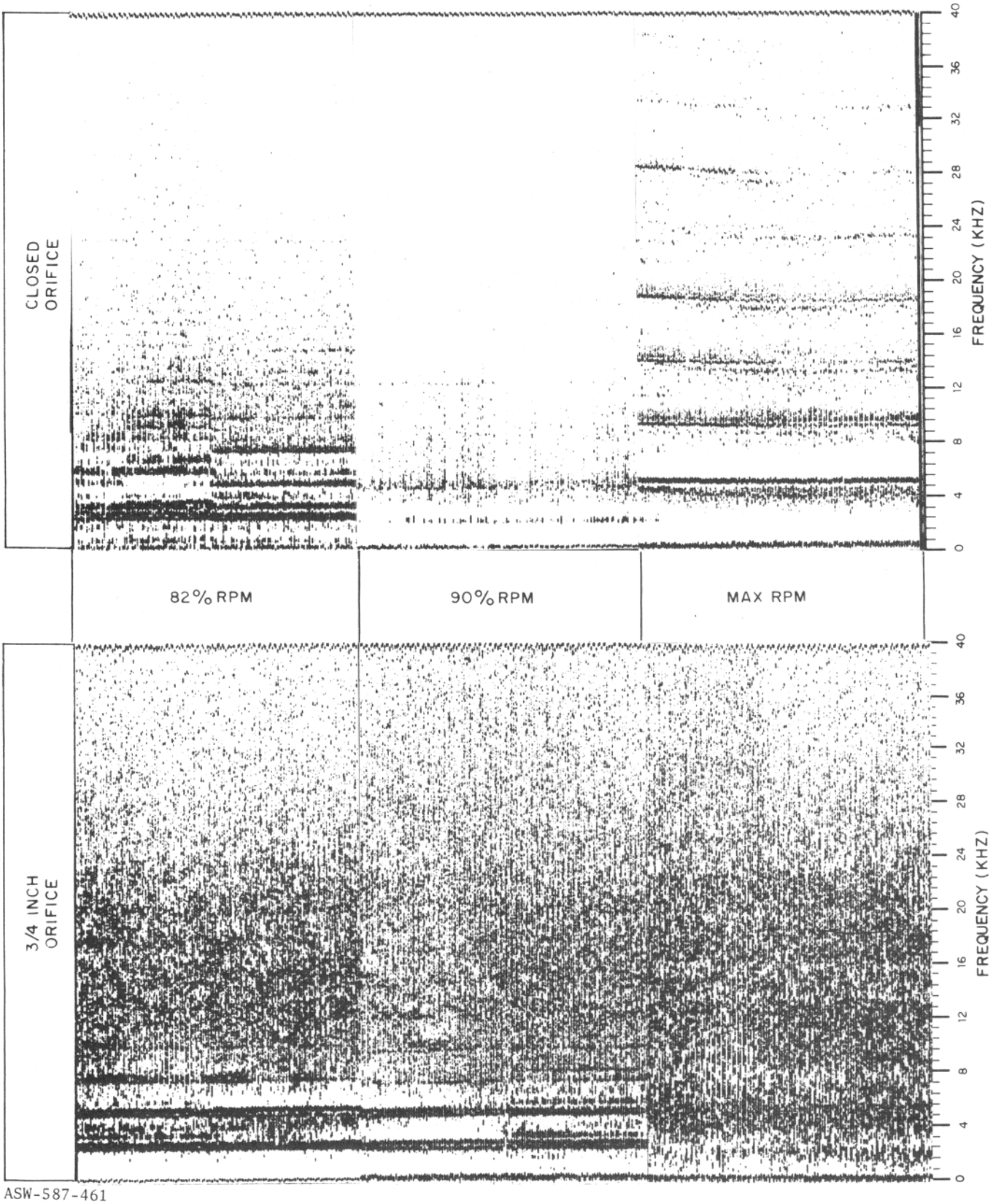

ASW-587-461

Figure 4-31. Spectral Comparison of 0.75 Inch Open and Closed Orifice at 82%, 90%, and Maximum RPM of the J-57 Port Engine as Sensed by Microphone No. 1

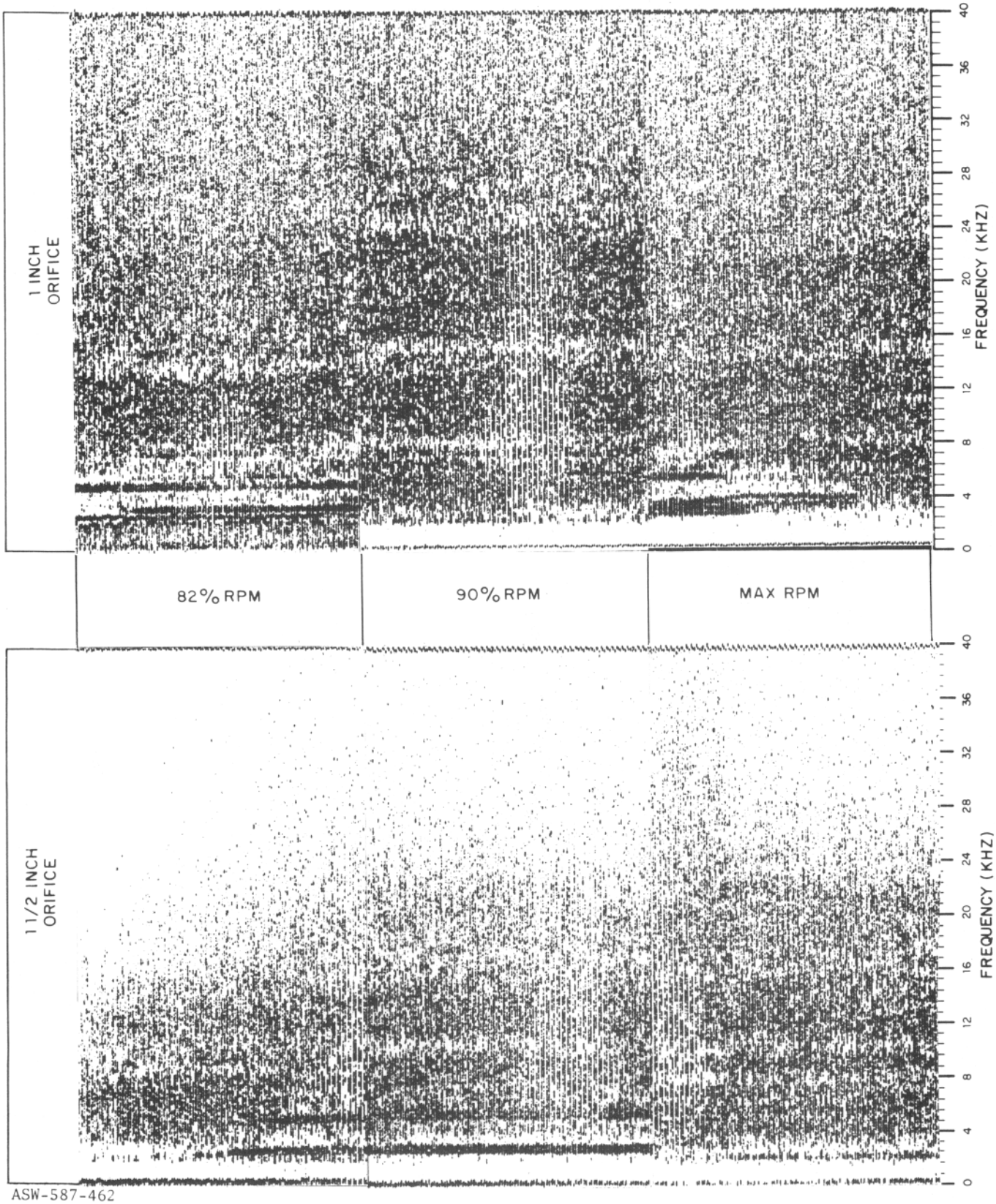

Figure 4-32. Spectral Comparison of 1.0 and 1.5 Inch Open and Closed Orifice at 82%, 90%, and Maximum RPM of the J-57 Port Engine as Sensed by Microphone No. 1

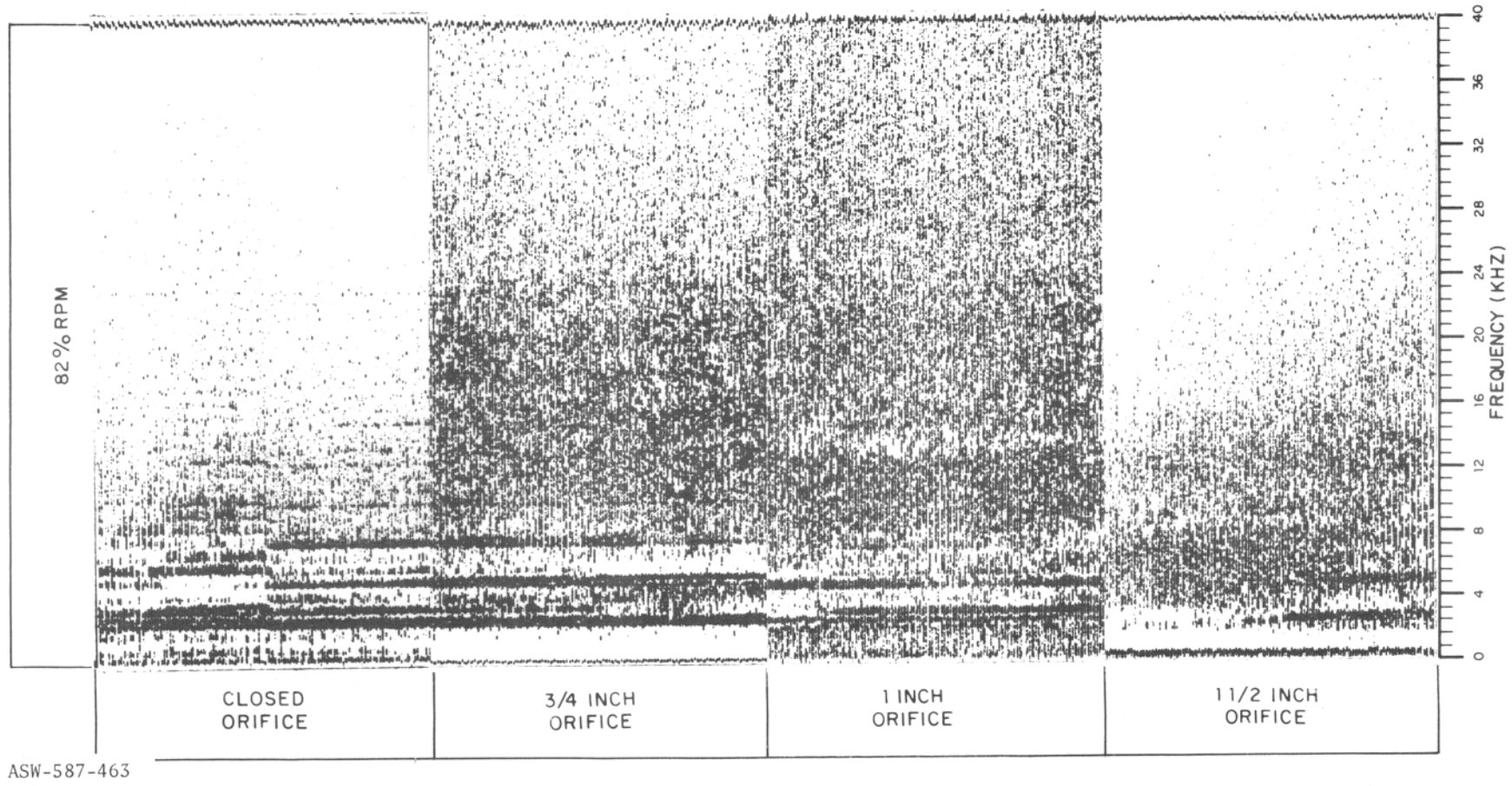

Figure 4-33. Spectral Comparison of Open and Closed Orifice at 82% RPM of the J-57 Port Engine as Sensed by Microphone No. 1

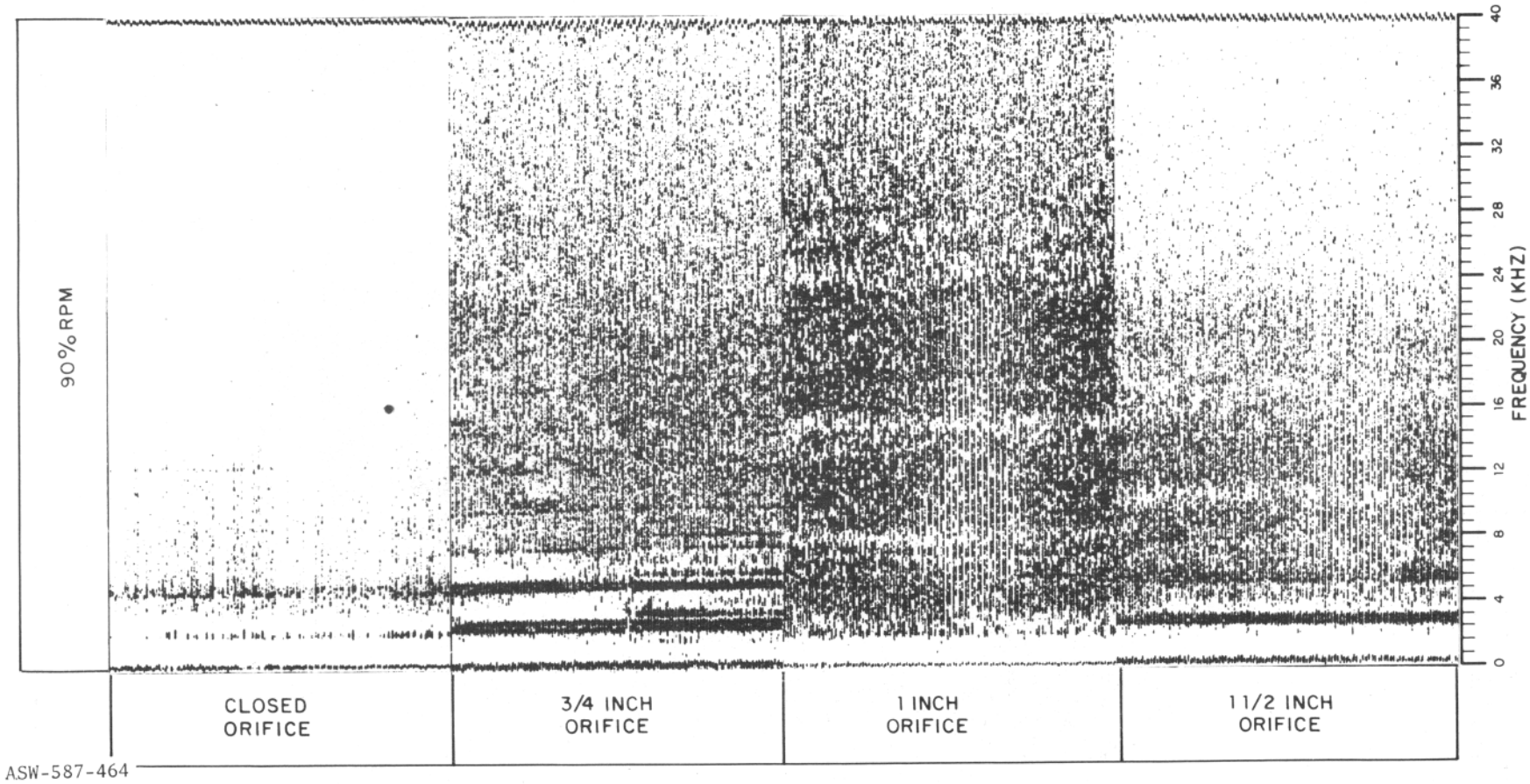

Figure 4-34. Spectral Comparison of Open and Closed Orifice at 90% RPM of the J-57 Port Engine as Sensed by Microphone No. 1

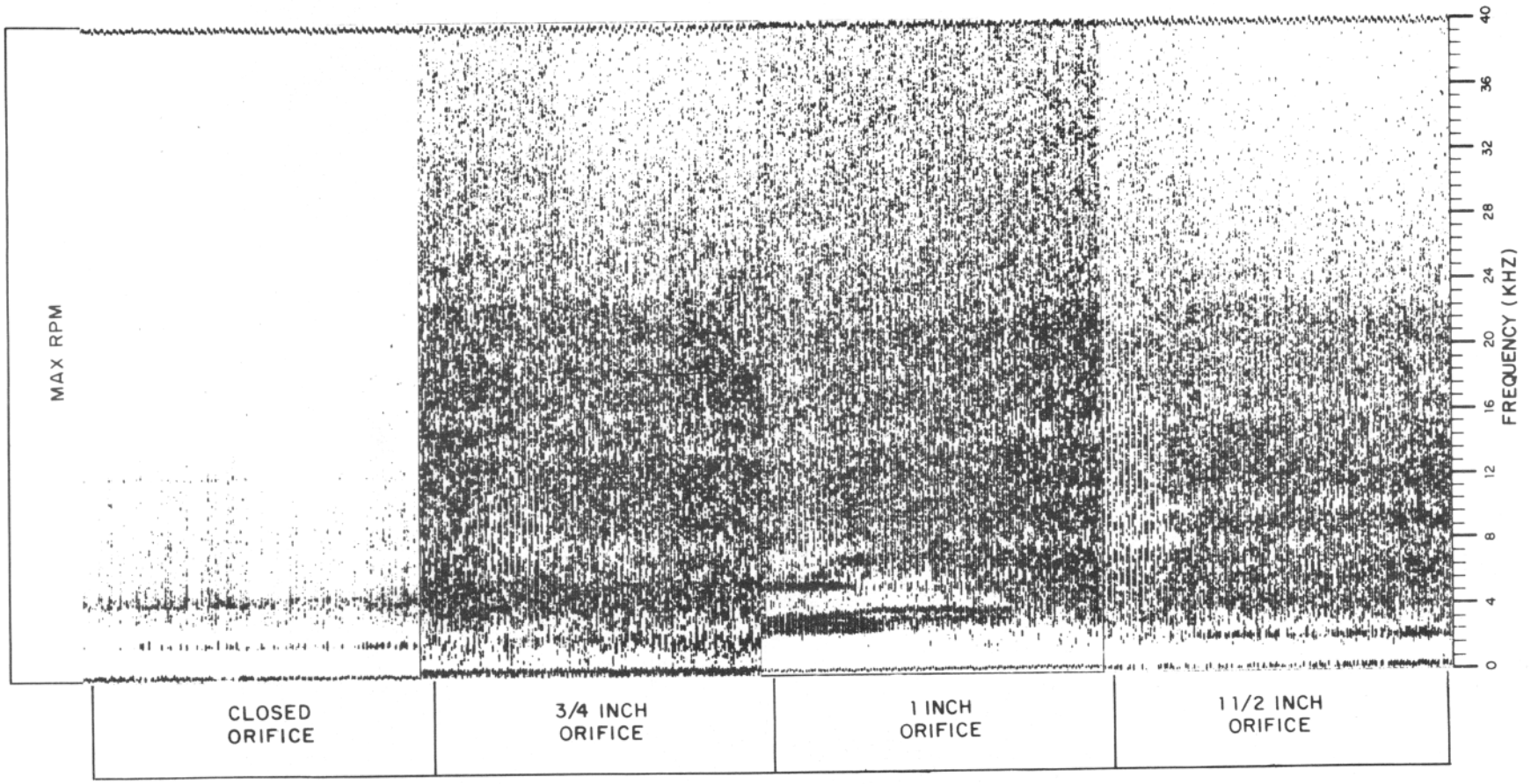

ASW-587-465

Figure 4-35. Spectral Comparison of Open and Closed Orifice at Maximum RPM of the J-57 Port Engine as Sensed by Microphone No. 1

4.5 Effect of Sensor Location on Acoustic Spectrum and Sound Pressure Levels

As has been apparent in previous discussions on engine speed and orifice size relationships, sensor location is a significant factor in the detection of sound pressure level and spectrum data. This factor is especially emphasized when microphone output versus orifice size is plotted for all microphones while engine speed is held constant.

Figure 4-36 is a plot of J-47 engine data at 90% RPM. Microphone No. 1 was located above, in front of, and pointing toward the orifice at a direct path distance of 30 inches. This microphone had the largest output and showed the greatest change. Microphone No. 3 was located forward, below, and pointing toward the orifice at a direct path distance of 22.5 inches. Microphone No. 4 was located aft and pointed toward the orifice at a direct path distance of 50 inches. Microphone No. 5 was mounted on a post approximately 105 inches away slightly above the orifice and was pointed toward the orifice. Microphones 3, 4, and 5 had significantly lower output levels than microphone No. 1 and showed less change. Microphone No. 2 was excluded from this test because of its different characteristics. All other microphones were of the same type.

Figure 4-37 is a plot of microphone output versus orifice size for the J-57 port engine running at maximum RPM. Microphones 2 and 4 were 29 and 34 inches, respectively, from the orifice and had the largest output and greatest change from the closed orifice condition. Microphone No. 1 was 43 inches from the orifice and showed the next greatest change. The curves for microphones 3 and 5 show relatively little change and have a higher closed orifice output than the three previous microphones. The latter is due to engine auxiliary machinery (fuel pumps, oil pumps, bearings, etc.) which were in close proximity to these microphones. Even if the increase in sound pressure level due to the machinery were not present, the microphone outputs would have been relatively small. As was apparent on the J-47 engine plot, distance is a factor in sound transmission. Microphones 3 and 4 were 85 and 79 inches, respectively, from the open orifice. A second factor which may have influenced the transmission of sound from the open orifice to the microphone was the engine cowling whose effect is unknown.

Variation in spectrum due to sensor location is apparent in Figure 4-38. This figure is a spectrogram composite of all five microphones and shows the changes in spectrum due to microphone location vividly. The J-57 port engine was running at 82% RPM and the modified burner can orifice was closed during this test. Although the changes are very noticeable in this figure, it is typical of most tests. (Refer to Appendix A through D.)

The effect of microphone location is also present in the energy grams. Figures 4-39 and 4-40 show spectrograms and energy grams of a burn-through test conducted on the J-57 part engine at maximum RPM. Microphone No. 4, which was close to the orifice, sensed a clean and easily

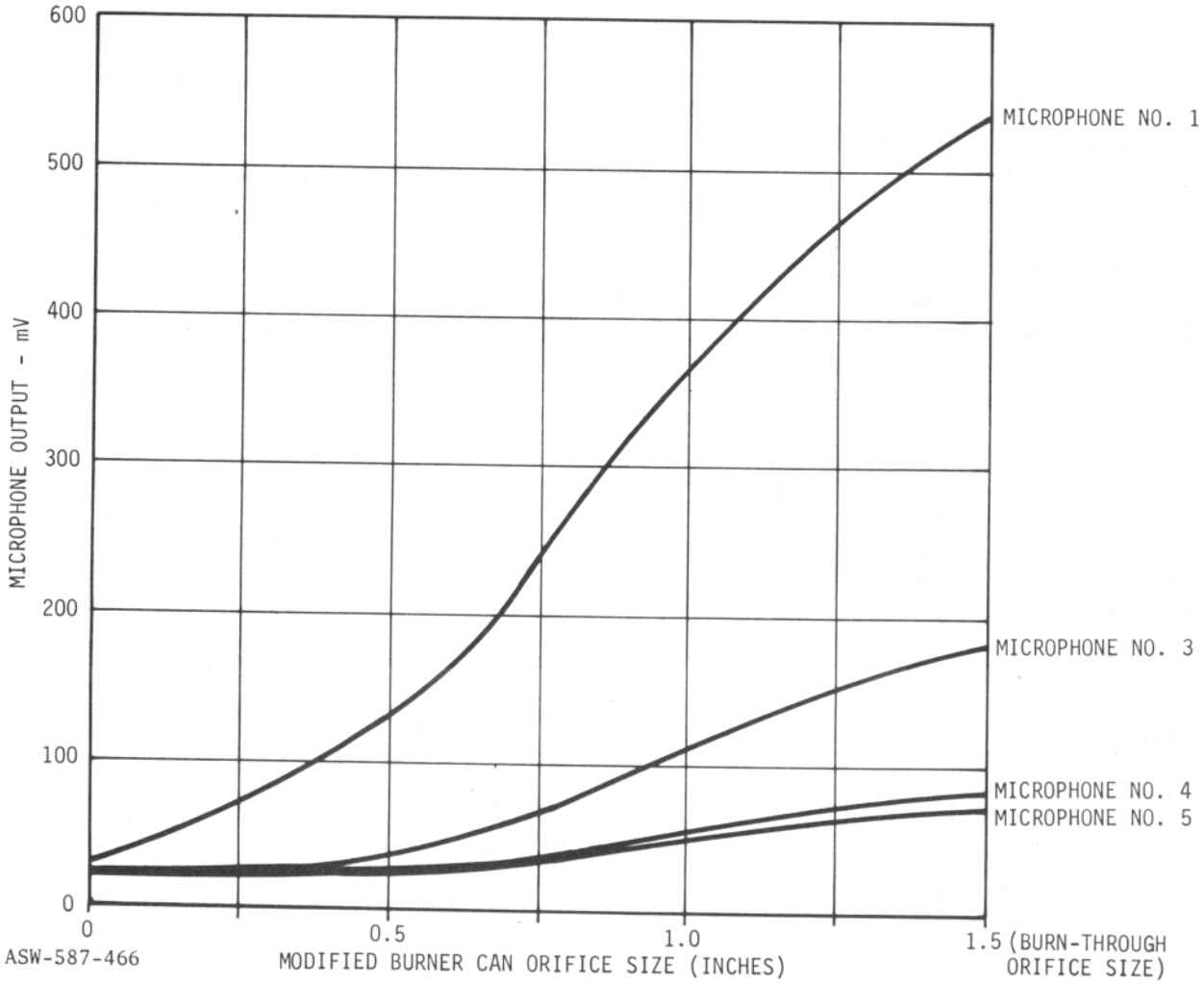

Figure 4-36. J-47 Engine Orifice Size and Sound Pressure Level Relationship of Microphones at 90% RPM

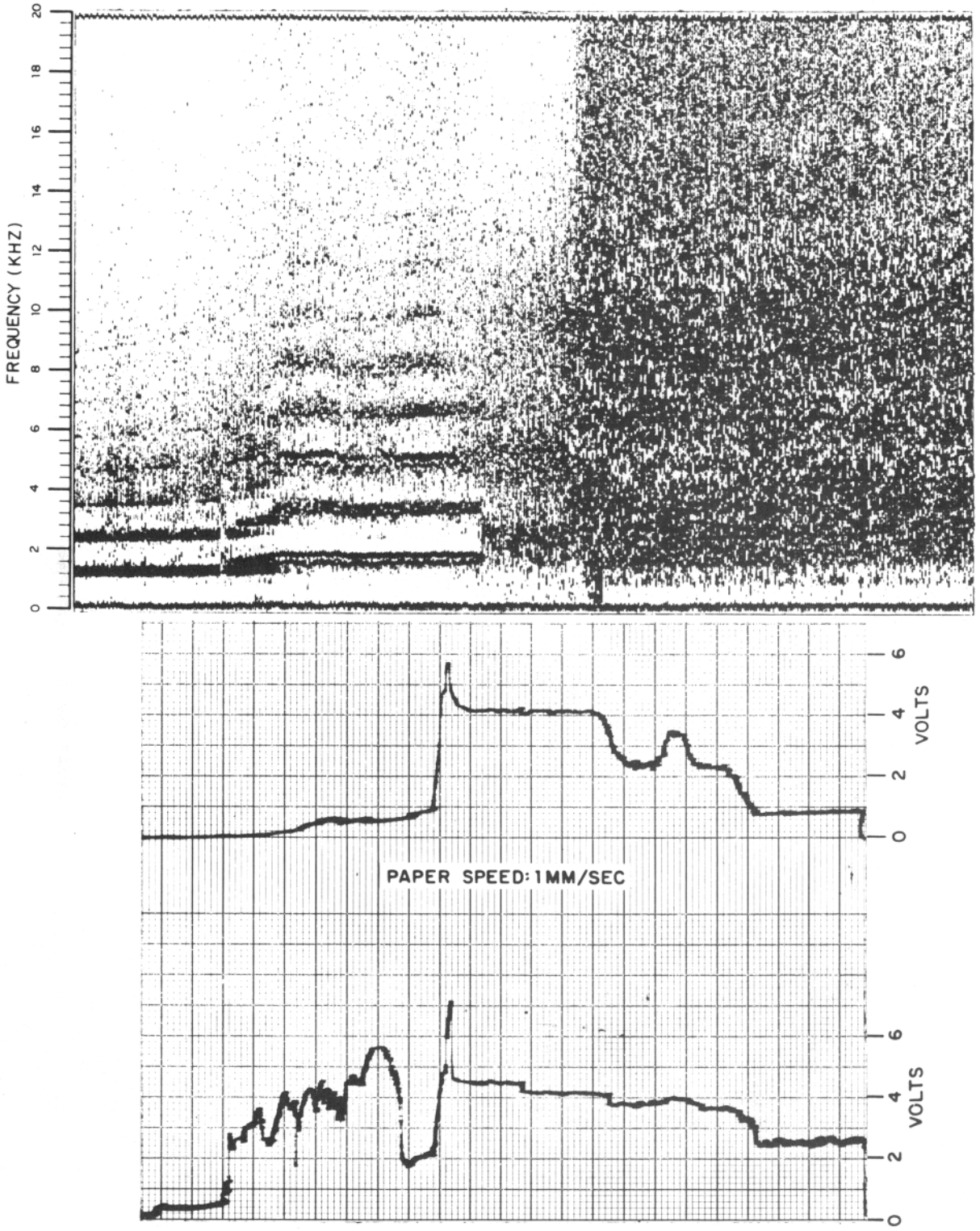

ASW-587-469

Figure 4-39. Burn-Through Failure on the J-57 Port Engine at Maximum RPM as Sensed by Microphone No. 5

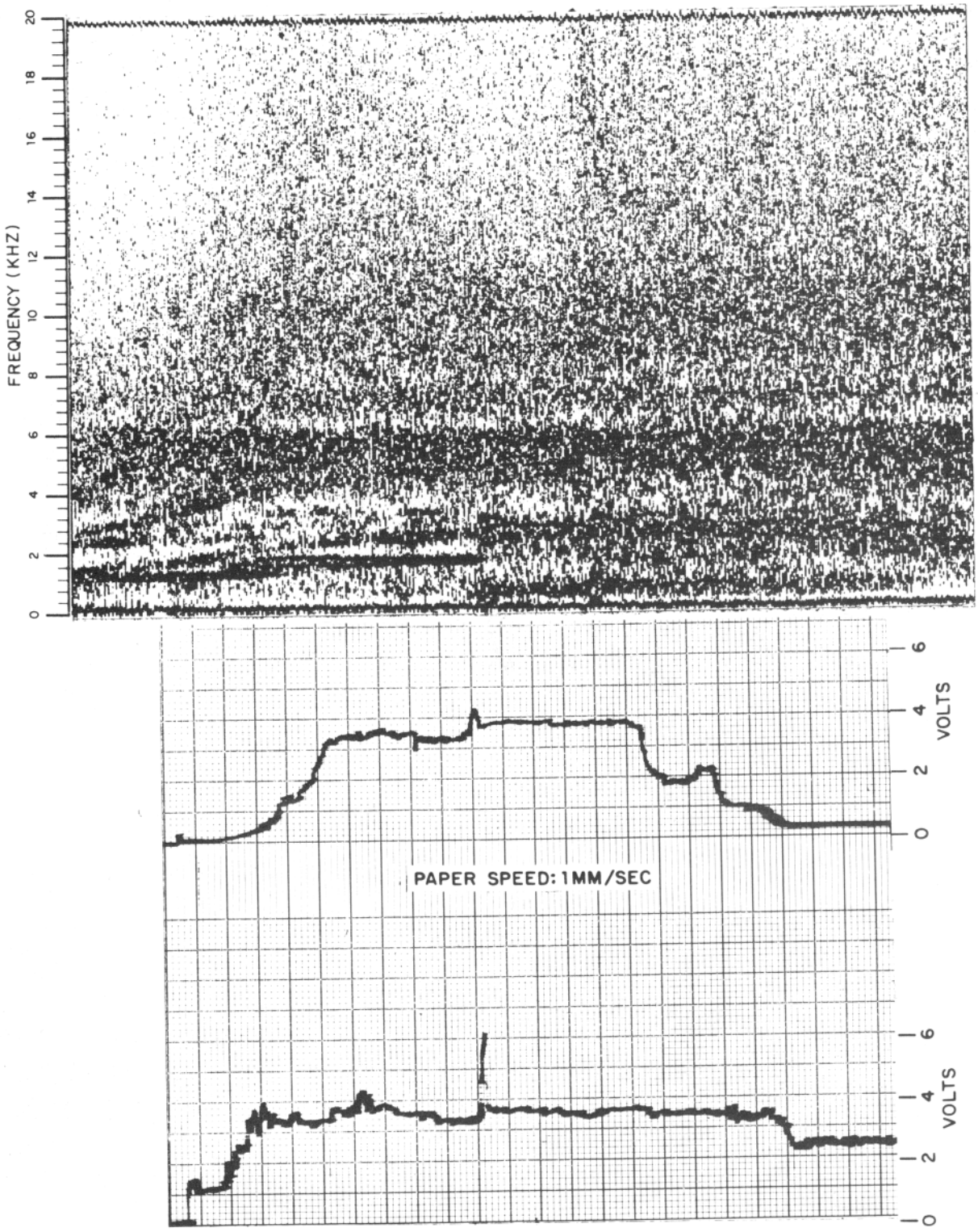

ASW-587-470

Figure 4-40. Burn-Through Failure on the J-57 Port Engine at Maximum RPM as Sensed by Microphone No. 7

detected burn-through on both grams while microphone No. 5, farther away, hardly sensed the burn-through making detection extremely difficult. The most noticeable difference in spectral content between microphones 4 and 5 is the spectrum below 5 kHz. The unfiltered and filtered mean square analysis traces in Figure 4-39 show that most of the startup and pre-burn-through frequencies of microphone No. 4 are below 5 kHz. Figure 4-40, which shows the same data for microphone No. 5, indicates that this microphone sensed a high proportion of frequencies above 5 kHz during startup and pre-burn-through which very nearly equate to the burn-through spectrum. These high frequencies, sensed by microphone No. 5, are from auxiliary engine machinery.

4.6 Effect of Extraneous Sound Sources

A series of tests were run to determine the interference effect of extraneous engine noise on the engine under test. Microphones were installed on the center test engine (J-57 port engine). The engine on the left (J-47 engine) and then the engine on the right (J-57 starboard engine) were run with the center test engine quiet. In addition, a burn-through test was run on the center test engine while the J-47 engine was running at maximum RPM. The results of these tests are presented in Appendix C. There was very little interference due to other engines operating in close proximity to the engine on which the sensors were mounted either when quiet or when operating.

Another interference factor, which was not a planned part of the program, became evident while the data was being analyzed. An air-start was used on the J-57 engine creating significant interference. Figure 4-41 shows the spectrum analysis of microphone No. 5, which was closest to the air-start connection, and mean square analysis traces (filtered and unfiltered) of the air-start operating. As can be seen in the figure, the spectrum of the air-start is very broad. A comparison of the mean square analysis traces (filtered and unfiltered) shows that the major portion of the spectrum is above 5 kHz and could influence the design of a burn-through detector based on acoustic techniques. Most commercial and military aircraft in inventory use an auxiliary power unit (APU) built into the aircraft for ground power and starting purposes. Further testing should be accomplished to determine the characteristics and effect of APU sound sources.

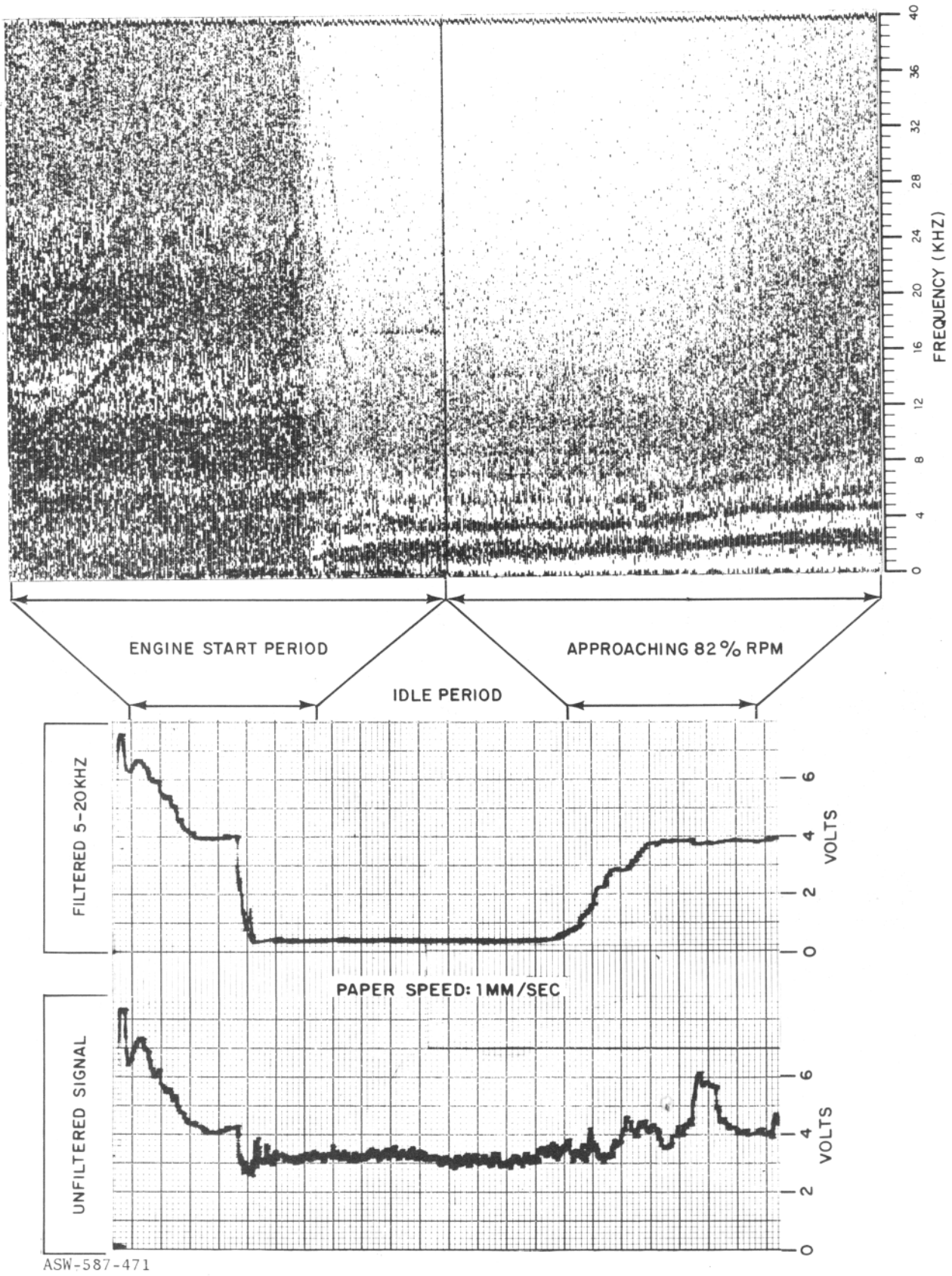

Figure 4-41. Effect of Air-Start on J-57 Port Engine Spectrum as Sensed by Microphone No. 5

5.0 SUMMARY OF RESULTS

5.1 Acoustic Spectrum

Spectrum analysis of the broadband instrumentation microphone recordings revealed that discrete engine machinery frequencies are present up to approximately 35 kHz. The analysis also revealed that the acoustic spectrum is composed primarily of complex, non-periodic signals or random noise which is present in varying degrees across the entire processor bandwidth of 0 to 40 kHz. Data analysis above 40 kHz revealed a minimal amount of random noise which has no apparent useful application to burn-through detection.

5.2 Characteristic Line Spectra at Burn-Through

Analysis of the grams at burn-through indicated that there were no characteristic discrete frequency lines associated with burn-through. The spectrum appeared in all cases to be composed of broadband random noise which, due to its intensity, usually masked out the discrete engine machinery lines. Engine-produced spectra are primarily below 10 kHz and burn-through produced spectra are primarily above 5 kHz.

5.3 Sound Pressure Level Relationship to Orifice Size and Engine Speed

Results of tests run on the open J-47 engine indicate that there is an increase in sound pressure level as the orifice size is increased and as the engine speed is increased. The cowled J-57 engine has characteristic machinery frequencies which comprise the predominent portion of the spectrum at low speeds and result in a high sound pressure level. As engine speed is increased, the sound pressure level drops, then increases at a lesser rate than for the J-47 engine. An increase in orifice size increased the sound pressure level. Overall, the J-57 engine is quieter than the J-47 engine.

5.4 Acoustic Spectrum Relationship to Orifice Size and Engine Speed

Analysis of the grams indicate that the spectrum, composed primarily of random noise, increases in density and frquency as engine speed is increased for a given orifice size. Likewise, for a given engine speed, random noise increases in density and frequency as the orifice size is increased. The J-57 engine spectral density change was less than that of the J-47 engine. At low speed,the J-57 engine characteristically resonates, producing a quantity of discrete frequency lines primarily below 10 kHz.

5.5 Effect of Sensor Location on Acoustic Spectrum and Sound Pressure Levels

Sensor location with respect to the orifice has a significant effect on both acoustic spectrum and sound pressure levels. Sound pressure

levels vary more than 7.5 times between microphones due to location on the J-47 engine at 90% RPM with a 1.5-inch open orifice. Differences of 3 times exist on the J-57 engine at maximum RPM with a 1.5-inch open orifice. In addition, the farther away from the orifice the less sensitive the microphone is to changing sound pressures. The farthest away and therefore least sensitive microphone sound pressure level changes 230% from closed orifice to 1.5 inch open orifice at 90% RPM on the J-47 engine while the most sensitive microphone changes 1,350% under the same conditions. The least sensitive microphone on the J-57 engine changes 125% while the most sensitive changes 300% from closed to 1.5 inch open orifice at maximum RPM. These changes are directly related to sensor location.

Spectral changes due to sensor location are equally as significant as sound pressure level changes. Although spectral changes are very apparent due to loaction, the most significant factor is the effect on burn-through failure detection (see Figures 4-39 and 4-40). Figure 4-40 accents the fact that microphones farther away from the orifice typically are less sensitive to the failure to the extent that a spectral change is not visible when a failure occurs. It was also observed that the proximity of the sensor to auxiliary engine machinery (1 to 3 feet from generators, gear boxes, and fuel pumps) affects the ability of the sensor to detect burn-through failures. Figure 4-38 shows the effect of auxiliary machinery on the spectrum. Microphones No. 3 and 5 we close to auxiliary machinery, where microphones No. 1, 2, and 4 were farther away in the order listed. The mashing effect of the auxiliary machinery noise is very visible.

5.6 Effect of Extraneous Sound Sources

Engines running in close proximity to the engine under test had little effect on sound pressure level or spectral content. It was observed that an air-start has greater sound pressure levels and spectral content than a burn-through failure. The characteristics of auxiliary power units are unknown and should be considered in any future programs.

6.0 CONCLUSIONS

The data gathered and analyzed during the course of this program indicate that burn-through failures can be detected by acoustic means. Signals produced by burn-through failure have been observed to be composed of random noise primarily above 5 kHz. There are no apparent discrete frequency lines produced by burn-through failures.

In addition to the random nature of burn-through spectra, several other factors were noted which have application to burn-through detection. These include sensor location, burn-through duration, erratic sound pressure levels due to engine resonances, extraneous sound source interference, and random variation in spectral density at burn-through.